UNIVERSIDADE DE BRASÍLIA
CAMPUS UNIVERSITÁRIO DARCY RIBEIRO
FACULDADE DE MEDICINA
PROGRAMA DE PÓS-GRADUAÇÃO EM PATOLOGIA MOLECULAR

WEMBLEY RODRIGUES VILELA

Efeito da sobrecarga lipídica sobre a bioenergética neural: Abordagens *in vivo* e *in vitro*

BRASÍLIA

SETEMBRO DE 2024

UNIVERSIDADE DE BRASÍLIA
CAMPUS UNIVERSITÁRIO DARCY RIBEIRO
FACULDADE DE MEDICINA
PROGRAMA DE PÓS-GRADUAÇÃO EM PATOLOGIA MOLECULAR

WEMBLEY RODRIGUES VILELA

Efeito da sobrecarga lipídica sobre a bioenergética neural: Abordagens *in vivo* e *in vitro*

Tese de doutorado apresentada à Faculdade de Medicina da Universidade de Brasília como parte dos requisitos para obtenção do título de doutor em Patologia Molecular

Área de Concentração: Bioquímica.

Orientadora: Profª. Drª. Andreza Fabro de Bem

Co-orientador: Prof. Dr. Julio Cesar Batista Ferreira

BRASÍLIA

SETEMBRO DE 2024

Vilela, Wembley Rodrigues
VV699e Efeito da sobrecarga lipídica sobre a bioenergética neural: Abordagens in vivo e in vitro / Wembley Rodrigues Vilela; orientador Andreza Fabro de Bem; co-orientador Julio Cesar Batista Ferreira. -- Brasília, 2024.
97 p.

Tese(Doutorado em Patologia Molecular) -- Universidade de Brasília, 2024.

1. Disfunção metabólica. 2. Mitocôndria. 3. Cognição. 4. Hipocampo. 5. Microglia. I. de Bem, Andreza Fabro, orient. II. Ferreira, Julio Cesar Batista, co-orient. III. Título.

WEMBLEY RODRIGUES VILELA

Efeito da sobrecarga lipídica sobre a bioenergética neural: Abordagens *in vivo* e *in vitro*

Tese de doutorado apresentada ao Programa de Pós-Graduação em Patologia Molecular da Universidade de Brasília como parte dos requisitos para obtenção do título de doutor.

Data de aprovação: 18/09/2024

Banca Examinadora:

Prof Dra. Andreza Fabro de Bem, Universidade de Brasília – Presidente

Prof. Dr. Mychael Vinícius da Costa Lourenço – Membro Titular

Dra. Daiane Fátima Engel – Membro Titular

Prof. Dra. Kelly Grace Magalhães – Membro Titular

Prof. Dra. Andréa Queiroz Maranhão – Membro Suplente

Decido esse trabalho
à minha mãe 

AGRADECIMENTOS

Em primeiro lugar, gostaria de agradecer à Deus, por absolutamente tudo! Pela saúde, paz, vitalidade, e por todo o amor que tenho e recebo de todos os meus.

À minha Mamis Marilene Rodrigues da Silva, que sempre foi meu exemplo direto de amor, educação, parceria e honestidade. Obrigado por ser minha mãe e por todo o amor, dedicação... por tudo ❤️

À toda a minha família, meu pai Welton, minha tia Ilda, meu vô Carmino *(In memoriam)*, vó Creuzinha, e à todos os outros membros dessa família, que proporcionaram um ambiente de muito amor e acolhimento para o meu desenvolvimento humano.

À minha orientadora Andreza Fabro de Bem, pela confiança e dedicação na minha formação pessoal e profissional ❤️

Aos meus professores do Lab de Bem, Jair e Paula, pelos ensinamentos e paciência.

Aos professores dos laboratórios aos quais fizemos parcerias, Julio Cesar, Gilberto Xavier, Alicia Kowaltowski (USP), João Duarte (Lund University), Rosa Paolicelli (University of Lausanne), pelas oportunidades e ensinamentos.

A todos os meus professores, que fizeram parte dessa jornada acadêmica desde o jardim de infância, até o doutorado.

Aos meus amigos de trabalho do Lab de Bem em Brasília, Wellinghton, Louise, Nathasha, Letícia, Whitney e Ana Bia, e especialmente ao Victor, por todo o apoio acadêmico e emocional durante a pós-graduação.

Aos meus amigos e colegas dos laboratórios parceiros, Luiz Bechara, Lisley Ramalho, Bárbara Krum, Débora Scheffer, Itamar Couto (USP), Nicolle Platt, Annelise Francisco, Nadiia Kravchencko, Zeinab Rafiee, João Vieira (Lund University), Gloria Colombo (University of Lausanne), por todo apoio acadêmico e pessoal durante essa trajetória.

Aos meus amigos pessoais por todo o apoio de sempre, especialmente a Dhyéssica Thome, Lucas Natan, Edney Bezerra, Gizele Barbosa, Alini Dessbessel e Adriany Fonseca.

À todos os funcionários da Universidade de Brasília, São Paulo, Lund e Lausanne, direta ou indiretamente proporcionaram um ambiente propício para a realização desta pesquisa.

À CAPES, CNPq e FAPDF pelo apoio financeiro, e especialmente ao programa CAPES/STINT, pela oportunidade de realizar o intercâmbio na Suécia.

O que você faz com amor e cuidado tem uma chance de fazer diferença, tanto para você como para a vida de outras pessoas. Tudo o que se faz sem amor e sem convicção é fadado ao fracasso e à perda de tempo, para você e para os outros" (Wim Wenders).

APRESENTAÇÃO

Esta tese está organizada em três partes, sendo constituída dos seguintes itens:

Parte I: Resumo, Resumo em Inglês (Abstract), Lista de Abreviaturas, Lista de Figuras, Revisão Bibliográfica, Justificativa e Objetivos;

Parte II: Resultados escritos na forma de artigo científico, dividido em capítulos;

Parte III: Conclusão e Perspectivas Futuras, Referências Bibliográficas citadas na Parte I e Parte III e Anexos

Os experimentos que deram origem ao capítulo I *(*Protocolo *in vivo)*, foram realizados no Instituto de Ciências Biomédicas (ICB) e Instituto de Biologia (IB) da Universidade de São Paulo (USP) São Paulo, Brasil, nos laboratórios do Prof. Julio Cesar Batista Ferreira, Prof. Gilberto Fernando Xavier e Prof. Alicia Juliana Kowaltowski e estão descritos na forma de artigo científico publicado na Revista "Journal of Bioenergetics and Biomembranes". Os experimentos do capítulo II (Protocolo *in vitro)*, foram realizados no ICB da USP, no laboratório do Prof. Julio Cesar Batista Ferreira, no Departamento de Ciência Médica Experimental, na Universidade de Lund, Suécia, sob a supervisão do Professor João M. N. Duarte, e no Departamento de Ciências Biomédicas, na Universidade de Lausanne, Suíça, supervisionado pela Prof. Rosa Chiara Paolicelli. Essa colaboração internacional foi possível através de uma bolsa pelo programa CAPES/STINT, durante o período de 12/2022 a 11/2023. Todos os experimentos foram realizados com a supervisão e orientação da professora Andreza Fabro de Bem.

SUMÁRIO

Parte I

RESUMO

A ingestão excessiva de dietas rica em gorduras saturadas é fator de risco não somente para o desenvolvimento de doenças metabólicas, mas afeta particularmente o cérebro. Evidências revelam que o declínio cognitivo e sinais de neurodegeneração são observados em modelos pré-clínicos e estudos clínicos de doenças metabólicas associadas a ingesta de dietas hiperlipídicas. Nós hipotetizamos que a mitocondria é primordialmente afetada pela sobrecarga lipídica, tendo por consequências *in vivo*: a disfunção hipocampal e neocortical, e fenotipicamente, o declínio cognitivo; e a polarização microglial para um fenótipo neurodegenerativo, *in vitro*, sendo o prejuízo bioenergético prevenido pelo ácido graxo de cadeia curta butirato. Para os experimentos *in vivo*, ratos Wistar machos de 8 semanas receberam dieta controle ou dieta hiperlipídica (DH) associada ao L-NAME na água de beber. DH+L-NAME induziu obesidade, hipertensão e aumento do colesterol sérico. Essa disfunção metabólica foi associada a prejuízo na fase de aprendizado espacial no labirinto aquático de Morris. A função mitocondrial e taxa de captação e a capacidade de retenção de cálcio no neocórtex não foi prejudicada nos ratos expostos a DH+ L-NAME. Já a disfunção mitocondrial no hipocampo foi evidenciada pela diminuição do consumo de oxigênio (O_2) relacionado à produção de ATP, tendência de diminuir a capacidade máxima mitocondrial e aumento na expressão da proteína OPA1 no hipocampo de ratos expostos a DH+L-NAME, sem alterações em outras proteínas relacionadas à dinâmica mitocondrial. Em conjunto os dados demonstram que a DH+L-NAME estabelecem uma relação entre a disfunção energética no hipocampo e o impacto sobre o processo de aprendizagem. Nos experimentos *in vitro*, células de microglia da linhagem BV2 foram cultivadas em baixa glicose, em inglês *"low glucose"*, LG, ou alta glicose, em inglês *"high glucose"*, HG, (5.5 e 25mM, respectivamente), e estimuladas por 24h com palmitato (100 e 200 µM. A exposição ao palmitato diminuiu a viabilidade celular em condições de HG, comparado ao LG. Efeitos do tratamento com palmitato foram observados na expressão dos genes CD68, Il-1β e IL-10, e também foi observado efeito do palmitato em genes de metabolismo lipídico, sem alterações em genes do metabolismo de glicose. O meio HG induziu aumento nos valores de respiração oxidativa e fluxo glicolítico em relação ao LG, e o tratamento com palmitato reduziu drasticamente os valores de ambos os fluxos, oxidativo e glicolítico. O co-tratamento com o butirato não foi eficiente para mitigar as alterações de função mitocondrial induzidas pelo

palmitato. Em cultura primária de microglia, o palmitato não induziu alterações na área mitocondrial e nem no metabolismo de sinaptossomas. Nossos resultados indicam uma maior propensão das células BV2 a sofrerem os efeitos tóxicos do palmitato quando cultivadas em HG. Palmitato foi capaz de aumentar a expressão de genes relacionados à inflamação e metabolismo lipídico. Além disso, o meio HG aumentou o fluxo metabólico, sendo esse diminuído pelo palmitato, independente do meio de cultura utilizado. Esse conjunto de dados sugere que a sobrecarga lipídica, *in vivo* e *in vitro*, compromete a bioenergética de células neurais, predispondo a características inflamatórias e um fenótipo de neurodegeneração.

Palavras-chave: disfunção metabólica, mitocôndria, cognição, hipocampo, microglia, palmitato.

ABSTRACT

The excessive intake of diets rich in saturated fats is a risk factor not only for the development of metabolic diseases, but particularly affects the brain. Evidence shows that cognitive decline and signs of neurodegeneration are observed in preclinical models and clinical studies of metabolic diseases associated with the intake of high-fat diets. We hypothesize that mitochondria are primarily affected by lipid overload, resulting in *in vivo* hippocampal and neocortical dysfunction, and phenotypically, cognitive decline; and microglial polarization toward a neurodegenerative phenotype, *in vitro*, with bioenergetic impairment being prevented by the short-chain fatty acid butyrate. For *in vivo* experiments, 8-week-old male Wistar rats received a control diet or a high-fat diet (HFD) associated with L-NAME in their drinking water. HFD+L-NAME induced obesity, hypertension and increased serum cholesterol. This metabolic dysfunction was associated with impaired spatial learning in the Morris water maze. Mitochondrial function and the calcium uptake rate and retention capacity in the neocortex were not impaired in rats exposed to HFD+L-NAME. Mitochondrial dysfunction in the hippocampus was evidenced by decreased oxygen consumption (O_2) related to ATP production, a tendency to decrease maximum mitochondrial capacity, and increased expression of the OPA1 protein in the hippocampus of rats exposed to HFD+L-NAME, without changes in other proteins related to mitochondrial dynamics. Together, the data demonstrate that HFD+L-NAME establishes a relationship between energy dysfunction in the hippocampus and the impact on the learning process. In *in vitro* experiments, BV2 microglial cells were cultured in low glucose, LG, or high glucose, HG, (5.5 and 25 mM, respectively) and stimulated for 24 h with palmitate (100 and 200 µM). Palmitate exposure decreased cell viability in HG conditions, compared to LG. Effects of palmitate treatment were observed on the expression of CD68, Il-1β and IL-10 genes, and palmitate also had an effect on lipid metabolism genes, with no changes in glucose metabolism genes. HG medium induced an increase in oxidative respiration and glycolytic flux values compared to LG, and palmitate treatment drastically reduced the values of both oxidative and glycolytic fluxes. Co-treatment with butyrate was not efficient in mitigating the changes in mitochondrial function induced by palmitate. In a primary culture of microglia, palmitate did not induce changes in the mitochondrial area or in the metabolism of synaptosomes. Our results indicate a greater propensity of BV2 cells to suffer the toxic effects of palmitate when cultured in HG. Palmitate was able to increase the expression of genes related to inflammation and lipid metabolism. In addition, the HG medium increased the

metabolic flux, which was decreased by palmitate, regardless of the culture medium used. This set of data suggests that lipid overload, *in vivo* and *in vitro*, compromises the bioenergetics of neural cells, predisposing to inflammatory characteristics and a neurodegeneration phenotype.

Keywords: metabolic dysfunction, mitochondria, cognition, hippocampus, microglia, palmitate.

LISTA DE ABREVIATURAS

AGCC	Ácidos Graxos de Cadeia Curta
ALT	Alanina Aminotransferase
AST	Aspartato Aminotransferase
ATP	Adenosina tri-fosfato
Ca^{2+}	Íon Cálcio
CTE	Cadeia Transportadora de Elétrons
DH	Dieta Hiperlipídica
DNA	Ácido Desoxirribonucleico
DRP-1	Proteína Relacionada à Dinamina 1
EIM	Espaço Inter-Membrana
ERO	Espécies Reativas de Oxigênio
FADH2	Flavina Adenina Dinucleutídeo
Fis1	Proteína de Fissão mitocondrial 1
GPCR	Receptores acoplados à proteína G
GTPases	Enzimas hidrolases que hidrolisam a Guanosina Tri-Fosfato
HG	Alta Glicose
IL	Interleucina
LDL	Lipoproteína de Baixa Densidade
LG	Baixa Glicose
L-NAME	N-ω-nitro-L-arginina metil éster
LPS	Lipopolissacarídeo
MFF	Fator de Fissão Mitocôndrial
NADH	Nicotinamida Adenina Dinucleutídeo

NFκB	Fator Nuclear κ B
NO	Óxido Nitrico
OPA-1	Proteína de Atrofia Ótica 1
OXPHOS	Fosforilação Oxidativa
O_2	Oxigênio molecular
SNC	Sistema Nervoso Central
STZ	Estreptozotocina
TNF-α	Fator de Necrose Tumoral α
UPF	Alimentos Ultraprocessados

LISTA DE FIGURAS DA REVISÃO BIBLIOGRÁFICA

1. REVISÃO BIBLIOGRÁFICA

Mundialmente, estamos sendo desafiados com a facilidade de acesso a alimentos contendo alta densidade energética, especialmente pelo padrão ocidentalizado, que contém excesso de açúcares e gordura, e baixo valor nutricional, que combinado com o crescente aumento do sedentarismo, tende a agravar problemas de saúde pública como obesidade, doenças cardiovasculares, risco aumentado de câncer e doenças neurodegenerativas (JOKINEN, 2015; KNIGHT et al., 2014; WHO, 2020). O elevado consumo de dietas ocidentalizadas está associado com alterações cardiometabólicas já na infância e adolescência, destacando-se a resistência à insulina, maior circunferência abdominal e dislipidemias como hipertrigliceridemia e elevado colesterol LDL (ROCHA et al., 2017), e em adultos, onde há adicionalmente associação com a hipertensão arterial (ALAMNIA; SARGENT; KELLY, 2023; LEE et al., 2023). No Brasil, cerca de 20% da ingestão calórica da população acima de 10 anos é oriunda de alimentos ultraprocessados (UPF, do inglês ultraprocessed foods), que contém quantidades excessivas de gorduras e açúcares, flavorizantes e aditivos sintéticos e pobre em grãos integrais e fibras, sendo que esse percentual cresceu 1% dentro do período de 10 anos (LOUZADA et al., 2023).

Em contrapartida, a adesão a um padrão dietético mais saudável, contendo maior quantidade de vegetais está associado a menor probabilidade de desenvolver componentes da síndrome metabólica, como elevada pressão arterial e glicemia, e maior circunferência abdominal (KHEIRANDISH et al., 2024). Essas evidências sugerem que consumo excessivo de dietas ocidentalizadas impactam a homeostase metabólica corporal, com ênfase no sistema cardiovascular, e em outros órgãos metabólicos, como o fígado (TUTUNCHI et al., 2021; XIAO et al., 2023) e o cérebro (GOMES GONCALVES et al., 2023).

1.1 Evidências clínicas do impacto de dietas ocidentalizadas no sistema nervoso central (SNC)

No SNC, um dos processos comprometidos pelo consumo de dietas ocidentalizadas é a cognição. Um estudo publicado em 2022 que avaliou, longitudinalmente, o perfil de consumo de UPF de uma população de brasileiros adultos entre os anos de 2008 a 2019 demonstrou que os indivíduos que consumiram maior porcentagem de kcal/dia oriundos de alimentos UPF apresentaram maior consumo de

calorias totais, menor índice de atividade física e maior frequência de sintomas depressivos (GOMES GONCALVES et al., 2023). A performance cognitiva geral e de funções executivas dos indivíduos que consumiam mais do que 19.9% da ingestão calórica total oriunda de UPFs diminuiu 28% mais rápido em comparação àqueles que reportaram consumir até 19.9% de UPF (GOMES GONCALVES et al., 2023). Um outro estudo prospectivo que acompanhou indivíduos por 31 anos desde a infância, demonstrou que o risco cardiovascular e obesidade infantil promoveu o desenvolvimento da síndrome metabólica (conjunto de ao menos 3 alterações metabólicas concomitantes) na vida adulta. Paralelamente a síndrome metabólica, foi associada com pior performance em testes que avaliaram memória episódica, aprendizagem associativa e atenção sustentada nestes indivíduos (HAKALA et al., 2021). Estas evidências reforçam a associação entre uma alimentação rica em gorduras e açúcares, o desequilíbrio metabólico e a suscetibilidade a disfunção cognitiva.

Ademais, Melo e colaboradores evidenciaram um aumento nas concentrações de palmitato no líquido cerebrospinal de humanos, o que foi associado ao ganho de peso corporal, acúmulo de gordura abdominal, e à presença de doenças metabólicas, como diabetes, dislipidemias e/ou hipertensão. O palmitato é o ácido graxo mais abundante em dietas com alto teor de gordura saturada. Interessantemente, um aumento na concentração de palmitato no líquido cerebrospinal foi correlacionado a um pior desempenho cognitivo nos indivíduos com doenças metabólicas (MELO et al., 2020).

Um estudo recente agrupou indivíduos de acordo com seu padrão alimentar. Os indivíduos consumidores de uma dieta equilibrada, contendo nutrientes oriundos de produtos de origem animal, vegetal, fontes de fibras e alimentos processados apresentaram vantagem cognitiva, bioquímica e em padrões de neuroimagem, em comparação com indivíduos que consumiam dietas restritivas. Especificamente, os indivíduos consumidores da dieta equilibrada mencionada acima, apresentaram melhores escores cognitivos de tempo de reação, menor suscetibilidade a doenças mentais como doença de Alzheimer e esquizofrenia, melhores escores de bem-estar, ansiedade, depressão e menor risco de acidente vascular encefálico, do que pacientes que consumiam dietas com restrição alimentar de fibras (dietas ocidentalizadas, com alto teor de proteína animal), e vegetarianas. Ademais, esse subtipo equilibrado apresentou menores níveis de proteína C reativa e menor contagem de leucócitos do que o subtipo de dietas ocidentalizadas, bem como maior volume da massa cinzenta no cérebro, particularmente

nas regiões parahipocampais e nos lobos temporal e parietal, estruturas relacionadas com a formação e processamento de memórias (ZHANG, R. et al., 2024).

1.2 Impacto da sobrecarga lipídica sobre o metabolismo e a função cerebral: estudos pré-clínicos

Modelos experimentais de exposição à dietas ricas em gorduras saturadas e açúcares refinados são amplamente utilizados para a indução de disfunções metabólicas como a obesidade, hipertensão arterial, hiperglicemia e hipercolesterolemia, o que reproduz com robustez os dados verificados em humanos (DE BEM et al., 2020). Estudos prévios demonstram que a dieta hiperlipídica (DH), ou a combinação da DH com outras drogas, promove a desregulação de funções de diversos órgãos metabólicos periféricos. No coração, a DH acrescida de sacarose, promoveu disfunção mitocondrial pelo excesso de espécies reativas de oxigênio (ERO) e menor taxa de produção de ATP (COLE et al., 2011).

Ademais, um modelo de dupla abordagem de DH e a droga N-ω-nitro-L-arginina metil éster (L-NAME) na água de beber, induziu síndrome metabólica acompanhada insuficiência cardíaca (SCHIATTARELLA et al., 2019; SUN et al., 2024). O L-NAME é um inibidor não seletivo da enzima óxido nítrico sintase, diminuindo assim a disponibilidade de óxido nítrico (NO, do inglês *"nitric oxide"*) celular. O NO, por sua vez, é fundamental no controle de diversos processos biológicos como proliferação celular, mitogênese, e por ser um poderoso vasodilatador, é essencial para uma adequada reatividade vascular, onde tem se demonstrado que o NO protege a vasculatura de danos associados ao risco cardiovascular, como aumento na pressão arterial, glicose e lipídeos sanguíneos (WU et al., 2021). No capítulo 1 desta tese, abordamos essa dupla abordagem de DH+L-NAME sobre parâmetros metabólicos e cognitivos.

No fígado, a DH com sacarose induziu esteatose e aumento sérico das enzimas hepáticas ALT e AST, além de elevados marcadores de inflamação no tecido hepático (ISHIMOTO et al., 2013). No pâncreas, a DH promove a hipertrofia das ilhotas pancreáticas e intolerância à glicose, acompanhado de hipertrofia do tecido adiposo branco e branqueamento do tecido adiposo marrom (GAO, M.; MA; LIU, 2015).

Alterações cerebrais também são evidentes em modelos pré-clínicos de sobrecarga lipídica. O consumo de DH induz aumento de marcadores inflamatórios no

hipotálamo a curto prazo, e morte de neurônios hipotalâmicos com o consumo crônico (THALER et al., 2012). Elevados níveis de marcadores inflamatórios no córtex pré-frontal também foram observados após o consumo crônico de DH em camundongos (MANDWIE et al., 2021). Todos esses dados demonstram como órgãos periféricos e o SNC são afetados pela disfunção metabólica induzida pelo consumo de DH.

1.2.1 O hipocampo e a disfunção hipocampal induzida pela sobrecarga lipídica

Como mencionado no tópico anterior, a disfunção metabólica induzida por DH tem impactos em órgãos metabólicos periféricos e no SNC, e particularmente a formação hipocampal é extremamente sensível à sobrecarga lipídica. A formação hipocampal é uma região do lobo temporal medial que é responsável pelo controle de emoções, aprendizado e consolidação de memórias de curto e longo prazo (MCDONALD; MOTT, 2017). Avaliações pós mortem de indivíduos com amnésia retrógrada e anterógrada indicam redução do volume hipocampal, acompanhado de lesões com perda celular em diversas regiões da formação hipocampal, sendo que a magnitude da perda de memória está positivamente correlacionada com a extensão da área hipocampal afetada (REMPEL-CLOWER et al., 1996; ZOLA-MORGAN; SQUIRE; AMARAL, 1986) .

Em roedores, o consumo de dietas hiperlipídicas e hipercalóricas impactam funções hipocampais, sendo observados prejuízos na memória de reconhecimento de curta e longa duração (DIAZ et al., 2021; DUTHEIL et al., 2016), memória espacial e aprendizagem (TREVINO et al., 2015), comportamento tipo depressivo e anedônico (DUTHEIL et al., 2016). Em modelos de desordem metabólica induzida por dieta, o prejuízo cognitivo é acompanhado de alterações químicas e funcionais no hipocampo, como o aumento de marcadores inflamatórios (DUTHEIL et al., 2016), sinais de neurodegeneração e apoptose (TREVINO et al., 2015), desbalanço do sistema antioxidante (DIAZ et al., 2021; TREVINO et al., 2015), ativação de células gliais (TREVINO et al., 2015; ZHUANG et al., 2022), redução de espinhas dendríticas e marcadores sinápticos (COPE et al., 2018; DIAZ et al., 2021; TREVINO et al., 2017; ZHUANG et al., 2022).

Dados do nosso grupo corroboram a disfunção hipocampal induzida por DH. Verificamos que a ingestão de DH por poucos dias (menos de 1 semana) foi capaz de causar prejuízo cognitivo em memória de reconhecimento, comportamento tipo-

depressivo, aumento da permeabilidade da barreira hematoencefálica e redução na capacidade oxidativa de mitocôndria hipocampais de camundongos Swiss (DE PAULA et al., 2021). Melo e colaboradores também evidenciaram prejuízo cognitivo dependente de funções hipocampais em um modelo *in vivo* de sobrecarga do ácido graxo saturado palmitato no hipocampo (MELO et al., 2020).

Além da dieta isoladamente, outros modelos de disfunção metabólica são estabelecidos pela associação da dieta com drogas e substâncias tóxicas ao organismo. Recentemente, publicamos um estudo no qual induzimos um modelo de diabetes mellitus tipo 2 em camundongos juvenis administrando DH e baixa dose de estreptozotocina (STZ), um antibiótico que é particularmente tóxico para as células β-pancreáticas, induzindo sua destruição. Nesse estudo, camundongos juvenis apresentaram intolerância à glicose e disfunção mitocondrial em órgãos relacionados ao metabolismo, particularmente o tecido adiposo marrom, e também no hipocampo, onde, além da disfunção bioenergética, evidenciamos astrogliose e prejuízo de memórias dependente de funções hipocampais (VILELA, W. R. et al., 2023). Como mencionado anteriormente, a associação de DH com L-NAME promove alterações metabólicas e cardíacas, sendo também observados alterações hepáticas (CORDERO-HERRERA et al., 2020). No capítulo 1 desta tese, avaliamos o efeito da associação DH e L-NAME em ratos sobre o comportamento e bioenergética cerebral. Além da disfunção metabólica periférica, verificamos que os ratos expostos à DH+L-NAME apresentaram atraso de aprendizagem e disfunção bioenergética hipocampal (VILELA, WEMBLEY R. et al., 2024). Ambas as abordagens evidenciam que as alterações metabólicas periféricas têm impacto direto na função cerebral, especialmente para a função cognitiva. Dentre os mecanismos celulares observados, alterações mitocondriais e de marcadores inflamatórios, estão presentes como reflexo das disfunções hipocampais e comportamentais observados nos modelos de disfunção metabólica (DE PAULA et al., 2021; DIAZ et al., 2021; TREVINO et al., 2015; VILELA, WEMBLEY R. et al., 2024).

1.3 A mitocôndria e a bioenergética cerebral

O cérebro é altamente dependente do contínuo aporte metabólico de substratos para o desempenho das funções neurais. A demanda energética cerebral é alta e paradoxal, visto que são limitadas as reservas de substratos energéticos no cérebro, o que demanda um alto fluxo sanguíneo finamente ajustado para suprir as necessidades, e uma

flexibilidade de ajuste quando há uma maior atividade em dada região (ATTWELL; LAUGHLIN, 2001). Estima-se que o cérebro consuma 120 gramas de glicose por dia, o que equivale a 20% do consumo de glicose corporal em repouso. Em situações de repouso, a rota metabólica favorecida é a fosforilação oxidativa (OXPHOS), enquanto tarefas que demandam uma atividade cerebral maior como plasticidade sináptica, memória e aprendizado, requerem contribuição adicional da glicólise e metabolismo do lactato (GOYAL et al., 2014; YASSINE et al., 2023). Quando há uma restrição no suprimento de glicose, as células cerebrais utilizam os corpos cetônicos derivados do fígado como o acetoacetato e o 3-hydroxibutirato como fonte energética temporária, até o reestabelecimento do suprimento de glicose (KAPOGIANNIS; AVGERINOS, 2020). A fosforilação oxidativa, principal processo bioenergético cerebral, acontece na mitocôndria, organela celular que controla a oxidação de substratos para a geração de energia na forma de adenosina trifosfato (ATP). A mitocôndria é também essencial no metabolismo redox, homeostase de cálcio e na sobrevivência celular (FRIEDMAN; NUNNARI, 2014; OSELLAME; BLACKER; DUCHEN, 2012).

O processo de geração de ATP nos eucariotos se inicia no citoplasma celular com as enzimas da via glicolítica, onde uma série de enzimas catabolizam glicose a piruvato, com a geração de 2 moléculas de ATP. O piruvato entra na matriz mitocondrial através do carreador de piruvato mitocondrial, sendo oxidado a Acetil CoA, que entra no ciclo do ácido cítrico e cataboliza a formação das coenzimas reduzidas NADH e $FADH_2$. As coenzimas reduzidas, por sua vez, são oxidadas nos complexos energéticos, localizados nas cristas mitocondriais, e os elétrons são transportados através dos complexos I, II, III e IV e da ubiquinona, até chegarem em seu aceptor final, o O_2, reduzindo-o a água. Durante o processo de transporte de elétrons, os complexos I, III e IV bombeiam prótons da matriz para o espaço inter-membrana (EIM), formando um gradiente de prótons, que posteriormente retornará para a matriz através da ATP sintase (complexo V), sendo esse o mecanismo de geração de ATP através da oxidação de substratos (Figura 1) (NUNNARI; SUOMALAINEN, 2012; OSELLAME et al., 2012).

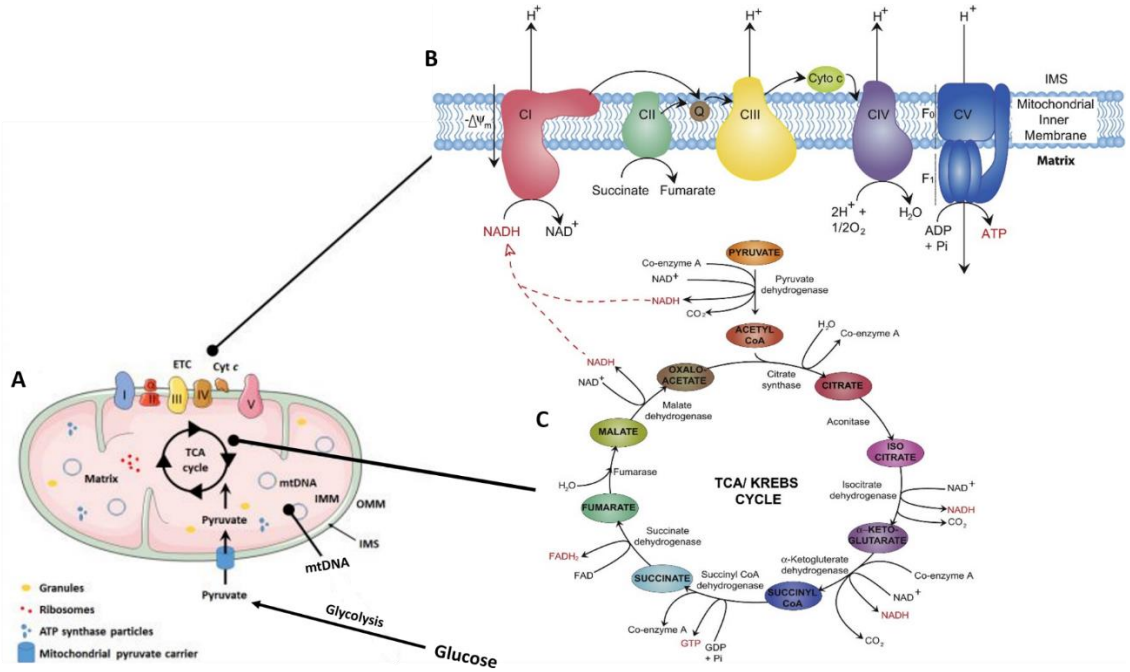

Figura 1. A mitocôndria e o processo de geração de energia pela fosforilação oxidativa. (A) Estrutura da mitocôndria, composta por ribossomos, DNA mitocondrial, grânulos de RNA, membranas externa, interna e o espaço inter-membrana (EIM). O processo de geração de energia se inicia com a entrada de glicose na célula, onde será oxidada a piruvato pelas enzimas da via glicolítica. O piruvato entra na matriz mitocondrial, onde será oxidado a Acetil-CoA, (C) e este entrará no ciclo do ácido cítrico, a fim de formar coenzimas reduzidas NADH e $FADH_2$, e o succinato, que serão posteriormente oxidadas nos complexos localizados nas cristas mitocondriais. (B) O NADH, o $FADH_2$ e o succinato transferem seus elétrons para os complexos I e II, e através da oxirredução das outras enzimas da cadeia transportadora de elétrons (CTE), culminando na redução do O_2 (aceptor final de elétrons) a água. A transferência de elétrons através da CTE mantém o potencial da membrana pelo bombeamento de prótons para o EIM. Nesta etapa final, o gradiente de prótons retorna à matriz pela ATP sintase, onde ADP é fosforilado para formar ATP. (A) Adaptado de (GRASSO et al., 2020) sob licença Creative Commons Attribution 4.0 International, (B e C) adaptados de (OSELLAME et al., 2012) sob a licença Creative Commons Attibution 3.0 Unported.

Alterações da função e estrutura mitocondrial podem comprometer a eficiência energética da organela, e a função celular como um todo. Dentre um processo crucial para a manutenção da morfologia, destaca-se a dinâmica mitocondrial (ALAVI; FUHRMANN, 2013). O processo de dinâmica mitocondrial controla a estrutura física das redes mitocondriais, continuamente alternando entre fusão e fissão para se ajustar às demandas celulares e energéticas (ALAVI; FUHRMANN, 2013). O processo de fusão é caracterizado pela junção de duas mitocôndrias em uma só, sendo mediado por três GTPases relacionada à dinamina, as mitofusinas 1 e 2, que catalisam a fusão da membrana

externa, e a proteína de atrofia ótica 1 (OPA1), que catalisa a fusão da membrana interna da mitocôndria (BAKER; PATEL; KHACHO, 2019). Esse processo forma mitocôndrias alongadas que são postuladas a terem uma atividade fosforilativa mais eficiente, além desse processo atenuar os danos às proteínas e preservar o DNA mitocondrial (MISHRA, P.; CHAN, 2016).

Já o processo de fissão caracteriza-se pela partição de uma mitocôndria em dois fragmentos, sendo mediado pela proteína citosólica DRP-1 (proteína relacionada à dinamina 1), que é recrutada para a membrana externa mitocondrial, e se liga a outras proteínas receptoras como Fis1, MFF, Mid49 e MiD51, desencadeando a cisão da organela (BAKER et al., 2019). Esse processo é importante no transporte de mitocôndrias e na eliminação de fragmentos mitocondriais que se tornaram disfuncionais (MISHRA, P.; CHAN, 2016). Esses fragmentos danificados são destinados à mitofagia, e o fragmento que não está danificado é preservado, podendo ser posteriormente fusionado com outra mitocôndria (OSELLAME et al., 2012). O processo de fissão frequentemente é associado à uma menor atividade fosforilativa, quando comparado com mitocôndrias mais alongadas (MISHRA, P.; CHAN, 2016). A dinâmica mitocondrial está esquematizada na Figura 2.

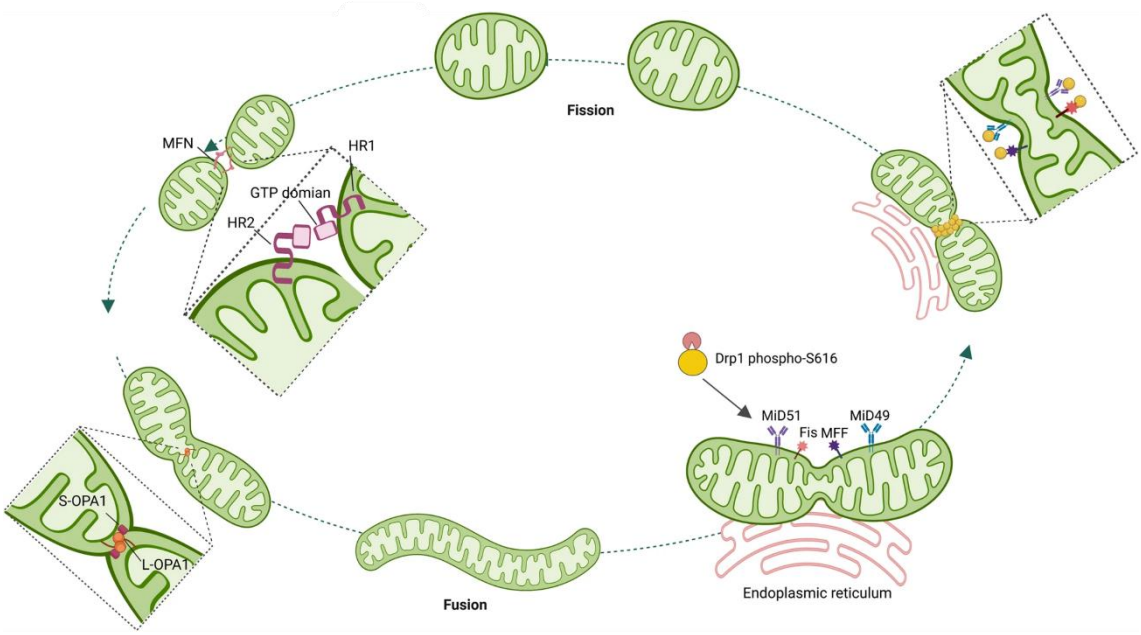

Figura 2. A dinâmica mitocondrial – fusão e a fissão. As principais proteínas envolvidas na fusão mitocondrial são as mitofusinas (MFN) 1 e 2, envolvidas na junção

da membrana externa das mitocôndrias, que posteriormente terão suas membranas internas fusionadas com o auxílio da proteína OPA1. Esse processo forma mitocôndrias mais alongadas. O processo de fissão mitocondrial é mediado pela interação da proteína citosólica Drp1, que é ativada pela fosforilação no resíduo S616, com seus receptores MiD 49 e 51, MFF e Fis, localizados na membrana externa da mitocôndria, e catalisam a cisão da organela em dois fragmentos. Drp1: proteína relacionada à dinamina 1; MFF: fator de fissão mitocondrial; MFN: mitofusina; OPA1: proteína de atrofia ótima 1. Adaptado de (CHEN; ZHAO; LI, 2023) sob licença Creative Commons Attribution 4.0 International.

A DH induz alterações morfológicas mitocondriais no cérebro, sendo notável disformidades nas cristas mitocondriais, acompanhados de elevação na produção de ERO e alteração no potencial de membrana mitocondrial (CHUNCHAI et al., 2018). No hipocampo de camundongos, alterações no balanço da expressão de proteínas de dinâmica mitocondrial, induzidas por DH, direcionados para um perfil pró-fissão, foi relacionado com menores níveis de geração de ATP, e prejuízo de memória espacial, bem como comportamento tipo-depressivo (YANG et al., 2021). Ademais, camundongos alimentados com DH apresentaram mitocôndrias fragmentadas, o que repercutiu em redução da atividade de enzimas antioxidantes e da enzima citocromo oxidase, da CTE (RUEGSEGGER et al., 2019). Esses dados demonstram que alterações na dinâmica mitocondrial hipocampal estão associados à um desbalanço energético e redox das células que compõem o tecido.

O íon Ca^{2+} é um regulador de diversas vias de sinalização, e sua homeostase é fortemente associada à função mitocondrial. A mitocôndria pode captar grandes quantidades de Ca^{2+}, atuando como um reservatório e controlando a quantidade do íon no citosol, e acredita-se que esse transiente de Ca^{2+} está relacionado com o controle da demanda energética pela regulação da produção de ATP (VILAS-BOAS et al., 2023). Vilas-Boas e colaboradores demonstraram que a captação de Ca^{2+} por mitocôndrias hepáticas promove o aumento da respiração oxidativa acoplada à geração de ATP, bem como a depleção dos estoques de Ca^{2+} limita a capacidade respiratória máxima (VILAS-BOAS et al., 2023). No hipocampo, a capacidade de retenção de cálcio está diminuída em um modelo murino de obesidade e resistência insulínica induzida por DH, apresentando também uma perda de memória de curto prazo (PARK; CHO; KIM, 2018). Esses camundongos apresentaram redução na respiração oxidativa e aumento da geração de ERO, além de aumentar a sensibilidade da abertura do poro de transição de

permeabilidade mitocondrial. A disfunção mitocondrial no hipocampo induz ativação da cascata apoptótica, culminando em morte celular (PARK et al., 2018).

A função mitocondrial em células neurais é fundamental para o suporte da maquinaria sináptica, sendo considerada como um fator limitante da sinaptogênese e plasticidade neuronal (LUQUE-CONTRERAS et al., 2014). As células neurais são compostas pelos neurônios e as células da glia, constituídas pelos astrócitos, oligodendrócitos e a microglia (Figura 3). Os neurônios são os responsáveis pela processamento e transmissão das informações elétricas na forma de sinapses; os astrócitos são vitais no controle do fluxo sanguíneo para o parênquima cerebral, nutrição neuronal e potencialização da atividade sináptica (GUILLAMON-VIVANCOS; GOMEZ-PINEDO; MATIAS-GUIU, 2015); os oligodendrócitos são os responsáveis pela formação da bainha de mielina, uma membrana rica em lipídeos que envolvem o axônio, aumentando a velocidade de condução do impulso elétrico (ALLEN; BARRES, 2009).

1.4 Papel da microglia na (dis)função cerebral

As microglias, células imunes residentes do SNC, são vitais para o remodelamento sináptico, manutenção da homeostase de mielina, além de possuir uma quimiotaxia robusta e intensa ação fagocítica e de vigilância constante do SNC. Elas são responsáveis pela eliminação de micróbios, células mortas, sinapses disfuncionais, agregados proteicos e qualquer outro antígeno solúvel que possa deixar o SNC em perigo (HICKMAN et al., 2018; MICHELL-ROBINSON et al., 2015). Ademais, por ser a fonte primária de citocinas no SNC, a microglia possui um papel de destaque na indução e manutenção da neuroinflamação e pode modular diversas respostas celulares (COLONNA; BUTOVSKY, 2017).

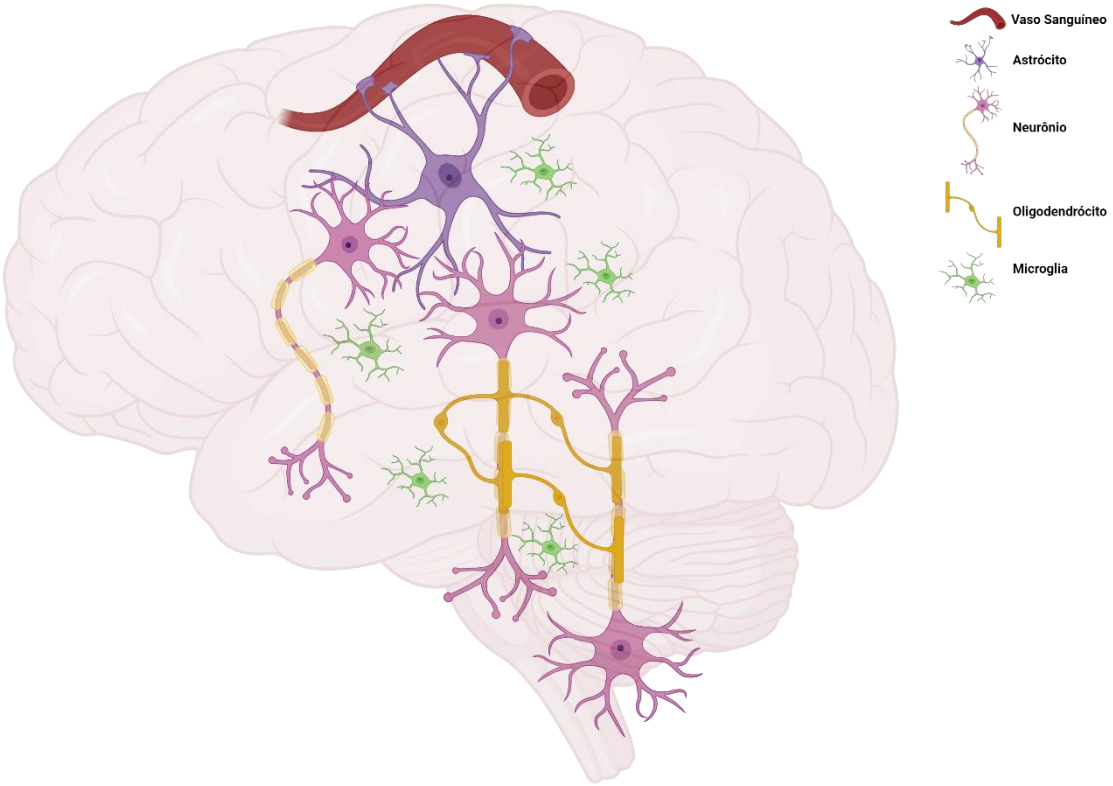

Figura 3. As células neurais. Diferentes tipos de glia interagem com os neurônios e os vasos sanguíneos. Os oligodendrócitos envolvem os axônios para aumentar a velocidade da condução elétrica do potencial de ação. Os astrócitos estendem seus processos fazendo a comunicação com o vaso sanguíneo e os terminais sinápticos. A microglia mantém o parênquima cerebral sob vigilância contra qualquer dano ou infecção. Imagem criada pelo Biorender.com, sob licença número WV27FS1OVL.

A microglia é crucial na saúde neuronal e neurogênese desde o desenvolvimento pré-natal, onde guia neurônios e axônios a formarem os circuitos primários (SQUARZONI; THION; GAREL, 2015), e também no cérebro desenvolvido, controlando a taxa de poda sináptica (PAOLICELLI et al., 2011), além de modular a plasticidade das sinapses através da modulação da liberação de citocinas, espécies reativas de oxigênio, óxido nítrico e fatores neurotróficos (VEZZANI; VIVIANI, 2015). Entretanto, quando o SNC sofre algum estímulo inflamatório ou é afetado por alguma doença, a microglia quiescente, responsável pelas funções favoráveis à integridade sináptica, morfológica e funcionalmente se polariza para um fenótipo responsivo, liberando citocinas inflamatórias e fatores neurotóxicos que comprometem a função sináptica (DAI et al., 2015).

Diversos autores demonstram alterações morfológicas e funcionais da microglia *in vitro* e *in vivo,* ocasionados por estímulos inflamatórios. Estudos em cultura celular demonstram remodelamento microglial frente a estímulos inflamatórios como o lipopolissacarídeo (LPS) (DAI et al., 2015; WANG et al., 2012) e ácidos graxos saturados oriundos de dieta (CHAUSSE et al., 2019; WANG et al., 2012). Os estímulos inflamatórios e dietéticos aumentaram a liberação de proteínas relacionadas à processos inflamatórios, como proteínas do completo de receptores do tipo Toll, TNF-α, IL-1β, IL-6 e favoreceram a translocação do fator nuclear κ B (NFκB) e a indução de apoptose em células BV2 (DAI et al., 2015; WANG et al., 2012). Ademais, as funções mitocondriais também foram comprometidas pelos estímulos inflamatórios, através da indução do metabolismo glicolítico e aumento na produção de ERO (CHAUSSE et al., 2019; WANG et al., 2012)

A microglia oriunda de roedores submetidos à DH reproduz o fenótipo inflamatório observado acima, induzindo maior expressão de genes relacionados à processos inflamatórios como inflamassoma NLRP3 e IL-1β, além de marcadores clássicos de polarização microglial, como o CD11b e o MHCII (BUTLER et al., 2020). Além disso, a microglia inflamatória oriunda de camundongos obesos apresentam uma maior atividade fagocítica de terminais sinápticos (HAO et al., 2016). A fagocitose possui uma implicação importante na degeneração sináptica, e acredita-se que uma poda sináptica hiperativa contribui para a degeneração sináptica e doenças neurodegenerativas (EVANS et al., 2020).

Em roedores, a DH está associada com aumento da polarização da microglia hipotalâmica, voltada para um perfil mais inflamatório (THALER et al., 2012; VALDEARCOS et al., 2017). Thaler e colaboradores também evidenciaram alterações morfológicas em células da glia de pacientes obesos (THALER et al., 2012). No hipocampo, o consumo de DH induziu polarização microglial, acompanhando de perda de neurônios hipocampais e prejuízo cognitivo de memória dependente de funções hipocampais (CHUNCHAI et al., 2018; HAO et al., 2016; JEON et al., 2012). Os efeitos da DH no hipocampo apresentam-se como alterações morfológicas da microglia, com menor número de ramificações, aumento no número de células microgliais e aumento de fagocitose de sinapses (CHUNCHAI et al., 2018; COPE et al., 2018; HAO et al., 2016; JEON et al., 2012). Os efeitos deletérios da ativação microglial no hipocampo sobre o declínio cognitivo e a fagocitose de espinhas dendríticas foram prevenidos pela inibição

farmacológica da ativação microglial por minociclina (COPE et al., 2018). Ademais, a microgliose hipocampal e o dano cognitivo induzido por DH também foi prevenido com o Infliximab, anticorpo monoclonal que neutraliza os efeitos do TNF-α, o que reforça o papel da ativação inflamatória na polarização microglial e sua contribuição para a perda cognitiva (MELO et al., 2020).

1.4.1 Alteração bioenergética da microglia em cenários inflamatórios

A microglia homeostática, que desempenha um papel crucial na vigilância da homeostase tecidual no SNC, depende principalmente da fosforilação oxidativa (OXPHOS) como sua principal fonte de energia. Em contraste, a microglia polarizada para um perfil inflamatório sofre mudanças em sua morfologia e função, caracterizada pela secreção de mediadores inflamatórios e alterações bioenergéticas. Essas alterações incluem o deslocamento metabólico do metabolismo predominantemente oxidativo para um perfil mais glicolítico, essencial para sustentar o estado reativo dessas células (BERNIER; YORK; MACVICAR, 2020; FOLICK; KOLIWAD; VALDEARCOS, 2021; KATOH et al., 2017). No estudo de Nair e colaboradores, o deslocamento metabólico para a glicólise foi acompanhado pela fragmentação de mitocôndrias após estímulo com LPS em cultura primária de micróglia. A fragmentação mitocondrial reforça a hipótese de mitocôndrias menos oxidativas (NAIR et al., 2019). Dados recentes do nosso grupo corroboram esse deslocamento metabólico para um perfil glicolítico, acompanhado de aumento de marcadores clássicos de inflamação, após células BV2 serem estimuladas com LPS (DE PAULA et al., 2024).

A sobrecarga lipídica *in vitro* induzida por palmitato também impacta o metabolismo energético da microglia, embora a literatura sobre o assunto seja escassa e controversa. Enquanto uns autores demonstram uma menor função oxidativa (BUTLER et al., 2023; DE PAULA et al., 2024), outro estudo demonstrou nenhum efeito do palmitato na respiração oxidativa, embora o mesmo tenha aumentado o fluxo glicolítico (CHAUSSE et al., 2019). Essas evidências demonstram que o palmitato altera a fisiologia energética da microglia, e que é necessária uma maior compreensão bioquímica desses eventos. Um resumo dos efeitos da DH e do palmitato na fisiologia da microglia está esquematizado na Figura 4.

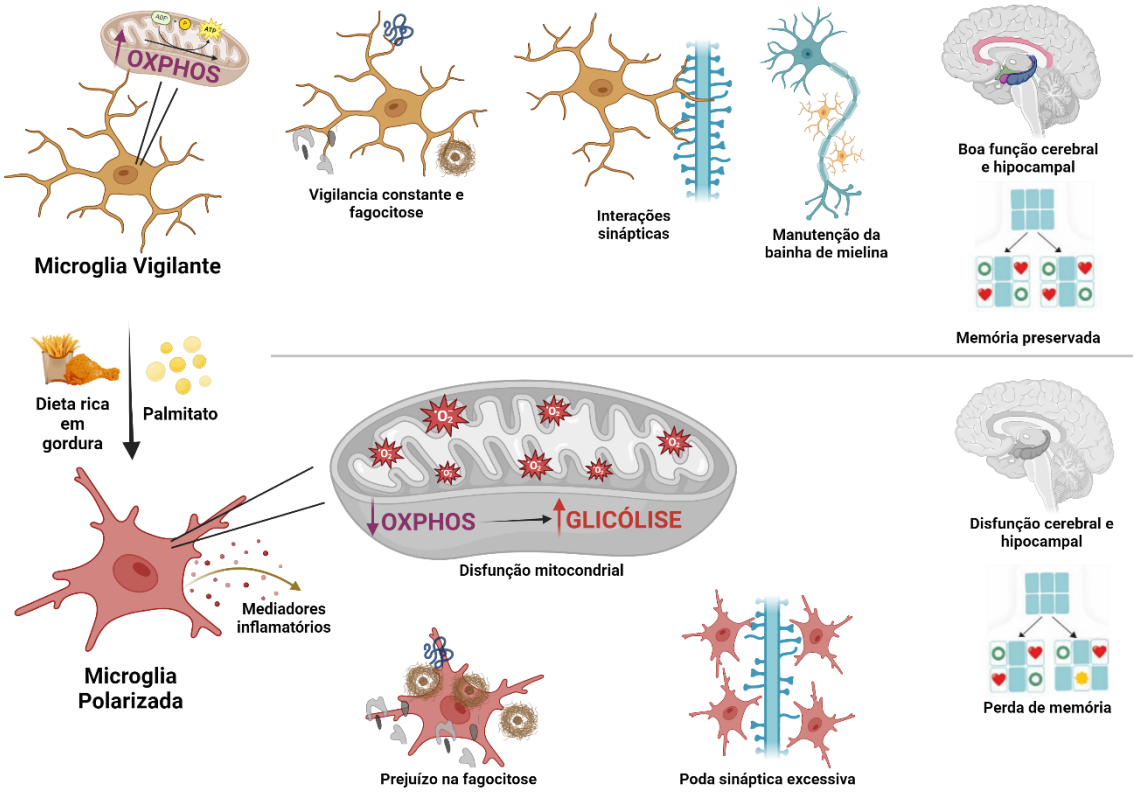

Figura 4. Efeitos da sobrecarga lipídica na fisiologia microglial. Em condições homeostáticas, a microglia demanda um perfil energético altamente oxidativo. Essa alta eficiência energética favorece as funções de vigilância constante do parênquima cerebral, fagocitose de antígenos solúveis e agregados proteicos, além de interagir com os neurônios e oligodendrócitos para otimizar a função sináptica. Esse cenário favorece uma boa função cerebral e hipocampal, e a manutenção de funções cognitivas otimizadas. Entretanto, em cenários de sobrecarga de lipídeos saturados por dieta ou exposição direta aos ácidos graxos saturados, a microglia pode se polarizar para um perfil associado à neurodegeneração, onde é observado a liberação de mediadores inflamatórios e um deslocamento do perfil energético para a glicólise. Essas alterações inflamatórias e metabólicas propiciam uma reduzida ação fagocítica de proteínas disfuncionais e uma maior fagocitose de terminais sinápticos, o que podem comprometer a função sináptica cerebral e associa-se com o prejuízo cognitivo induzido por esse modelo de sobrecarga de lipídeos saturados. Imagem criada pelo Biorender.com, sob licença número UY27FS258D.

1.5 O butirato como estratégia terapêutica às disfunções metabólicas e cerebrais

Propondo uma estratégia terapêutica direcionada à redução das alterações microgliais induzidas por estressores metabólicos, a utilização de ácidos graxos de cadeia curta (AGCC) figura-se como uma alternativa plausível para este fim. Os AGCC são metabólitos das bactérias intestinais, oriundos da fermentação de fibras dietéticas, proteínas e peptídeos que não são digeridos (KOH et al., 2016). As bactérias intestinais são extremamente sensíveis à intervenção dietética, sendo que sua composição e

abundância relativa são altamente variáveis na população. A DH induz disbiose intestinal e redução na plasticidade hipocampal, o que acompanha prejuízo de memória espacial (CHUNCHAI et al., 2018). Na microglia hipocampal, a DH induz proliferação e redução no prolongamento de seus processos. Nesse estudo, as alterações neuronais, micróglias e cognitivas foram prevenidas pela administração de prebióticos (ingredientes alimentares digeridos pelas bactérias intestinais) e probióticos (microorganismos vivos, nesse caso o *Lactobacillus paracasei HII01*) (CHUNCHAI et al., 2018), que aumentaram as concentrações de AGCC (FUSCO et al., 2023). Os prébióticos e probióticos possuem efeitos locais e sistêmicos. Em ratos expostos à DH, a administração de ambos (prebióticos e probióticos), em conjunto ou separadamente, reduziu marcadores inflamatórios no cólon e a adiposidade, e restaurou parâmetros metabólicos de homeostase glicêmica e perfil lipídico à níveis do grupo controle. No cérebro, essa mesma abordagem terapêutica reduziu o estresse oxidativo no hipocampo dos ratos alimentados com DH (CHUNCHAI et al., 2018).

Os AGCC são mediadores a serem considerados na modulação metabólica decorrente do consumo de prebióticos e probióticos, bem como no impacto benéfico a função cerebral. Os três principais AGCC são o acetato, o propionato e o butirato, que possuem cadeias carbônicas de dois, três e quatro carbonos, respectivamente (MARKOWIAK-KOPEC; SLIZEWSKA, 2020). Dentro dos AGCCs, o butirato tem recebido atenção particular por seus efeitos benéficos no metabolismo energético e homeostase intestinal. Embora seja o menos abundante dentre os AGCCs citados (~60% acetato, 25% propionato e 15% butirato, em humanos), o butirato representa a maior fonte energética para os colonócitos, e modula a saúde gastrintestinal atuando como um inibidor da histona deacetilase, além de atuar em diversos receptores específicos acoplados à proteína G (GPCRs) (LIU et al., 2018). Ademais, diversos estudos *in vivo* e *in vitro* demonstram a importante modulação da respotsa imune e inflamatória sistêmica e na barreira intestinal (TAN et al., 2014).

A administração de butirato previniu as alterações metabólicas induzidas pela DH, incluindo ganho de peso, resistência à insulina (HENAGAN et al., 2015), dislipidemias e redução da termogênese (GAO, Z. et al., 2009) em modelos experimentais de obesidade. Melhora em parâmetros mitocondriais do músculo esquelético também foram observada após a administração de butirato, com maior densidade de fibras musculares oxidativas e aumento na expressão de proteínas musculares esqueléticas. Marcadores de biogênese

mitocondrial hepática também foram aumentados com administração de butirato (GAO, Z. et al., 2009).

Os AGCC também impactam a função cerebral. Em estudos *in vivo*, o butirato é importante na manutenção da integridade da barreira hematoencefálica e na função e maturação da microglia (KOH et al., 2016; MISHRA, S. P. et al., 2020), além de atenuar a neuroinflamação em camundongos expostos à DH (CAVALIERE et al., 2022). A função mitocondrial no córtex cerebral também é impactada pelo butirato, pela atenuação do estresse oxidativo e da redução da capacidade de produção de ATP, induzidas pela DH (CAVALIERE et al., 2022). Ademais, Stilling e colaboradores demonstraram que o butirato protege os neurônios dos danos da isquemia, melhora parâmetros cognitivos e atenua a neurodegeneração (STILLING et al., 2016).

Em cultura celular, um mix de acetato e butirato preveniu a inflamação estimulada por LPS em microglia, pela redução da translocação do fator nuclear-κB (CAETANO-SILVA et al., 2023). Ademais, o butirato melhorou parâmetros, em linhagem de neurônios, de disfunção mitocondrial e morte celular, induzidos pela sobrecarga de glicose (CHO et al., 2024). Em altas doses (10 mM), o butirato modulou neurônios Neuro-2a para um perfil mais oxidativo (XU et al., 2021). Esse conjunto de evidências demonstram como o butirato oferece um potencial terapêutico para tratar e prevenir doenças metabólicas e reestabelecer a função mitocondrial e energética central e periférica.

1.6 Particularidades no cultivo celular de microglia

Em cultura celular, uma questão metodológica, que é frequentemente negligenciada, é a concentração de glicose no meio de cultura. Especialmente na microglia, por ser uma célula altamente reativa, a concentração de glicose pode alterar ou favorecer alterações metabólicas induzidas por outro estímulo. Entre as refeições, a concentração de glicose sanguínea em indivíduos saudáveis é de 4-6 mmol/L, sendo que a concentração de glicose no parênquima cerebral é de apenas 1-2 mmol/L (PATCHING, 2017). Em cultura celular, frequentemente usa-se os meios contendo baixa glicose (LG, do inglês *"low glucose"*) que contem 5,5 mmol/L e o meio contendo alta glicose (HG, do inglês *"high glucose"*), contendo 25mmol/L. É de suma importância adequar o meio de cultura às necessidades específicas do tipo de cultivo celular a ser realizado, entretanto, é

fundamental haver um consenso na literatura sobre a concentração de glicose utilizada para cada tipo celular.

Em cultura de uma linhagem de células hepáticas, os autores caracterizaram o cultivo das células em HG como um modelo de glicotoxicidade. Alteração na taxa de apoptose, aumento de ERO e diminuição da atividade fosforilativa mitocondrial, foram observados nestas células em comparação com células cultivadas em meio LG (ALNAHDI; JOHN; RAZA, 2019). Em células BV2, o meio contendo HG, aumenta a proliferação celular e proteínas de inflamação, além de condicionar as células a sofrerem os efeitos do LPS de uma forma mais severa (HSIEH et al., 2019; ZHANG, X. et al., 2015). Em cultura primária de microglia, o cultivo em HG aumenta a proporção de células com morfologia amoebóide, em comparação com células cultivadas em LG. Esse formato menos ramificado é frequentemente associado à um perfil inflamatório e associado à dano tecidual (VUONG et al., 2017). Vale ressaltar que as controvérsias bioenergéticas da microglia exposta ao palmitato, abordadas no tópico 1.4.1 da Revisão Bibliográfica desta tese, podem ter relação com a concentração de glicose no meio de cultura, visto que foi observado um deslocamento de um perfil oxidativo para um glicolítico em células cultivadas em LG (DE PAULA et al., 2024), porém células cultivadas em HG não apresentaram prejuízo bioenergético (CHAUSSE et al., 2019). Esses dados sugerem que as concentrações de glicose no meio podem direcionar a intensidade da resposta ao estímulo aplicado.

Levando em consideração o papel crucial da mitocôndria na manutenção energética e homeostase celular, hipotetizamos que a sobrecarga de lipídeos saturados induz disfunções metabólica, cognitiva e mitocondrial *in vivo*, e alterações na função de células de microglia, *in vitro*. Também avaliamos se o cultivo de células de microglia em HG predispõe estas células a sofrerem efeitos mais expressivos do palmitato e se o AGCC butirato é capaz de prevenir a disfunção metabólica em cultura celular de micróglia.

2. JUSTIFICATIVA

O consumo excessivo de alimentos com alto teor de gordura e açúcar desencadeia sobrepeso e obesidade, problemas de saúde pública com alta prevalência, morbidade e mortalidade, e geralmente estão associados a comorbidades cardiovasculares, câncer e comprometimento cognitivo na idade adulta, bem como o aumento do risco de doenças neurodegenerativas. Essa sobrecarga energética oriunda de ácidos graxos saturados afeta diretamente o metabolismo mitocondrial de diversas células no organismo, sendo que as células do sistema nervoso central, em especial a microglia, respondem extremamente rápido a esse estímulo, promovendo um microambiente inflamatório propício à disfunção neuronal, e consequente alterações cognitivas.

Neste sentido, a compreensão dos eventos mitocondriais decorrentes da sobrecarga lipídica em tecidos e células fundamentais para o bom funcionamento da maquinaria cognitiva, permite desenvolver estratégias farmacológicas a fim de prevenir ou reverter a disfunção celular no sistema nervoso central, que reflete fenotipicamente no declínio cognitivo.

3. OBJETIVOS

3.1 Objetivo geral

Investigar o efeito da sobrecarga de ácidos graxos (AG) saturados sobre as funções metabólicas, mitocondriais e desfechos fenotípicos em modelos experimentais *in vivo* e *in vitro*.

3.2 Objetivos específicos

a) Avaliar o impacto da exposição a DH+L-NAME sobre parâmetros metabólicos e a performance cognitiva em ratos Wistar.

b) Avaliar o impacto da exposição a DH+L-NAME na função e fisiologia mitocondrial no hipocampo e neocórtex de ratos Wistar.

c) Avaliar o impacto do palmitato sobre a viabilidade celular e a transcrição de genes relacionados à atividade microglial, inflamação, metabolismo de lipídeos e glicose em condições experimentais de LG ou HG.

d) Avaliar o impacto do palmitato sobre o perfil bioenergético em cultura de microglia em condições experimentais de LG ou HG.

e) Avaliar o potencial efeito do butirato como uma estratégia para prevenir as possíveis alterações metabólicas induzidas por palmitato em microglias em cultura.

f) Avaliar o efeito do palmitato sobre a área mitocondrial e a fagocitose de sinaptossomas em cultura primária de microglia.

Parte II

4. CAPÍTULO I – A disfunção metabólica induzida por DH+ L-NAME preferencialmente afeta mitocôndrias hipocampais, impactando a memória espacial em ratos

Manuscrito publicado na revista “Journal of Bioenergetics and Biomembranes”, no dia 20 de fevereiro de 2024, intitulado: **Metabolic dysfunction induced by HFD + L-NAME preferentially affects hippocampal mitochondria, impacting spatial memory in rats.**
Disponível em: https://doi.org/10.1007/s10863-024-10005-2

https://doi.org/10.1007/s10863-024-10005-2

RESEARCH

Metabolic dysfunction induced by HFD + L-NAME preferentially affects hippocampal mitochondria, impacting spatial memory in rats

Wembley R. Vilela[1,2,7] · Lisley S. Ramalho[2] · Luiz R. G. Bechara[2] · João V. Cabral-Costa[3] · Julian D. C. Serna[3] · Alicia J. Kowaltowski[3] · Gilberto F. Xavier[4] · Julio C. B. Ferreira[2] · Andreza Fabro de Bem[1,5,6]

Received: 24 August 2023 / Accepted: 31 January 2024

Abstract

High-fat diet-induced metabolic changes are not restricted to the onset of cardiovascular diseases, but also include effects on brain functions related to learning and memory. This study aimed to evaluate mitochondrial markers and function, as well as cognitive function, in a rat model of metabolic dysfunction. Eight-week-old male *Wistar* rats were subjected to either a control diet or a two-hit protocol combining a high fat diet (HFD) with the nitric oxide synthase inhibitor L-NAME in the drinking water. HFD plus L-NAME induced obesity, hypertension, and increased serum cholesterol. These rats exhibited bioenergetic dysfunction in the hippocampus, characterized by decreased oxygen (O_2) consumption related to ATP production, with no changes in H_2O_2 production. Furthermore, OPA1 protein expression was upregulated in the hippocampus of HFD + L-NAME rats, with no alterations in other morphology-related proteins. Consistently, HFD + L-NAME rats showed disruption of performance in the Morris Water Maze Reference Memory test. The neocortex did not exhibit either bioenergetic changes or alterations in H_2O_2 production. Calcium uptake rate and retention capacity in the neocortex of HFD + L-NAME rats were not altered. Our results indicate that hippocampal mitochondrial bioenergetic function is disturbed in rats exposed to a HFD plus L-NAME, thus disrupting spatial learning, whereas neocortical function remains unaffected.

Highlights

- A two-hit protocol using HFD + L-NAME induces metabolic dysfunction in rats.
- Spatial memory is impacted in HFD + L-NAME rats.
- Hippocampal but not neocortex bioenergetics is affected in HFD + L-NAME rats.
- OPA-1 expression is upregulated in the hippocampus of HFD + L-NAME rats.
- Cortical calcium dynamics was not affected by HFD + L-NAME.

Keywords Metabolic dysfunction · Cognition · Mitochondria · Hippocampus · Neocortex · Bioenergetics

Introduction

In recent decades, there has been a significant rise in the prevalence of metabolic diseases such as hypertension, type 2 diabetes mellitus, hypercholesterolemia, and obesity, making them major public health concerns worldwide (Saklayen 2018). One out of three adults are now estimatedto have metabolic syndrome (Hirode and Wong 2020),defined by the co-occurrence of at least three cardiometabolic risk factors (Alberti et al. 2009). This metabolic dysfunction is associated with increased risk of cardiovascular diseases, various types of cancers, and stroke (Alberti et al. 2009; Mottillo et al. 2010). Additionally, emerging evidence suggests a link between metabolic dysfunction and cognitive decline, as well as an increased risk of dementia (Siervo et al. 2014; Livingston et al. 2020; Mellendijk et al. 2015).

Clinical evidence shows the impact of metabolic dysfunction on cognitive function. For instance, a 14-year follow-up study conducted on middle-aged adults revealed that subjects with metabolic dysfunction, particularly those with hypertension and hyperglycemia, exhibited reduced

Published online: 20 February 2024

cognitive performance, as evidenced in tasks assessing word fluency and delayed word recall (Knopman et al.2009). Furthermore, a 31-year follow-up study indicated that cardiovascular risk factors in childhood persist until adulthood and contribute to obesity, hypertension, and elevated total cholesterol, which were associated with poorer performance of episodic memory, associative learning and sustained attention tasks (Hakala et al. 2021).

Several animal models have been employed to replicate metabolic dysfunction in research settings (Bem et al. 2020). Most of them use energy-dense diets alone, such as high fat diet (HFD) (Cavaliere et al. 2019), or high carbohydrate diets (Trevino et al. 2015; Moreno-Fernandez et al. 2018), either alone or in combination with drugs that potentiate metabolic effects, such as streptozotocin (Nath et al. 2017; Vilela et al. 2023) or N-ω-nitro-L-arginine methyl ester (L-NAME) (Cordero-Herrera et al. 2020). Recent preclinical studies provide compelling evidence that metabolic dysfunction critically impairs brain func- tions beyond the cardiovascular system (Vilela et al. 2023; Diaz et al. 2021).

Mitochondria are critically affected by the consumption of energy-dense food (Aoun et al. 2012; Putti et al. 2015). Mitochondrial dysfunction contributes to the pathogen- esis of metabolic disturbances in several tissues (Pinti etal. 2019). Especially in the brain, mitochondria regulate energy-requiring neurotransmission and calcium homeostasis, which are fundamental mechanisms for synaptic activity, learning, and memory (Moreira et al. 2007). Recent studies conducted by our group revealed that mitochondrial bioenergetics in both central and peripheral tissues were adversely affected by HFD in different stages of life, and this metabolic disruption is associated with cognitive impairments (Vilela et al. 2023; Paula et al. 2021). Additionally, Yang and colleagues observed that excessive lipid intake restricts mitochondrial biogenesis and alters the expression of mitochondrial dynamic proteins in the hippocampus of mice (Yang et al. 2021).

Considering the critical role of mitochondrial function in cellular homeostasis, particularly within in the central nervous system (CNS), we hypothesize that impaired mitochondrial function in the CNS may underlie possible cognitive impairments induced by HFD + L-NAME in adult rats.

Methods

Animals and experimental design

A scheme of the complete experiment is presented in Fig. 1a. Eight-week old male Wistar rats were housed in acrylic cages (3–4 rats/cage) under controlled conditions, with temperatures at 23-25ºC, and 12 h light/dark cycle (lights on at 6 a.m.) They had *ad libitum* access to food and water. The rats were organized into two groups and fed with either a standard rodent diet (Ctrl; 70% carbohydrates, 20% protein and 10% fat) or a high-fat diet (HFD; 20% carbohydrates, 20% protein and 60% fat) along sixteen weeks (both from PRAGSOLUÇÕES Biociências®, Jaú, SP, Brazil. See complete nutritional information on table S1). L-NAME (Sigma-Aldrich®) (150 mg/L) was administered to the rats receiving the HFD through their drinking water throughout the whole period of dietary intervention until euthanasia. Body weights were registered at the beginning and end of the experimental protocol. After 12 weeks of treatment, rats were submitted to cholesterol analysis. At 15 weeks of treatment, cognitive function was assessed using the reference memory task in the Morris Water Maze and, in the following week, blood pressure was measured and the rats sacrificed. Visceral white adipose tissue was collected and weighted. The hippocampus and neocortex were collected for mitochondrial respirometry, calcium dynamics and western blotting analysis.

Total cholesterol

Caudal blood was collected and total serum cholesterol levels were measured using commercially available enzymatic-colorimetric kit. Cholesterol esters presented on the sample are hydrolyzed and oxidized, and the products released have maximum absorptivity at 500 nm (LABTEST® comercial kits, Cat #76).

Blood pressure

Blood pressure was determined noninvasively using a computerized tail-cuff system, which measures blood pressure photoeletrically by the ascertainment of the pressure at which the blood flow (interrupted by the cuff) returns to the tail (BP2000, Visitech Systems, Apex, North Carolina, USA). Briefly, the rats were introduced into an acrylic restrainer with a tail-cuff system, above a surface constantly heated at 33ºC. Blood pressure measurements were started by inflation of the tail cuff to more than 200 mm Hg and release of the pressure. The tracings rise sharply when pressure is applied to the system, and falls of gradually during deflation. Systolic blood pressure is taken as the first onset of pulse registered after deflation of pressure, and diastolic blood pressure was considered the last pulse observed before total deflation (Johns et al. 1996).

Morris water maze

Hippocampal-dependent spatial memory was assessed in a Morris Water Maze, as described by Santos and

Colleagues (Santos et al. 2012). The swimming pool was a round, black, fiberglass tank, 200 cm in diameter,50 cm in height, filled to a depth of 25 cm with water(26 °C ± 1) rendered opaque by the addition of milk. A movable circular plastic platform (9 cm in diameter), mounted on a plastic column about 2 cm below the water surface, allowed the subjects to escape from the water.The pool was located in a 3.15 × 4.00 m room with several salient cues hanging on the walls. A video camera posi- tioned approximately 290 cm over the center of the pool was connected to a computer, and the videos obtained were analyzed using AnyMaze®. For descriptive data analysis, the pool was divided into four equal-area quad- rants, which bordered each other along imaginary lines. Each trial involved placing the rat near the border of the pool (in one out of eight starting locations) and allow- ing it to swim until finding the platform. If the rat didnot find the platform within 120 s, it was guided manu-ally to the platform, where it remained for a 10-s period. The platform was located at a single fixed location in the center of the northeast (NE) quadrant (here named target quadrant). Each animal was exposed to four trials per ses- sion (one session per day), each trial having a different starting point, with an inter-trial interval (ITI) of 10 min. Acquisition of the spatial reference memory was assessed by the decrease of latency to find the platform along trials and sessions. The rats were trained for 7 days. On day 8, a Probe Test was carried out by removing the platform and allowing the animals to swim freely for 180 s. The time the animal spent within the target quadrant, the latency to reach and the number of crossings in an area measuring two times the platform area concentric to its location (named counter) were measured to assess retention of the spatial memory.

High-resolution respirometry

Oxygen consumption was evaluated using high-resolution respirometry (HRR) in an Oroboros 2k Oxygraph (Oroboros Instruments, Innsbruck, Austria) at 37ºC. The oxygraph system is a closed chamber, which determine changes in O_2 concentration, and because of that, any variation in the O_2 concentration, is attributed to the samples that consume and use the substrates/drugs added into the experiment, to assess the specific mitochondrial states (Hutter et al. 2006). Rats received ketamine and xylazine i.p. (80:8/mg/kg, respectively) for complete analgesia and were then euthanized by cervical dislocation. The hippocampus was collected immediately after euthanasia and homogenized in 300 µl isolation buffer [IB: 300 mM sucrose, 10 mM Hepes, 2 mM EGTA, 0.1% bovin serum albulmin (BSA)] using a 5 mL glass-glass homogeneizer.

The neocortex was collected and homogenized in 5 mL IB using a 30 mL glass-glass homogenizer. Neocortex homogenates were centrifuged at 600 g. All centrifugations were performed at 4ºC for 10 min. Then, the supernatant was collected and centrifuged at 12,000 g. Finally, the supernatant was discarded, and the pellet was resuspended in 10 mL of IB and centrifuged at 12,000 g. The remaining pellet was resuspended in 500 µL of IB.

The samples (~0.150 mg/mL) were added to a 2 mL cuvette containing reaction buffer (RB: 125 mM sucrose, 65 mM KCl, 2 mM KH_2PO_4, 2 mM $MgCl_2$, 10 mM Hepes, 0.1 mM EGTA, 0,01%BSA). Substrates (all purchased from Sigma-Aldrich) were added sequentially to assess O_2 flux, as it follows: pyruvate (P), malate (M), glutamate (G) and succinate (S) (PMGS, 2.5 mM each, diluted in RB) to assess state 2. State 3 (phosphorylating) was assessed after the addition of 500 µM ADP, and state 4 (leak) after the addition of oligomycin (OMY: 0.1 µg/mL). Maximum respiration was evaluated after the addition of titrated uncoupler carbonyl cyanide 3-chlorophenylhydrazone (CCCP, final concentration 1–3 µM). 0.5 µM rotenone was added to assess Complex-II electron transport system and non-mitochondrial residual respiration was evaluated with Antimycin A (AA: 1 µM).

H_2O_2 release

Mitochondrial H_2O_2 release was measured using 25 µM Amplex Red (Molecular Probes A12222) and 0.5 U/mL horseradish peroxidase (Sigma P8125) system. Amplex Red is oxidized in the presence of extramitochon- drial horseradish peroxidase bound to H_2O_2, generating resorufin, which can be detected using a fluorescence spectrophotometer (λex = 563/λem = 587 nm, F-2500 Hitachi—Hitachi). To estimate H_2O_2 release during State 3 and State 4 respiratory rates, and in uncoupled mitochondria, we added 1 mM ADP, 1 µg/mL oligomycin, and 0.1 µM FCCP, respectively. Calibration was conducted by adding H_2O_2 at known concentrations (A240 = $43.6M^{-1}.cm^{-1}$) to the experimental buffer.

Western blotting

The protein expression was evaluated by Western Blotting, a technique that separates the proteins by molecular weight through gel electrophoresis, detects and identifies samples blotted onto a membrane, by antibody binding of one or more proteins (Gavini and Parameshwaran 2023). Hippocampal samples were subjected to SDS-PAGE in polyacrylamide gels (8–15%, depending on the protein molecular weight). After electrophoresis, proteins were electrotransferred to nitrocellulose membranes. Equal gel loading and transfer efficiency were monitored using

0.1% Ponceau S staining of the blot membrane. Blotted membranes were then blocked (5% powdered milk in 10 mM Tris-HCl pH 7.6, 150 mM NaCl, and 0.1% Tween 20 (TBST) for 1 h at room temperature and incubated overnight at 4 °C with specific antibodies, diluted in 5% bovine serum albumin (BSA) and TBST, against Mfn1 (Santa Cruz Biotechnology, Cat# SC50300, dilution 1:500), Mfn2 (Abcam, Cat# AB56889, dilution 1:1000), OPA1 (Abcam, Cat# AB42364, dilution 1:1000), OMA1 (Proteintech, Cat# 17116-1-AP, dilution 1:1000), YME1L (Proteintech, Cat# 11510-1-AP, dilution 1:1000), pDRP^{S616} (Cell Signaling, Cat# 3455, dilution 1:1000), DRP-1 (Cell Signaling, Cat# D6C7, dilution 1:1000), Fis1 (Enzo Life Scinces, Cat# 210-907-R100, dilution 1:1000), and β-Actin (Sigma-Aldrich, Cat# A5316, dilution 1:1000). Binding of the primary antibody was detected with the use of peroxidase-conjugated secondary antibodies (rabbit, mouse or goat for 100 min at room temperature, dilution 1:10000) and developed using enhanced chemiluminescence detected by autoradiography. Quantification analysis of blots was performed in Image J software (Image J Corporation based on NIH image). The protein contents were quantified by the Bradford method. Samples were normalized to relative changes in housekeeping protein β-Actin, and expressed as the percentage of control.

Calcium dynamics

Isolated brain mitochondria (500 µg) were incubated in 2 mL of experimental buffer (125 mM sucrose, 65 mM KCl, 10 mM Hepes, 2 mM phosphate, 2 mM $MgCl_2$, and 0.2% bovine serum albumin, adjusted to pH 7.2 with KOH),plus 0.1 µM Calcium Green 5 N and either 2.5 mM Pyruvate/Malate (PM) or 1 mM succinate, in the presence of 2 µM rotenone (S + ROT). Calcium Green 5 N is a fluorescence probe that increases its fluorescence emis-sion upon calcium binding, and it was measured with a F4500 Hitachi Fluorimeter (ʎex = 506/ʎem = 532 nm), at 37 °C, under constant stirring. Several additions of 10 µM Ca^{2+} were made, with a 3-minute interval. Each addition causes a spike in signal that decreases gradually due to calcium uptake into the mitochondrial matrix. The Ca^{2+} loads were added until mitochondrial membrane perme- ability transition (mPT) induction, where it collapses the mitochondrial membrane potential and results in release of the accumulated calcium from the matrix, causing a sudden and sustained increase in fluorescence signal. One trace was conducted for each animal (n = 5). The relation- ship between Calcium Green 5 N fluorescence (F) and[Ca^{2+}] concentrations was established using the equation [Ca^{2+}] = K_d.(F-F_{min})/(F_{max}-F). The K_d value was empiri- cally determined as the value at which the change in fluorescence (ΔF) after each calcium addition is equivalent to a 10 µM change in calcium concentration (Δ[Ca^{2+}]). The maximal (F_{max}) and minimal (F_{min}) fluorescence were determined at the end of each trace using 100 µL of 100 mM Ca^{2+} and 100 mM EGTA solutions, respectively. Calcium retention capacity was determined as the total amount of calcium Ca^{2+} taken up by mitochondria until the induction of mPT (nmol Ca^{2+}. mg protein^{-1}). Calcium uptake rates were determined as the slope of the linear portion (nmol Ca^{2+}. mg protein^{-1}. s^{-1}) at the beginning of the first calcium addition (Serna et al. 2020).

Statistical analysis

All data were expressed as mean ± SEM and were ana- lyzed with either SAS or GraphPad Prism 6.0®. Kol- mogorov-Smirnov normality test was performed on all samples. Water-maze latency scores were analysed usinga repeated measures analysis of variance (ANOVA) with Groups as the between, and Days and Trials as the within- subjects factors (SAS Institute, Inc., Cary, NC). Data involving time within each quadrant in the Morris Water Maze, substrates and treatments on calcium homeosta- sis were analyzed using two-way ANOVA followed by Sidak post-hoc test. All other experiments were analyzedby unpaired Student *t-test* for Gaussian distribution and Mann-Whitney test for non-gaussian distribution. Results were considered statistically significant for $p < 0.05$.

Results

HFD + L-NAME induced metabolic dysfunction inadult *Wistar* rats

A HFD associated with L-NAME added in the drinking water for 16 weeks (Fig. 1a) induced metabolic dysfunction in *Wistar* rats, as evidenced by increments in body weight (Fig. 1b), visceral adiposity (Fig. 1c), plasma cholesterol levels (Fig. 1d), and blood pressure, as indicated by systolic (Fig. 1e) and diastolic measurements (Fig. 1f). Adult rats exposed to HFD + L-NAME for 16 weeks exhibited obesity (Fig. 1b, $t_{(14)} = 2.966$, $p = 0.0102$) characterized by increased abdominal fat deposition, as reflected by the visceral mass of white adipose tissue (WAT) (Fig. 1c, $t_{(14)} = 3.280$, $p = 0.0055$). Moreover, the two-hit protocol elevated total cholesterol (Fig. 1d, $t_{(16)} = 2.215$, $p = 0.0416$) and increased peripheral vascular resistance, demonstrated here by elevated systolic (Fig. 1e, $t_{(14)} = 9.715$, $p < 0.0001$) and diastolic blood pressure (Fig. 1f, $t_{(14)} = 12.79$, $p < 0.0001$) compared to controls.

Hippocampal-dependent spatial learning wasimpaired in rats exposed to HFD + L-NAME

To assess hippocampal-dependent cognitive functions, the animals were submitted to the Reference Memory Morris Water Maze test. The rats were exposed daily to the pool with a hidden platform located two centimeters below the water surface, and the time taken to reach the platform from different starting points along the pool's edge was recorded in four trials (the ITI was 10 min). Statistics revealed significant main Group ($F_{1,13} = 9.13$, $p = 0.0098$), Day ($F_{6,78} = 16.37$, $p < 0.0001$) and Trial ($F_{3,39} = 6.79$, $p = 0.0009$) effects, and a significant Day x Trial interaction effect ($F_{18,234} = 1.87$, $p = 0.0189$). As Fig. 2a shows, both HFD + L-NAME rats and Controls improve with repeated training, as revealed by a substantial reduction of the latency scores, both along days and trials, particularly at the initial testing sessions, when the navigation task is being acquired. Even though HFD + L-NAME subjects improve along repetitivetraining, they exhibit a poorer performance as comparedto control subjects, expressed as longer latencies all along testing (Fig. 2a). This result suggests that HFD + L-NAME- induced hippocampal learning impairment, even thoughexistent, was not complete, since these subjects did improve along repetitive training. During the Probe Test, the plat- form was removed from the pool and the subjects' search for the missing platform in its previously presented location reflected their memory for that location. The performance of the HFD + L-NAME rats did not differ significantly from that of the controls. This was evidenced from the lack of significant differences in the time spent within the target quadrant (Fig. 2b, $t_{(13)} = 0.4111$, $p = 0.6877$), the latency to reach the counter (Fig. 2c, $t_{(12)} = 1.341$, $p = 0.2049$) and the number of entries within the counter (Fig. 2d, $t_{(13)} = 0.04191$, $p = 0.9672$). Additionally, a 2-way ANOVA for Probe Test data including the total time spent within each Quadrant as the within-subjects factor and Group as the between-subjects factor, revealed lack of significant main Group effect (Figure S1, $F_{(1,52)} = 2.889 \times 10^{-6}$, $p = 0.9987$) and a significant main Quadrant effect (Figure S1, $F_{(3,52)} = 5.556$, $p = 0.0022$). ANOVA also revealed lack of significant Group x Quadrant interaction effect (Figure S1, $F_{(3,52)} = 1.436$, $p = 0.2428$). Sidak's pos hoc multiple comparisons test revealed that HFD + L-NAME subjects exhibit a preference for the target quadrant (NE, where the platform had been located), over the NW quadrant (Figure S1, $p = 0.0274$).

HFD + L-NAME induces bioenergetic dysfunction specifically in the hippocampus, without affecting the neocortex

Figure 3a shows a representative tracing from the oximetry performed in both groups. HFD + L-NAME rats presented close to significant decrease in both hippocampal oxygen consumption in state 3 (Fig. 3b, $t_{(11)} = 2.158$, $p = 0.0539$)and in maximum respiratory capacity (Fig. 3b, $t_{(11)} = 1.972$,

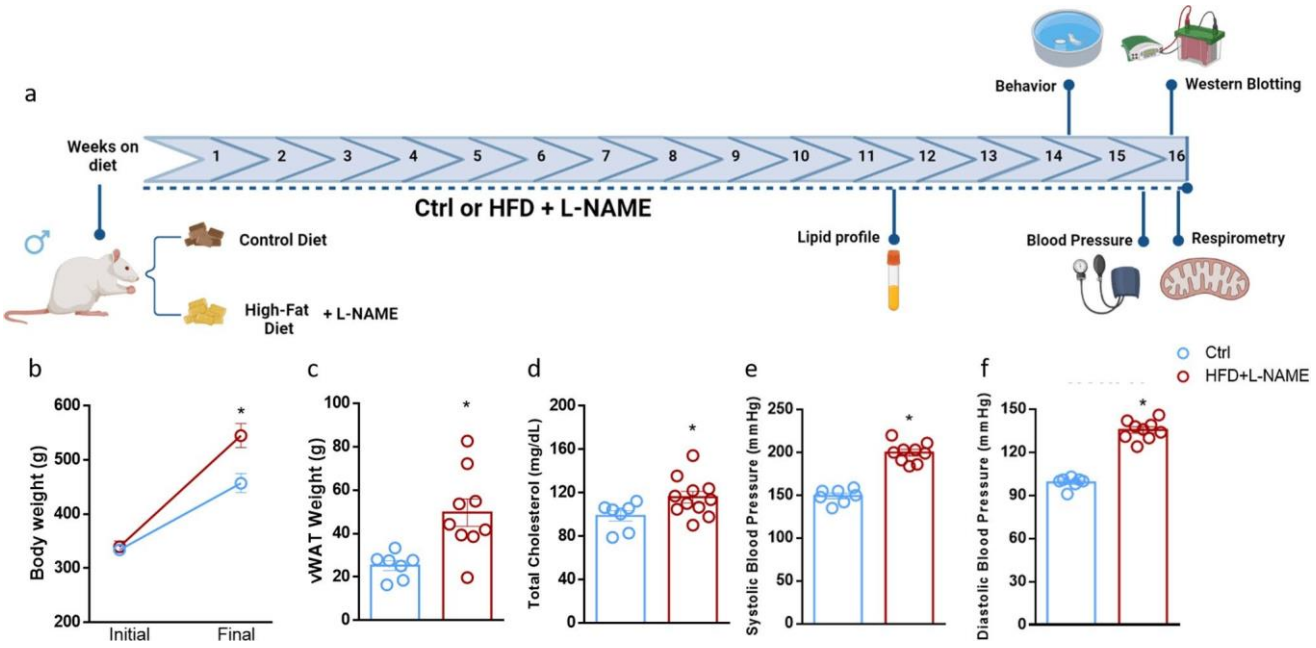

Fig. 1 HFD + L-NAME induces obesity, hypercholesterolemia and hypertension in *Wistar* rats. **a** Experimental design: 8-week-old male *Wistar* rats were fed, for 16 weeks, with either Ctrl diet or HFD + L-NAME (150 mg/L) in drinking water. L-NAME was given throughout the HFD period. Created with BioRender.com. **b** Initial vs. final body weight. **c** Visceral WAT weight. **d** Total cholesterol measured at 12 weeks of treatment. **e** Systolic and **f** diastolic blood pressure measured at 16 weeks of treatment. $N = 7$–11 per group. Data are expressed as mean ± SEM. Statistical analysis made by student´s *t-test*. *$p < 0.05$ vs. Ctrl

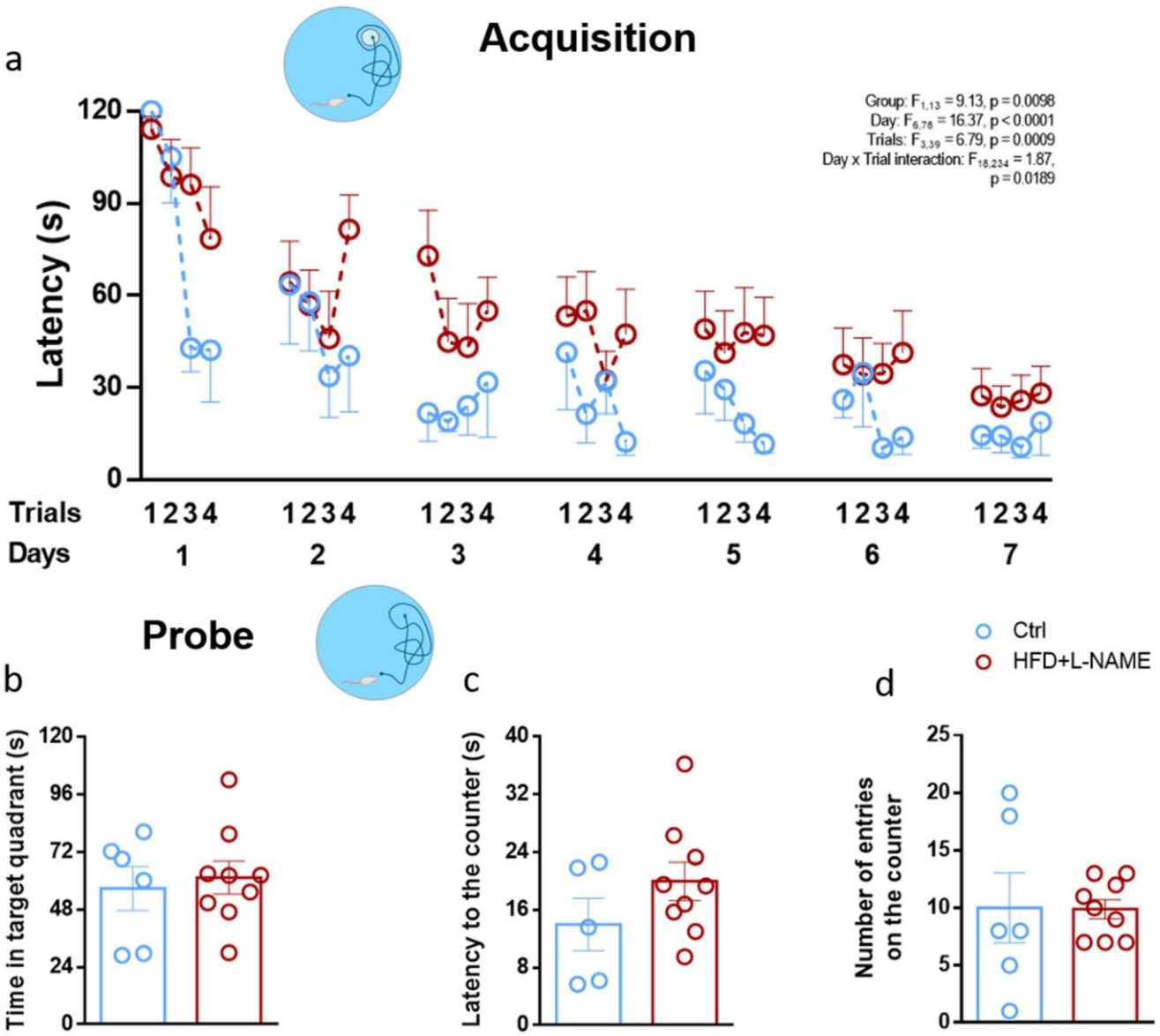

Fig. 2 HFD + L-NAME induces disruption of acquisition of the Reference Memory task in the Morris Water Maze. **a** Average latency scores (per trial) to find the platform over 7 days of acquisition training. Each animal performed 4 trials per day. **b** Time spent within the target quadrant, **c** latency to reach the counter and **d** number of entries on the counter, during the Probe Test (day 8). Images created with BioRender.com. N = 6–9 per group. Data are expressed as mean ± SEM. Statistical analysis involved three way ANOVA (for graph A) and student´s *t-test* (for the other graphs)

p = 0.0743) compared to Ctrl rats. In contrast, there were no significant differences between groups in state 2 (Fig. 3b, $t_{(11)} = 1.008$, $p = 0.3351$) and state 4 (Fig. 3b, $t_{(11)} = 0.8229$, $p = 0.4281$). HFD + L-NAME rats exhibited decreased oxygen consumption related to ATP production (Fig. 3c, $t_{(11)} = 2.261$, $p = 0.0450$) compared to Ctrl rats. Addition-ally, there were no significant differences in H_2O_2 production in hippocampus homogenate in respiratory states 2 (Fig. 3d, $t_{(10)} = 0.9242$, $p = 0.3772$), 3 (Fig. 3d, $t_{(11)} = 1.100$, $p = 0.2947$), 4 (Fig. 3d, $t_{(11)} = 0.1779$, $p = 0.8620$), and uncoupled (Fig. 3d, $t_{(10)} = 0.8285$, $p = 0.4267$).

Furthermore, HFD + L-NAME did not induce bioenergetic changes in isolated mitochondria from cerebral cortex in states 2 (Fig. 4a, $t_{(11)} = 0.6486$, $p = 0.5299$), 3 (Fig. 4a, $t_{(12)} = 0.06436$, $p = 0.9497$), 4 (Fig. 4a, $t_{(12)} = 0.5492$, $p = 0.5930$), or uncoupled (Fig. 4a, $t_{(12)} = 0.3899$, $p = 0.7034$) when compared to the Ctrl group. H_2O_2 production in isolated brain mitochondria was not altered by HFD + L-NAME, as compared to Ctrl rats, in states 2 (Fig. 4b, $t_{(12)} = 1.774$, $p = 0.1014$), 3 (Fig. 4b, $t_{(12)} = 1.077$, $p = 0.3027$), 4 (Fig. 4b, $t_{(12)} = 1.677$, $p = 0.1193$), and uncoupled (Fig. 4b, $t_{(12)} = 1.164$, $p = 0.2671$).

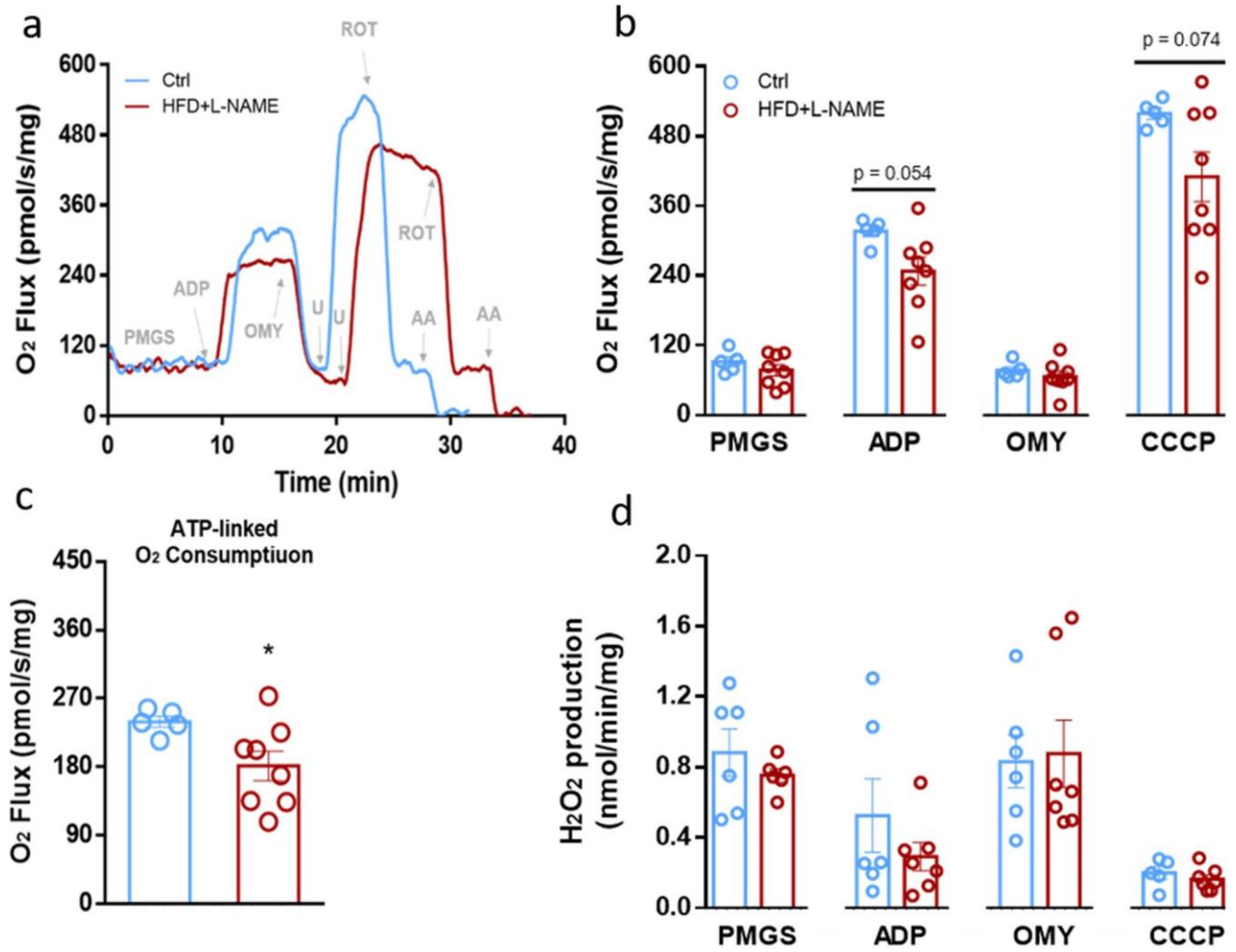

Fig. 3 HFD + L-NAME reduces oxidative phosphorylation in the hippocampus, without altering H_2O_2 production. HRR was performed to evaluate mitochondrial respiratory states: State 2 (PMGS), state 3 (ADP), state 4 (OMY) and state 4 uncoupled (U = CCCP). **a** Representative oxygraph from the experiment. **b** O_2 flux (pmol/s) *per* mg protein in State 2 (PMGS), state 3 (ADP), state 4 (OMY), and state 4 uncoupled (CCCP) respiratory states. **c** ATP-linked O_2 consumption, calculated by the difference between state 3 and state 4. **d** H_2O_2 production in states 2, 3, 4 and uncoupled. $N = 5–8$ per group. Data are expressed as mean ± SEM. Statistical analysis made using Student *t-test*. *$p < 0.05$ vs. Ctrl

Moreover, HFD + L-NAME treatment did not alter brain mitochondrial calcium retention capacity using either complex I (pyruvate/malate) (Fig. 4c, $t_{(16)} = 0.5885$, $p = 0.8103$) or complex II-related (succinate plus rotenone) (Fig. 4c,$t_{(16)} = 0.6949$, $p = 0.7471$) substrates. Only substrate interac- tion was present (Fig. 4c, substrate factor: $F_{(1, 16)} = 8.634$,$p = 0.0096$; treatment factor: $F_{(1, 16)} = 0.8236$, $p = 0.3776$; interaction: $F_{(1, 16)} = 0.00566$, $p = 0.9410$). Additionally, brain calcium uptake rates were not altered using either complex 1 (Fig. 4d, $t_{(16)} = 0.2330$, $p = 0.9671$) or complex II-related (Fig. 4d, $t_{(16)} = 2.028$, $p = 0.1155$) substrates between both groups. Substrate interaction was again significant(Fig. 4d, substrate factor: $F_{(1, 16)} = 72.85$, $p < 0.0001$; treat- ment factor: $F_{(1, 16)} = 2.557$, $p = 0.1294$; interaction: $F_{(1, 16)} = 1.611$, $p = 0.2224$).

OPA1 expression is increased in the hippocampus of HFD + L-NAME rats

Hippocampal mitochondrial morphology-controlling protein was evaluated using western blotting. The expression of OPA1 protein was increased in the hippocampus homogenate of HFD + L-NAME rats compared to controls (Fig. 5c, $t_{(12)} = 2.602$, $p = 0.0231$). Other proteins related to fusion were evaluated, but there were no significant group differences in the expression of Mfn1 (Fig. 5a, $t_{(8)} = 0.6757$, $p = 0.5183$), Mfn2 (Fig. 5b, $t_{(10)} = 0.5854$, $p = 0.5713$), OMA1 (Fig. 5d, $t_{(12)} = 1.148$, $p = 0.2735$) and YME1L (Fig. 5e, $t_{(12)} = 0.5448$, $p = 0.5959$). Proteins related to fission werealso evaluated, and there were no significant group differences in the expression of $pDRP^{s616}$ (Fig. 5f, $t_{(10)} = 1.006$,

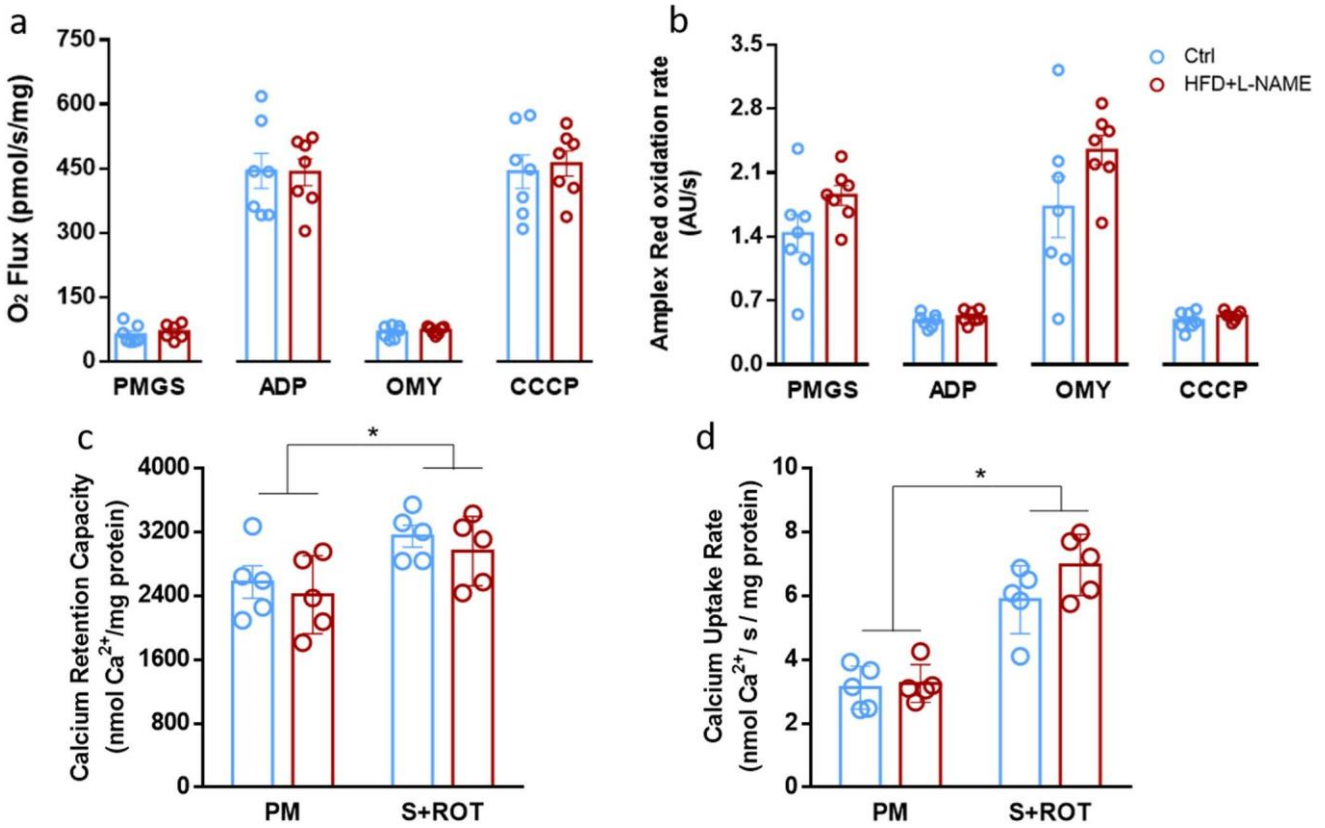

Fig. 4 HFD + L-NAME did not alter brain oxygen consumption, H_2O_2 production or calcium dynamics. **a** O_2 flux (pmol/s) *per* mg protein in State 2 (PMGS), state 3 (ADP), state 4 (OMY) and state 4 uncoupled (CCCP) respiratory states. **b** H_2O_2 estimated through Amplex Red oxidation rate. **c** Calcium retention capacity and **d** uptake rate measured by Calcium green fluorescence, using pyruvate/malate or succinate and rotenone as substrates. $N = 5–7$ per group. All data are expressed as mean ± SEM. Statistical analysis run using Student *t-test (*for graphs **a** and **b**) and two way ANOVA (for graphs **c** and **d**). $^*p < 0.05$

$p = 0.3382$), Drp-1 (Fig. 5g, $t_{(8)} = 1.164$, $p = 0.2778$), and Fis1 (Fig. 5h, $t_{(12)} = 0.5040$, $p = 0.6234$).

Discussion

The present study aimed to characterize the mitochondrial profiles in the hippocampal and neocortex of a rat model of metabolic dysfunction. The intervention with HFD + L-NAME induced metabolic changes including obesity, hypertension, and increased total serum cholesterol. In the brain, HFD + L-NAME led to hippocampal bioenergetic dysfunction, which was associated with impaired acquisition of the Reference Memory version of the Morris' Water Maze task. Our study employed a two- hit protocol combining HFD with L-NAME in the drinking water to accelerate metabolic disturbance, especiallythe increase in peripheral vascular resistance. Similar protocols have been shown to induce metabolic changes such as obesity, insulin resistance, in addition to hepatic steato- sis (Cordero-Herrera et al. 2020) and cardiac dysfunction (Kitakata et al. 2021).

The metabolic alterations observed in our study were accompanied by a disturbance in the acquisition of spatial learning, which were overcome by repetitive training, while retention of the spatial memory remained intact. Memory formation is a complex process involving acquisition (learning), consolidation (physically store memory traces with protein synthesis), and recall (during re-exposure to the learning context) (Quillfeldt 2016). In tasks that require repetitive training, such as the Morris Water Maze, these processes interact with each other, making it difficult to pinpoint the exact timing of memory storage. These processes require synaptic plasticity, whereby receptors and intracellular signaling pathways are involved in orchestrating structural and functional neuronal changes, ultimately inducing and sustaining long-term potentiation (LTP), which is involved in the basis of memory formation (Bliss and Cooke 2011).

The Morris Water Maze test revealed a disturbance in the acquisition phase of Reference Memory in HFD + L-NAME rats. On the other hand, repetitive training allowed these rats to improve their performance and to reach a performance close to that seen in the Ctrl group. Thus, it is not

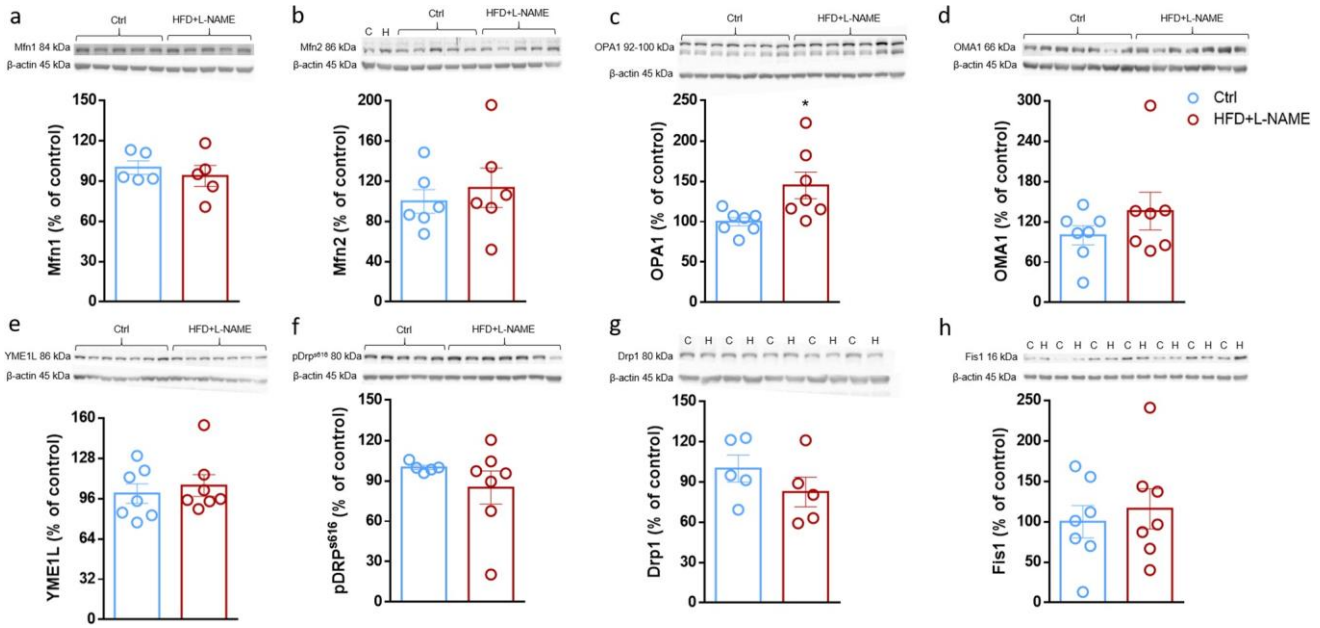

Fig. 5 HFD + L-NAME increases expression of OPA1 in the hippocampus. Mitochondrial fusion (**a-e**) and fission (**f-h**) protein levels in hippocampus homogenates. Representative blot images are included at the top of each figure. C = Control group, H = HFD + L-NAME group. N = 5–7 per group. Data are expressed as mean ± SEM. Statistical analysis made using Student *t-test*. *$p < 0.05$ vs. Ctrl

surprisingly that during the Probe Test (with the platform removed from the pool), HFD + L-NAME rats did not show any impairment in their search for the former platform location. It is important to highlight both that the starting point in the Probe Test was the south cardinal point ("S") of the pool and that the NW and NE (this latter the target) quadrants are equidistant from the starting point and symmetrically opposed to each other. Therefore, comparisons of the time spent within these two quadrants allow to exclude any possible bias related to the starting point (S). In contrast, the southern quadrants (SW and SE) encompass the start- ing point. Even though starting within the southern quad- rants, the times spent within the SW and SE quadrants weresmaller when compared to those seen for the NE quadrant (Figure S1). In addition, the time spent within the NE was significantly greater as compared to that seen in the NW quadrant (Figure S1). These figures reinforce that both groups remember the former plataform location within the NE quadrant.

These findings are consistent with data of other studies that have reported cognitive dysfunctions in diet-induced metabolic dysfunction in rats. For instance, Treviño and colleagues reported that spatial and recognition memory impairments were associated with hippocampal inflammation, oxidative stress (Trevino et al. 2015), reduced dendritic arborization, and diminished synaptophysin (Trevino et al. 2017) in hypercaloric diet-induced metabolic dysfunctional subjects.

Sprague Dawley rats subjected to a two-hit protocol combining a cafeteria diet with a 2-vessel occlusion model exhibited impaired spatial memory which was accompanied by reduced cerebral blood volume, white matter atrophy, and changes in hippocampal cell density (Livingston et al. 2020). Furthermore, hypertensive mice have been shown to exhibit reduced angiogenic proteins, increased TNF-α levels, and reduced capillary density in key regions involved in spatial memory formation (Tarantini et al. 2016).

Mitochondrial dysfunction seems to be a common feature of metabolic deregulation in various conditions such as HFD intake and obesity (Yang et al. 2021), hypertension (Zamorano-Leon et al. 2010), hypercholesterolemia (Yang et al. 2021; Mancini et al. 2021), and hyperglycemia (Vilela et al. 2023). Specifically in the hippocampus, mitochondrial alterations have been reported as a result of metabolic dysfunction, including increased mitochondrial oxidative stress, impaired electron transport chain and ATP production, and elevated autophagy markers (Gao et al. 2019).

Here we observed mitochondrial oxidative phosphorylation dysfunction and a trend towards decreased mitochondrial maximum respiration specifically in the hippocampus of HFD + L-NAME rats, while hippocampal oxidative status remained unchanged. Notably, bioenergetics, oxidative status and calcium homeostasis in neocortex were unaffected. These findings suggest that the hippocampal mitochondrial function may be more susceptible to metabolic stressors compared to neocortical regions.

A previous study reported mitochondrial alterations in the hippocampus and prefrontal cortex of obese mice, evidenced by altered activity of TCA cycle enzymes and decreased activity of respiratory complexes activity. Interestingly, the oxidative status was only downregulated in the hippocampus, remained intact in the prefrontal cortex, which add evidence to our hypothesis that hippocampal mitochondria are more sensitive to metabolic stressors, in this case the HFD (Mello et al. 2019). In contrast, Cavaliere and colleagues reported oxidative stress and impaired mitochondrial oxidative capacity in the brain cortex of high fat diet treated mice (Cavaliere et al. 2019).

Mitochondrial dynamics and the balance between morphology-related proteins can impact on bioenergetic efficiency (Kowaltowski et al. 2019). The lack of mitochondrial integrity, including the inability to clear damaged proteins and fragmented mitochondria, can limit ATP production and directly impact mitochondrial bioenergetics (Yang et al. 2021; Ruegsegger et al. 2019). Here we investigatedthe expression of mitochondrial morphology-related pro- teins in the hippocampus homogenate. Our data showed an increase in the fusion-related protein OPA1 expression in the hippocampus of HFD + L-NAME rats, while the expression of other morphology-controlling proteins remained unchanged.

These results conflict with data of previous studies showing that HFD consumption promotes mitochondrial fission and elevated pDRP1^{s616} levels in the hippocampus (Ruegsegger et al. 2019), as well as decreased ATP production and Mfn 1 and 2 expression levels in the hippocampus, leading to impaired spatial memory in mice (Yang et al. 2021). It is important to mention that we evaluated the changes in morphology-related proteins at a single time point; changes may have occurred earlier during the development of metabolic dysfunction. One can not discard the possibility that compensatory mechanisms occur in hippocampal mitochondria to maintain the homeostatic equilibrium of mitochondria dynamics and function.

Intracellular and intramitochondrial Ca^{2+} are central metabolic regulators that affect the activity of cytosolic and mitochondrial metabolic pathways. Mitochondria have a high capacity to take up Ca^{2+}, making them important calcium buffering organelles (Vercesi et al. 2018). Within mitochondria, Ca^{2+} ions regulate key metabolic pathways that determine ATP synthesis rates (Vilas-Boas et al. 2023). We evaluated calcium homeostasis in the neocortex and found no changes in mitochondrial calcium transport between groups. However, we observed an increase in calcium uptake rates and retention capacity when using substrates of complex-II over complex-I.

Park and colleagues showed diminished hippocampal calcium retention capacity in an obesity/insulin resistance mouse model, while physical exercise improved mitochondrial calcium homeostasis (Park et al. 2018). Interestingly, in isolated heart mitochondria, the rate of calcium entrance into the mitochondria is higher when the mitochondria received complex-II related substrates, indicating that in the presence of ROT + S, mitochondria can buffer calcium faster than when using complex I-driven substrates. This study also showed a 25% decrease in the time required to phosphorylate ADP with complex II-related substrates compared to complex I-related substrates, suggesting that ATP-synthase works faster when complex-II is the primary source of substrate oxidation (Belosludtseva et al. 2021). Furthermore, our high resolution respirometry data suggest that when using ROT + S as substrates, oxygen consumption is higher in the hippocampus, liver and heart compared to pyruvate and malate (Vilela et al. 2023). These data may indicate an increased activity of mitochondrial complex-II over complex-I, which is supported by higher activity of liver complex-II enzymes over complex-I (Flamment et al. 2009).

The present results revealed a co-occurrence of hippocampal mitochondrial dysfunction and a deficit in acquiring a hippocampal-dependent spatial memory task, without lack of observable cortical mitochondrial changes. These findings are consistent with previous research by Pintana and colleagues, who reported impaired spatial and learning memory associated with mitochondrial dysfunction and increased hippocampal ROS production in insulin-resistant rats (Pintana et al. 2013). The same laboratory also reported increased brain oxidative stress, hippocampal synaptic dysfunction and brain mitochondrial dysfunction along with spatial memory impairment in HFD-fed rats (Pratchayasakul et al. 2015). Moreover, Wang and colleagues reported impairments in recognition and spatial memory, reduced hippocampal mitochondrial ATP and membrane potentials, and increased ROS production in HFD-induced obese mice (Wang et al. 2015). The results of our study lend additional support to the notion that the integrity of hippocampalATP production and bioenergetics are essential for neuro- nal function underlying cognitive tasks, particularly spatial learning and memory.

Mitochondrial dysfunction seems to be a key element in metabolic dysfunction-related structural and functional changes in the hippocampus, rendering an environment that is more inflammatory and prone to dysfunctional synapses (Hao et al. 2016; Dutheil et al. 2016). Congruently, Park and colleagues demonstrated that long-term HFD-associated type 2 diabetes caused neuroinflammation and impaired hippocampal mitochondrial homeostasis by increasing mitophagy and reducing the number of synapses, dendritic spines and also the number of presynaptic mitochondria in adult mice (Park et al. 2021). This energy imbalance can

disrupt normal neuronal function and contribute to cognitive impairments.

In conclusion, our study demonstrates that exposure of adult rats to HFD + L-NAME induces metabolic dysfunction and affects hippocampal mitochondrial oxidative phosphorylation efficiency, thereby impacting the acquisition of a hippocampal-dependent spatial memory task. We also reinforce that the hippocampus is particularly sensitive to metabolic stressors, in our case the HFD + L-NAME insult, compared to neocortex, which then reflects on cellular function and disturbs performance of cognitive tasks that required its participation.

Supplementary Information The online version contains supplementary material available at https://doi.org/10.1007/s10863-024-10005-2.

Acknowledgements We gratefully acknowledge Dra. Paula Maria Quaglio Bellozi for the support in graphic design.

Author contributions W.R.V.: Conceptualization, Methodology, Validation, Formal analysis, Investigation, Data curation, Writing - original draft preparation, Visualization. L.S.R.: Conceptualization, Methodology, Validation, Formal analysis, Investigation, Visualization. L.R.G.B.: Conceptualization, Methodology, Validation, Formal analysis, Investigation, Visualization. J.V.C-C.: Investigation, Methodology, Visualization. J.D.C.S.: Investigation, Methodology, Visualization. A.J.K.: Conceptualization, Methodology, Resources, Writing - review & editing, Visualization. G.F.X.: Conceptualization, Methodology, Resources, Data curation, Writing - review & editing, Visualization. J.C.B.F.: Conceptualization, Methodology, Validation, Resources, Supervision, Project administration, Funding acquisition, Visualization. A.F.B.: Conceptualization, Methodology, Validation, Resources, Data curation, Writing - review & editing, Supervision, Project administration, Funding acquisition, Visualization.

Funding This study was supported by the Fundação de Amparo à Pesquisa do Estado de São Paulo (13/07937-8, 20/06970-5); Fundação de Apoio à Pesquisa do Distrito Federal (FAPDF grants: 00193–00000884/2021-89, 00193–0000002348/2022-07); Conselho Nacional de Desenvolvimento Científico e Tecnológico (CNPq grant 424809-2018-4); Coordenação de Aperfeiçoamento de Pessoal de Nível Superior (CAPES/STINT grant 88881.465507/2019-01); and Instituto Nacional de Ciência e Tecnologia e Neuro-ImunoModulação (INCT-NIM grant 485489/2014-1).

Data availability The data that support the findings of this study are available from the first author, W.R.V and the corresponding author, A.F.B., upon reasonable request.

Declarations

Ethical approval The procedures fulfilled the guidelines for animal care from the NIH (National Research Council, 2011) and were approved by the Ethics Committee on the Use of Animals at the University of São Paulo (CEUA/USP No 9236210120).

Competing interests Alicia J. Kowaltowski declare that she is editor of the Journal of Bioenergetics and Biomembranes. The authors declare that they have no known competing financial interests or personal relationships that could have influenced this work.

References

Alberti KG, Eckel RH, Grundy SM, Zimmet PZ, Cleeman JI, Donato KA et al (2009) Harmonizing the metabolic syndrome: a joint interim statement of the International Diabetes Federation Task Force on Epidemiology and Prevention; National Heart, Lung, and Blood Institute; American Heart Association; World Heart Federation; International Atherosclerosis Society; and International Association for the Study of Obesity. Circulation 120(16):1640–1645. https://doi.org/10.1161/CIRCULATIONAHA.109.192644

Aoun M, Feillet-Coudray C, Fouret G, Chabi B, Crouzier D, Ferreri C et al (2012) Rat liver mitochondrial membrane characteristics and mitochondrial functions are more profoundly altered by dietary lipid quantity than by dietary lipid quality: effect of different nutritional lipid patterns. Br J Nutr 107(5):647–659. https://doi.org/10.1017/S000711451100331X

Belosludtseva NV, Kireeva TA, Belosludtsev KN, Khunderyakova NV, Mironova GD (2021) Comparative study of functional changes in Heart Mitochondria in two modes of Epinephrine exposure modeling myocardial Injury in rats. Bull Exp Biol Med 171(6):727–731. https://doi.org/10.1007/s10517-021-05304-2

Bliss TV, Cooke SF (2011) Long-term potentiation and long-term depression: a clinical perspective. Clin (Sao Paulo) 66(Suppl 1):3–17. https://doi.org/10.1590/s1807-59322011001300002

Cavaliere G, Trinchese G, Penna E, Cimmino F, Pirozzi C, Lama A et al (2019) High-Fat Diet induces Neuroinflammation and mitochondrial impairment in mice cerebral cortex and synaptic fraction. Front Cell Neurosci 13:509. https://doi.org/10.3389/fncel.2019.00509

Cordero-Herrera I, Guimaraes DD, Moretti C, Zhuge Z, Han H, McCann Haworth S et al (2020) Head-to-head comparison of inorganic nitrate and metformin in a mouse model of cardiometabolic disease. Nitric Oxide 97:48–56. https://doi.org/10.1016/j.niox.2020.01.013

de Bem AF, Krolow R, Farias HR, de Rezende VL, Gelain DP, Moreira JCF et al (2020) Animal models of metabolic disorders in the study of neurodegenerative diseases: an overview. Front Neurosci 14:604150. https://doi.org/10.3389/fnins.2020.604150

de Mello AH, Schraiber RB, Goldim MPS, Garcez ML, Gomes ML, de Bem Silveira G et al (2019) Omega-3 fatty acids attenuate brain alterations in High-Fat Diet-Induced obesity model. Mol Neurobiol 56(1):513–524. https://doi.org/10.1007/s12035-018-1097-6

de Paula GC, Brunetta HS, Engel DF, Gaspar JM, Velloso LA, Engblom D et al (2021) Hippocampal function is impaired by a short-term High-Fat Diet in mice: increased blood-brain barrier permeability and neuroinflammation as triggering events. Front Neurosci 15:734158. https://doi.org/10.3389/fnins.2021.734158

Diaz A, Munoz-Arenas G, Venegas B, Vazquez-Roque R, Flores G, Guevara J et al (2021) Metforminium Decavanadate (MetfDeca) Treatment ameliorates hippocampal neurodegeneration and Recognition Memory in a metabolic syndrome model. Neurochem Res 46(5):1151–1165. https://doi.org/10.1007/s11064-021-03250-z

Dutheil S, Ota KT, Wohleb ES, Rasmussen K, Duman RS (2016) High-Fat Diet Induced anxiety and Anhedonia: impact on brain homeostasis and inflammation. Neuropsychopharmacology 41(7):1874–1887. https://doi.org/10.1038/npp.2015.357

Flamment M, Gueguen N, Wetterwald C, Simard G, Malthiery Y, Ducluzeau PH (2009) Effects of the cannabinoid CB1 antagonist rimonabant on hepatic mitochondrial function in rats fed a high-

fat diet. Am J Physiol Endocrinol Metab 297(5):E1162–1170. https://doi.org/10.1152/ajpendo.00169.2009

Gao W, Wang W, Zhang J, Deng P, Hu J, Yang J et al (2019) Allicin ameliorates obesity comorbid depressive-like behaviors: involvement of the oxidative stress, mitochondrial function, autophagy, insulin resistance and NOX/Nrf2 imbalance in mice. Metab Brain Dis 34(5):1267–1280. https://doi.org/10.1007/s11011-019-00443-y

Gavini K, Parameshwaran K (2023) Western blot. *StatPearls*. Treasure Island (FL) ineligible companies. Kodeeswaran Parameshwaran declares no relevant financial relationships with ineligible companies, Disclosure

Hakala JO, Pahkala K, Juonala M, Salo P, Kahonen M, Hutri-Kahonen N et al (2021) Cardiovascular Risk factor trajectories since childhood and cognitive performance in midlife: the Cardiovascular Risk in Young finns Study. Circulation 143(20):1949–1961. https://doi.org/10.1161/CIRCULATIONAHA.120.052358

Hao S, Dey A, Yu X, Stranahan AM (2016) Dietary obesity revers- ibly induces synaptic stripping by microglia and impairs hippo- campal plasticity. Brain Behav Immun 51:230–239. https://doi.org/10.1016/j.bbi.2015.08.023

Hirode G, Wong RJ (2020) Trends in the prevalence of metabolic syndrome in the United States, 2011–2016. JAMA 323(24):2526–2528. https://doi.org/10.1001/jama.2020.4501

Hutter E, Unterluggauer H, Garedew A, Jansen-Durr P, Gnaiger E (2006) High-resolution respirometry–a modern tool in aging research. Exp Gerontol 41(1):103–109. https://doi.org/10.1016/j.exger.2005.09.011

Johns C, Gavras I, Handy DE, Salomao A, Gavras H (1996) Models of experimental hypertension in mice. Hypertension 28(6):1064–1069. https://doi.org/10.1161/01.hyp.28.6.1064

Kitakata H, Endo J, Hashimoto S, Mizuno E, Moriyama H, Shirakawa K et al (2021) Imeglimin prevents heart failure with preserved ejection fraction by recovering the impaired unfolded protein response in mice subjected to cardiometabolic stress. Biochem Biophys Res Commun 572:185–190. https://doi.org/10.1016/j.bbrc.2021.07.090

Knopman DS, Mosley TH, Catellier DJ, Coker LH (2009) & Atherosclerosis Risk in Communities Study Brain, M. R. I. S. Fourteen-year longitudinal study of vascular risk factors, APOE genotype, and cognition: the ARIC MRI Study. *Alzheimers Dement*, *5*(3), 207–214, https://doi.org/10.1016/j.jalz.2009.01.027

Kowaltowski AJ, Menezes-Filho SL, Assali EA, Goncalves IG, Cabral-Costa JV, Abreu P et al (2019) Mitochondrial morphology regulates organellar ca(2+) uptake and changes cellular ca(2+) homeostasis. FASEB J 33(12):13176–13188. https://doi.org/10.1096/fj.201901136R

Livingston JM, McDonald MW, Gagnon T, Jeffers MS, Gomez-Smith M, Antonescu S et al (2020) Influence of metabolic syndrome on cerebral perfusion and cognition. Neurobiol Dis 137:104756. https://doi.org/10.1016/j.nbd.2020.104756

Mancini G, Dias C, Lourenco CF, Laranjinha J, de Bem A, Ledo A (2021) A High Fat/Cholesterol Diet recapitulates some Alzheimer's Disease-Like features in mice: focus on hippocampal mitochondrial dysfunction. J Alzheimers Dis 82(4):1619–1633. https://doi.org/10.3233/JAD-210122

Mellendijk L, Wiesmann M, Kiliaan AJ (2015) Impact of Nutrition on cerebral circulation and cognition in the metabolic syndrome. Nutrients 7(11):9416–9439. https://doi.org/10.3390/nu7115477

Moreira PI, Santos MS, Seica R, Oliveira CR (2007) Brain mitochondrial dysfunction as a link between Alzheimer's disease and diabetes. J Neurol Sci 257(1–2):206–214. https://doi.org/10.1016/j.jns.2007.01.017

Moreno-Fernandez S, Garces-Rimon M, Vera G, Astier J, Landrier JF, Miguel M (2018) High Fat/High glucose Diet induces metabolic syndrome in an experimental rat model. Nutrients 10(10). https://doi.org/10.3390/nu10101502

Mottillo S, Filion KB, Genest J, Joseph L, Pilote L, Poirier P et al (2010) The metabolic syndrome and cardiovascular risk a systematic review and meta-analysis. J Am Coll Cardiol 56(14):1113–1132. https://doi.org/10.1016/j.jacc.2010.05.034

Nath S, Ghosh SK, Choudhury Y (2017) A murine model of type 2 diabetes mellitus developed using a combination of high fat diet and multiple low doses of streptozotocin treatment mimics the metabolic characteristics of type 2 diabetes mellitus in humans. J Pharmacol Toxicol Methods 84:20–30. https://doi.org/10.1016/j.vascn.2016.10.007

National Research Council (2011) Guide for the care and use of laboratory animals, 8th edn. The National Academies Press, Washington, DC

Park HS, Cho HS, Kim TW (2018) Physical exercise promotes memory capability by enhancing hippocampal mitochondrial functions and inhibiting apoptosis in obesity-induced insulin resistance by high fat diet. Metab Brain Dis 33(1):283–292. https://doi.org/10.1007/s11011-017-0160-8

Park G, Lee JY, Han HM, An HS, Jin Z, Jeong EA et al (2021) Ablation of dynamin-related protein 1 promotes diabetes-induced synaptic injury in the hippocampus. Cell Death Dis 12(5):445. https://doi.org/10.1038/s41419-021-03723-7

Pintana H, Apaijai N, Chattipakorn N, Chattipakorn SC (2013) DPP-4 inhibitors improve cognition and brain mitochondrial function of insulin-resistant rats. J Endocrinol 218(1):1–11. https://doi.org/10.1530/JOE-12-0521

Pinti MV, Fink GK, Hathaway QA, Durr AJ, Kunovac A, Hollander JM (2019) Mitochondrial dysfunction in type 2 diabetes mellitus: an organ-based analysis. Am J Physiol Endocrinol Metab 316(2):E268–E285. https://doi.org/10.1152/ajpendo.00314.2018

Pratchayasakul W, Sa-Nguanmoo P, Sivasinprasasn S, Pintana H, Tawinvisan R, Sripetchwandee J et al (2015) Obesity accelerates cognitive decline by aggravating mitochondrial dysfunction, insulin resistance and synaptic dysfunction under estrogen-deprived conditions. Horm Behav 72:68–77. https://doi.org/10.1016/j.yhbeh.2015.04.023

Putti R, Migliaccio V, Sica R, Lionetti L (2015) Skeletal Muscle Mitochondrial Bioenergetics and morphology in high Fat Diet Induced obesity and insulin resistance: focus on Dietary Fat source. Front Physiol 6:426. https://doi.org/10.3389/fphys.2015.00426

Quillfeldt JA (2016) Behavioral methods to study learning and memory in rats. *In: Andersen, M, Tufik, S. (eds)* Rodent model as tools in ethical Biomedical Research. *Springer*, *Cham*

Ruegsegger GN, Vanderboom PM, Dasari S, Klaus KA, Kabiraj P, McCarthy CB et al (2019) Exercise and metformin counteract altered mitochondrial function in the insulin-resistant brain. JCI Insight 4(18). https://doi.org/10.1172/jci.insight.130681

Saklayen MG (2018) The global epidemic of the metabolic syndrome. Curr Hypertens Rep 20(2):12. https://doi.org/10.1007/s11906-018-0812-z

Santos TO, Mazucanti CH, Xavier GF, Torrao AS (2012) Early and late neurodegeneration and memory disruption after intracerebroventricular streptozotocin. Physiol Behav 107(3):401–413. https://doi.org/10.1016/j.physbeh.2012.06.019

Serna JDC, Caldeira da Silva CC, Kowaltowski AJ (2020) Functional changes induced by caloric restriction in cardiac and skeletal muscle mitochondria. J Bioenerg Biomembr 52(4):269–277. https://doi.org/10.1007/s10863-020-09838-4

Siervo M, Harrison SL, Jagger C, Robinson L, Stephan BC (2014) Metabolic syndrome and longitudinal changes in cognitive function: a systematic review and meta-analysis. J Alzheimers Dis 41(1):151–161. https://doi.org/10.3233/JAD-132279

Tarantini S, Tucsek Z, Valcarcel-Ares MN, Toth P, Gautam T, Giles CB et al (2016) Circulating IGF-1 deficiency exacerbates hypertension-induced microvascular rarefaction in the mouse hippocampus and retrosplenial cortex: implications for cerebromicrovascular and brain aging. Age (Dordr) 38(4):273–289. https://doi.org/10.1007/s11357-016-9931-0

Trevino S, Aguilar-Alonso P, Flores Hernandez JA, Brambila E, Guevara J, Flores G et al (2015) A high calorie diet causes memory loss, metabolic syndrome and oxidative stress into hippocampus and temporal cortex of rats. Synapse 69(9):421–433. https://doi.org/10.1002/syn.21832

Trevino S, Vazquez-Roque RA, Lopez-Lopez G, Perez-Cruz C, Moran C, Handal-Silva A et al (2017) Metabolic syndrome causes recognition impairments and reduced hippocampal neuronal plasticity in rats. J Chem Neuroanat 82:65–75. https://doi.org/10.1016/j.jchemneu.2017.02.007

Vercesi AE, Castilho RF, Kowaltowski AJ, de Oliveira HCF, de Souza-Pinto NC, Figueira TR et al (2018) Mitochondrial calcium transport and the redox nature of the calcium-induced membrane permeability transition. Free Radic Biol Med 129:1–24. https://doi.org/10.1016/j.freeradbiomed.2018.08.034

Vilas-Boas EA, Cabral-Costa JV, Ramos VM, Caldeira da Silva CC, Kowaltowski AJ (2023) Goldilocks calcium concentra- tions and the regulation of oxidative phosphorylation: too much, too little, or just right. J Biol Chem 299(3):102904. https://doi.org/10.1016/j.jbc.2023.102904

Vilela WR, Bellozi PMQ, Picolo VL, Cavadas BN, Marques KVS, Pereira LTG et al (2023) Early-life metabolic dysfunction impairs cognition and mitochondrial function in mice. J Nutr Biochem 117:109352. https://doi.org/10.1016/j.jnutbio.2023.109352

Wang D, Yan J, Chen J, Wu W, Zhu X, Wang Y (2015) Narin- gin improves neuronal insulin signaling, brain mitochondrial function, and cognitive function in High-Fat Diet-Induced obese mice. Cell Mol Neurobiol 35(7):1061–1071. https://doi.org/10.1007/s10571-015-0201-y

Yang C, Sui G, Li D, Wang L, Zhang S, Lei P et al (2021) Exog- enous IGF-1 alleviates depression-like behavior and hippocampal mitochondrial dysfunction in high-fat diet mice. Physiol Behav 229:113236. https://doi.org/10.1016/j.physbeh.2020.113236

Zamorano-Leon JJ, Modrego J, Mateos-Caceres PJ, Macaya C, Martin-Fernandez B, Miana M et al (2010) A proteomic approach to determine changes in proteins involved in the myocardial metabolism in left ventricles of spontaneously hypertensive rats. Cell Physiol Biochem 25(2–3):347–358. https://doi.org/10.1159/000276567

Authors and Affiliations

Wembley R. Vilela[1,2,7] · Lisley S. Ramalho[2] · Luiz R. G. Bechara[2] · João V. Cabral-Costa[3] · Julian D. C. Serna[3] Alicia J. Kowaltowski[3] · Gilberto F. Xavier[4] · Julio C. B. Ferreira[2] · Andreza Fabro de Bem[1,5,6]

✉ Andreza Fabro de Bem debemandreza@gmail.com; andrezadebem@unb.br

[1] Department of Physiological Sciences, University of Brasilia, Federal District, Brasília, DF 70910-900, Brazil

[2] Department of Anatomy, Institute of Biomedical Sciences, University of São Paulo, São Paulo, SP 05508-000, Brazil

[3] Departamento de Bioquímica, Instituto de Química, Universidade de São Paulo, São Paulo, SP 05508-000, Brazil

[4] Department of Physiology, Biosciences Institute, Universityof São Paulo, São Paulo, SP 05508- 090, Brazil

[5] Brazilian National Institute of Science and Technology on Neuroimmunomodulation, Oswaldo Cruz Foundation, Rio deJaneiro, RJ 21040-360, Brazil

[6] Department of Biomedical and Clinical Sciences, LinköpingUniversity, Linköping 581 85, Sweden

[7] Department of Experimental Medical Science, Faculty ofMedicine, Lund University, Lund 22362, Sweden

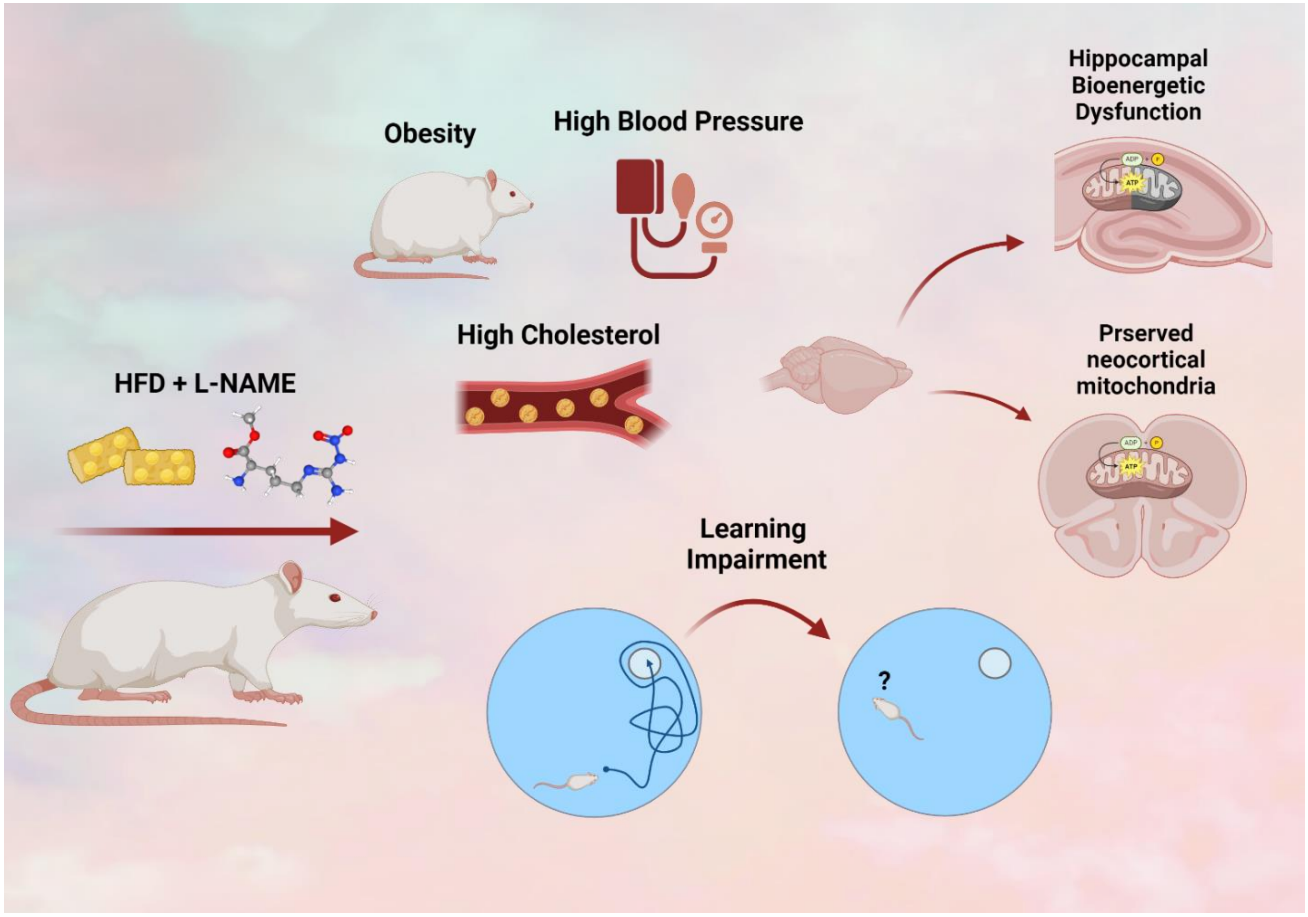

Graphical Abstract. HFD+L-NAME induced metabolic dysfunction and impairment on spatial learning acquisition in Wistar rats. Exposing 8-week-old male Wistar rats to 16 weeks of the 2-hit HFD+L-NAME, induced obesity, hypertension and hypercholesterolemia. These metabolic features were accompanied by impaired acquisition of the spatial version of the Morris Water Maze test, and downregulated hippocampal, but not neocortical mitochondrial bioenergetics. Image created with BioRender.com.

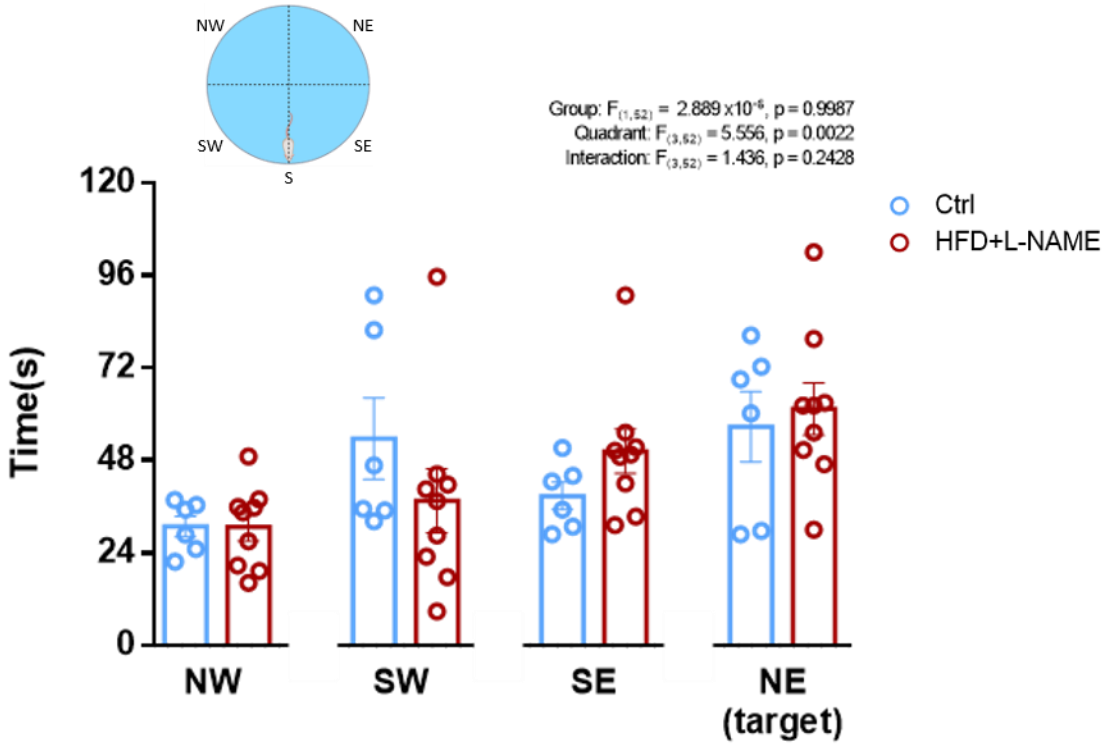

Figure S1. Means ± SEM of the time spent within each quadrant for HFD+L-NAME and Control subjects during the Probe Test in the Morris Water Maze. ANOVA revealed lack of significant Groups differences. Statistics also revealed that the subjects of both Groups spent significantly more time in the target quadrant (NE) as compared to the time spent within the all other quadrants, thus indicating that the subjects do remember the quadrant where the platform had been presented. On the upper left part of the figure, the diagram of the pool that shows the disposition of the NW, NE, SW and SE quadrants and the starting point in the south (S). N = 6-9 per group.

Table S1. Nutrient formulation of the standard (Ctrl) and high fat (HFD) diets.

	Control Diet (Ctrl)		High-fat Diet (HFD)	
Component	Kcal	%kcal	Kcal	%kcal
Starch	1194.4	30.7	0	0
Casein	758.4	19.5	1034	19.72
Dextrinized Starch	204	5.2	646	12.32
Sucrose	1300	33.4	356	6.79
Soy oil	213.3	5.5	290.7	5.54
Vitamin mix AIN-93	38	1	51.6	0.98
L-Cistin	11.36	0.3	15.6	0.3
Lard	171	4.4	2849.4	54.34
Total	3890.5	100	5243.3	100

Caloric amount corresponding to 1kg of food (PRAGSOLUÇÕES Biociências®).

5. CAPÍTULO II –As condições de glicose no meio de cultura ditam a toxicidade do palmitato, inflamação e disfunção metabólica em cultura de microglia

Manuscrito em preparação redigido em língua inglesa, não submetido à nenhuma revista

Glucose media conditions drive palmitate toxicity, inflammation and metabolic dysfunction in microglia

Wembley R. Vilela[1,2,3,4], Gloria Colombo[4], Nicolle Platt dos Santos[3,5], Luiz Roberto Grassmann Bechara[2], Gabriela Cristina de Paula[3,6], Julio Cesar Batista Ferreira[2], Rosa Chiara Paolicelli[4], João M.N. Duarte*[3], Andreza F. de Bem*[1]

[1]Laboratory of Bioenergetics and Metabolism, Physiological Sciences Department, Biology Institute, University of Brasilia, Brasília, DF, Brazil

[2]Laboratory of Integration of Biological Systems, Institute of Biomedical Sciences, University of São Paulo, São Paulo, SP, Brazil

[3]Department of Experimental Medical Science, Faculty of Medicine, Lund University, Lund, Sweden

[4]Department of Biomedical Sciences, Faculty of Biology and Medicine, University of Lausanne, Lausanne, Switzerland

[5]Department of Biochemistry, Center of Biological Sciences, Universidade Federal de Santa Catarina, Florianópolis, SC, Brazil

[6]Institute for Research in Biomedicine, Universitá della Svizzera Italian, Switzerland

*These authors contributed equally

Corresponding authors: Andreza Fabro de Bem (debemandreza@gmail.com; andrezadebem@unb.br), João M. N. Duarte (joao.duarte@med.lu.se)

ABSTRACT

As a brain immune cell, microglia exhibit directed responses to different stimuli, which can vary depending on the environmental conditions they encounter. This study aims to evaluate inflammatory, metabolic and phagocytic responsiveness of microglia to palmitate, a saturated fatty acid, in two distinct culture conditions: low glucose (LG) or high glucose (HG). BV2 cells were cultured in LG or HG concentrations (5.5 and 25mmol/L, respectively), and exposed to palmitate (100 and 200 µmol/L) or vehicle for 24 hours. In HG conditions, palmitate decreased cell viability, which was accompanied by an increase in inflammatory markers associated with a diseased-phenotype. Additionally, palmitate induced higher expression of genes related to lipid metabolism in both LG and HG, without affecting enzymes linked to glucose metabolism. HG condition led to an increase in the oxygen consumption rate (OCR) and glycolytic flux compared to LG-cultured cells, with palmitate reducing OCR and glycolytic flux in both conditions. The short-chain fatty acid butyrate did not prevent palmitate-induced mitochondrial dysfunction in BV2 cells. In primary microglia, palmitate did not affect mitochondria area and cargo metabolism. Our results indicate that BV2 cells are more prone to palmitate stress on viability assays when cultured in HG. In conclusion, our findings demonstrate a significant impact of palmitate on microglial bioenergetics and inflammation, with these effects being more pronounced under HG conditions.

Keywords: microglia, palmitate, glucolipotoxicity, mitochondria, phagocytosis.

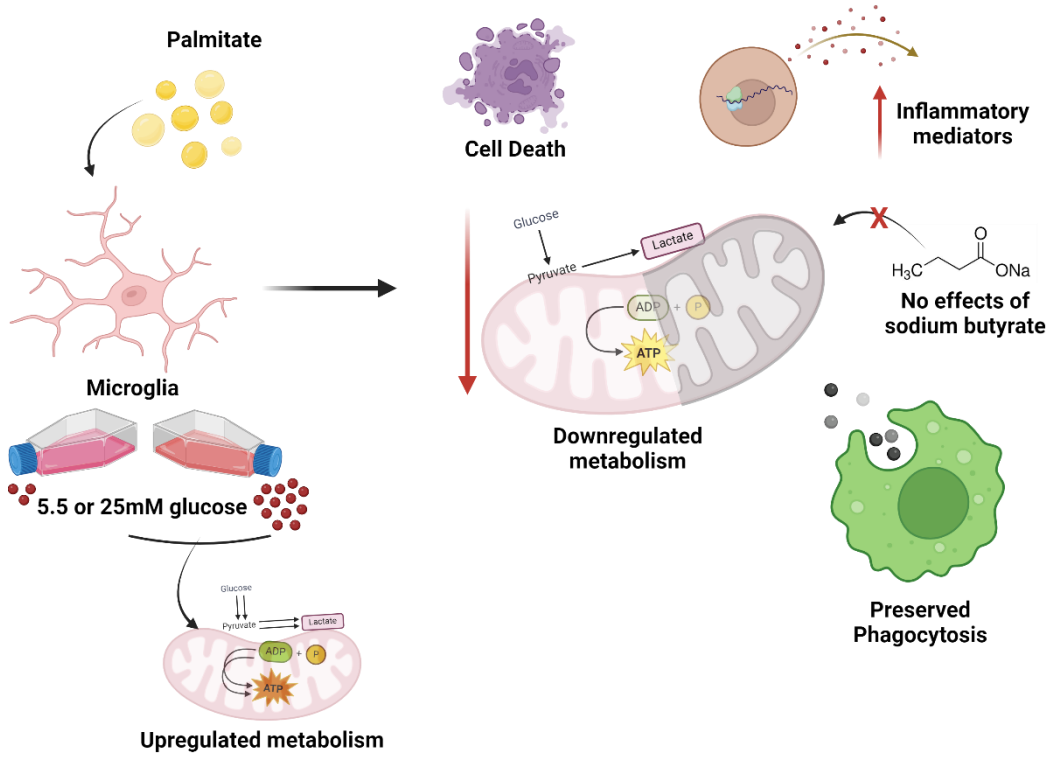

Graphical Abstract. Palmitate effects on microglial cells cultured in low or high glucose. High glucose itself increased metabolic rate in BV2 cells. Palmitate polarized microglia towards a disease-associated phenotype, inducing cell death, upregulating inflammatory mediators and shutting down mitochondria. Cell death effect was more pronounced when cells were cultured in high glucose. Palmitate did not impact phagocytosis of external cargo, and sodium butyrate did not prevent palmitate-changes on bioenergetics. Image created with BioRender.com under the license RP27FS2H3I.

Abbreviation List: AA: antimycin A, ACM: astrocyte conditioned medium, ANOVA: analysis of variance, ATP: adenosine triphosphate, BSA: bovine serum albumin, But: butyrate, CD68: cluster of differentiation 68, CNS: central nervous system, DAGL-β: Diacylglycerol lipase, DMEM: Dulbecco's modified eagle medium, ECAR: extracellular acidification rate, FA: fatty acid, FBS: fetal bovine serum, FCCP: Carbonyl cyanide p-(trifluoromethoxy) phenylhydrazone, GAPDH: glyceraldehyde-3-phosphate dehydrogenase, GC: glycolytic capacity, GPR: G-protein coupled receptor, HBSS: Hank's balanced salt solution, HFD: high-fat diet, HG: high glucose, HK: hexokinase, HSL: hormone sensitive lipase, IL- interleukin, LDH: lactate dehydrogenase, LG: low glucose, LPL: lipoprotein lipase, LPS: lipopolysaccharide, M-MLV: Moloney Murine Leukemia Virus, MTT: 3-(4,5-dimethylthiazol-2-yl)-2,5-diphenyl tetrazolium bromide, NADH: nicotinamide adenine dinucleotide, NF-κB: nuclear factor κB, NGA: non-

glycolytic acidification, NMR: non-mitochondrial respiration, OCR: oxygen consumption rate, OMY: oligomycin, OXPHOS: oxidative phospholarylation, PAL: palmitate, PBS: phosphate buffer saline, PFA: paraformaldehyde, P2X7R: P2X7 receptor, ROT: rotenone, ROS: reactive oxygen species, RS: reactive species, SCFA: Short-chain fatty acid, SFA: saturated fatty acid, TLR4: Toll-like receptor 4, TNF-α: tumor necrosis factor α, 2-DG: 2-Deoxy-D-glucose.

INTRODUCTION

Microglia are highly dynamic immune cells of the central nervous system (CNS), exhibiting robust chemotaxis, phagocytosis, and cytokine production. They play vital role in synaptic remodeling and maintaining brain homeostasis (HICKMAN et al., 2018; MICHELL-ROBINSON et al., 2015). As immune cells, microglia represent the first line of host defense against pathogens, constantly surveilling brain parenchyma and eliminating microbes, dead cells, dysfunctional synapses, protein aggregates, and other soluble antigens that endanger the CNS (PAOLICELLI; ANGIARI, 2019). If harmful stimuli persist, microglia continue responding, which may be detrimental to the CNS, leading to tissue damage through the release of inflammatory cytokines, synapse pruning, altered blood-brain barrier permeability, and myelination dysfunction (DAI et al., 2015; PAOLICELLI et al., 2022). Microglia are crucial for neuronal health and neurogenesis from prenatal development, where they guide neurons and axons to form primary circuits (SQUARZONI; THION; GAREL, 2015) and prevent synaptic loss and engulfment in developed brain (PAOLICELLI et al., 2011).

Lipid ligands play a crucial role in determining microglial function and phenotype, influencing their inflammatory, metabolic, and phagocytic profiles. Biological microglial ligands including lipopolysaccharide (LPS), derived from the cell wall of Gram-negative bacteria, and palmitate, typically act through toll-like receptors (TLR2 and TLR4), leading to a pro-inflammatory response. (CHUNCHAI et al., 2018; NAKAJIMA et al., 2023; WANG et al., 2012). Individuals consuming HFD, which is typically abundant in saturated fatty acids (SFA), exhibit elevated plasma levels of palmitate (ALNAHDI; JOHN; RAZA, 2019; QIU et al., 2022). In rodents, HFD induces microglial morphologic changes and the release of proinflammatory cytokine in both the hypothalamus (THALER et al., 2012; VALDEARCOS et al., 2017) and hippocampus, often accompanied by metabolic dysfunction and cognitive impairment (COPE et al., 2018).

In contrast, short-chain fatty acids (SCFAs), which are produced by gut bacteria through the fermentation of dietary fibers, proteins and peptides, particularly acetate, propionate and butyrate, act as ligands for G-protein coupled receptors (e.g., GPR 43 and GPR 41) and are described as modulators of the microglia inflammatory response (NAKAJIMA et al., 2023; ZHOU et al., 2023). These SCFAs play a role in maintaining BBB integrity and in the maturation and proper functioning of microglia (KOH et al., 2016; MISHRA et al., 2020). Moreover, a combination of acetate and butyrate has been shown to prevent excessive LPS-stimulated inflammation by reducing NF-κB translocation and TNF-α overexpression in primary microglia (CAETANO-SILVA et al., 2023). These interactions underscore the importance of lipid signaling in shaping microglial function and their role in neuroinflammation.

Microglia exhibit metabolic flexibility, enabling then to switch between glycolysis and oxidative metabolism in response to energy demand, allowing adaptation to various metabolic conditions (BERNIER; YORK; MACVICAR, 2020; CHAUSSE et al., 2019; NAIR et al., 2019; VOLOBOUEVA et al., 2013). This metabolic reprogramming is pivotal for regulating key immune functions of microglia, including phagocytosis, chemotaxis, cytokine production, and antigen presentation (LI, Y. et al., 2022). There is evidence that the SFA palmitate mimics the effects of HFD on microglial polarization and inflammatory response (BUTLER et al., 2020). However, the metabolic profile induced by palmitate remains controversial. Butler and colleagues reported an overall decrease in oxidative metabolism induced by palmitate in BV2 cells (BUTLER et al., 2023), whereas Chausse and colleagues found that palmitate increased glycolytic flux without affecting oxidative metabolism in these cells (CHAUSSE et al., 2019). Therefore, understanding palmitate-induced metabolic alterations is crucial, as these metabolic changes may dictate microglia phenotype and function.

In cell culture, a critical yet frequently neglected factor is the glucose concentration in the media. Some studies use low glucose, others high, and many do not specify the glucose amount. Alnahdi and colleagues used high glucose (HG) medium (25mmol/L glucose) as a model of glucotoxicity in a hepatic cell line, observing changes in apoptosis rate, increased reactive species (RS) production, diminished complex IV activity and ATP levels compared to low glucose (LG) medium (5.5 mmol/L glucose) (ALNAHDI et al., 2019). In BV2 cells, HG induces cell proliferation, upregulate stress and inflammatory proteins, and sensitizes cells to LPS inflammatory effects more than LG media (HSIEH et al., 2019). Higher glucose concentrations induce amoeboid cell shape (VUONG et al.,

2017) and increase LPS-induced TNF-α and IL-6 release in primary microglia (ZHANG et al., 2015), suggesting that the glucose concentrations can dictate the intensity of the response to triggers. However, it remains unknown how microglia would bioenergetically handle excess glucose, given the 4.5-fold increase in the energy substrate availability between media conditions.

In this study, we explored the effects of varying glucose concentrations in cell culture media, alongside the presence of palmitate in BV2 cells. Our findings reveal that HG media amplifies the impact of palmitate on cell viability and death. Lipotoxicity had a more pronounced effects on BV2 inflammatory gene expression and mitochondrial function than glucotoxicity, with no influence of palmitate on the phagocytic capacity of primary microglia. Furthermore, butyrate failed to mitigate palmitate-induced changes in oxygen consumption and in glycolytic flux in BV2 cells.

METHODS

BV2 cell culture

BV2 microglial cells (passage range 16-34) were cultured as previously detailed (DE PAULA et al., 2024) in a T75 flask (ThermoFisher Cat #156800) at 37ºC and 5% CO_2 in either low glucose (LG, 5.5 mmol/L) DMEM medium (ThermoFisher Cat# 11885084, Gibco), or high glucose (HG, 25 mmol/L) DMEM medium (Sigma-Aldrich Cat #D2902, supplemented with 3.5g/L glucose (Sigma-Aldrich Cat #G7528)). Both media contained 0.1 g/L sodium pyruvate and 0.584 g/L L-glutamine. 3.7g/L of sodium bicarbonate was added to HG media and pH was adjusted to 7.56 and sterile filtered. Both media were supplemented with 50 IU/ml penicillin/streptomycin (ThermoFisher Cat #15070063, Gibco) and 10% heat-inactivated fetal bovine serum (FBS, ThermoFisher, Cat# 10500064, Gibco).

Palmitate and butyrate treatments

The day after seeding BV2 cells, the culture medium was replaced by a treatment medium (DMEM low or high glucose without FBS, for at least 4h before treatment). Cells were then incubated with sodium palmitate (Sigma-Aldrich Cat# P9767) conjugated with fatty acid-free bovine serum albumin (BSA, Sigma-Aldrich, Cat #A3803). Palmitate-BSA complexes were prepared as described elsewhere (CHAUSSE et al., 2019). Briefly,

palmitate was dissolved in water to produce a 10 mmol/L solution and heated to 65ºC until the solution was totally clear. BSA was dissolved in water to produce a 10% (w/v)solution at 37°C. Palmitate-BSA conjugation was performed by adding proportionally 500 µL of lipid stock solution to each 2.5 ml of BSA stock solution every 5 min at 37ºC. After four fatty acid additions, the volume was completed with 500 µL of water to achieve a final stock solution of 4 mmol/L palmitate/0.757 mmol/L BSA. Conjugation produced a fatty acid:BSA ratio of approximately 5:1. BSA solutions were used as vehicle. Both solutions were filtered (0.22 µm) and stored at -20°C until use. Cells were treated with palmitate (100 or 200 µmol/L) or vehicle for 24 hours. As vehicle, we tested BSA concentrations of 9.46, 18.92 or 37.85 µmol/L.

For real time metabolic analysis, Sodium Butyrate (Sigma-Aldrich Cat #303410 was diluted in PBS to make a 10 mmol/L solution, and cells were treated with a 200 µmol/L concentration for 24 hours, concomitantly with 200 µmol/L pamitate.

Primary microglia culture

Primary microglial cells were obtained as previously described (MONSORNO et al., 2023). Mice pups at P3-5 were euthanized by decapitation and the brain was immediately collected and put into a 3mL ice-cold Hank's balanced salt solution (HBSS). Olfactory bulb and cerebellum were removed and the meninges were peeled off, with the aid of a magnifying glass, under the hood, in cold HBSS. The brains were transferred to a 3 mL TrypLE Express enzyme solution (Life Technologies, Cat # 12-604-021), grossly smashed and incubated for 20 min at 37º C. After 10 min of incubation, the tissues were mechanically homogeneized with the pipette, and incubated again to reach the required 20-min of incubation. Moreover, 10 mL DMEM HG, supplemented with 10% FBS and 50 IU/ml penicillin/streptomycin , was added into the homogenate, and cells were pelleted at 400 g for 4 min. The pellet was ressuspended in fresh culture medium and plate in T75 cell culture flask, and maintained at 37º C and 5% CO_2. The culture media was fully replaced to a new one after 48 h of plating, and then replaced 50% every two days, to keep maintaining the growth factors secreted by the glia. After about 2 weeks, microglia were harvested by detachment from the underlying astrocyte layer by tapping and smacking the flask. Cells were pelleted at 350 g for 5 min, and the remaining supernatant was used as astrocyte conditioned medium (ACM). The cells were ressuspended in ACM and seeded in poly-D-lysine-coated plates at $8x10^3$ seeding density. ACM was replaced 2

days after seeding, and two days further, the cells were treated with palmitate (100 or 200 μmol/L) or vehicle (18.92 or 37.85 μmol/L, respectively) for 24h in HG culture media.

Cell viability

For viability tests, cells were seeded in 96-well plates cultured ($7.5x10^3$ cells/well). After treatment, cells were incubated with 1 mg/mL 3-(4,5-dimethylthiazol-2-yl)-2,5-diphenyl tetrazolium bromide (MTT; ThermoFisher Cat #M6494) for 1.5 h. Following, the solution was removed and 100 μL dimethyl sulfoxide was added to solubilize the purple-colored formazan crystals. This color change was detected at 600 nm and served as surrogate of cell viability.

Cell death was detected by measuring the release of lactate dehydrogenase (LDH) into the culture medium. LDH activity was determined in both the medium and cell lysate after addition of 0.3%(v/v) Triton in PBS. A 150 μL mix containing Tris-HCL (0.2 mol/L, pH 7.3), 1.4 mmol/L sodium pyruvate and 308 μmol/L NADH was mixed with 50 μL of supernatant or with 10 μL of cell lysate plus 40 μL of MiliQ water. Oxidation of NADH was detected through the decrease in absorbance at 340 nm for 10 min at 25 °C. LDH release from cells was expressed as activity in supernatant*100 / (activity in supernatant + whole lysate).

Real time qPCR

BV2 cells were plated into 6-well plates ($4x10^4$ cells/well), and treated as described above. After, RNA was extracted with TRIzol according to the manufacturers' instructions (Thermofisher #15596026). RNA was quantified by spectrophotometry at 260 nm (Nanodrop). 500 ng of RNA was reverse transcribed with M-MLV qScriptXLT cDNA SuperMix (Quantabio, Cat #95161-500) and relative expression levels of target genes (Table 1) were measured by real-time qPCR, using PerfeCTa SYBR Green FastMix (Quantabio, Cat #95074-012). GAPDH and the ribosomal protein L14 were used as housekeeping genes.

Table 1. Nucleotide sequence of primers used for real-time PCR.

Primer target	Forward	Reverse
CD68	GGCGGTGGAATACAATGTGTCC	AGCAGGTCAAGGTGAACAGCTG
IL-1β	GAAGAGCCCATCCTCTGTGA	TTCATCTCGGAGCCTGA
HSL	GGCTCACAGTTACCATCTCACC	GAGTACCTTGCTGTCCTGTCC
DAGL-β	AGCGACGACTTGGTGTTCC	GCTGAGCAAGACTCCACCG
L14	GGCTTTAGTGGATGGACCCT	ATTGATATCCGCCTTCTCCC
LPL	AGGTGGACATCGGAGAACTG	TTTGTCCAGTGTCAGCCAGA
GAPDH	CTCCACTCACGGCAAATTCAAC	ACTCCACGACATACTCAGCAC
P2X7R	GAACACGGATGAGTCCTTCGTC	CAGTGCCGAAAACCAGGATGTC
IL-6	TCTGAAGGACTCTGGCTTTG	GATGGATGCTACCAAACTGGA
IL-10	ATGGTGTCCTTTCAATTGCTC	AGGATCTCCCTGGTTTCTCTT
HK1/2	TATCGGTCCAGCACGTATGC	AGAACCGTCTACGCCAACTG
Glycogen Synthase	GAGAACGCAGTGCTTTTCGA	TCATCCCCTGTCACCTTCG
TNF-α	TTGACCTCAGCGCTGAGTTG	CCTGTAGCCCACGTCGTAGC

Real time metabolic analysis

BV2 oxygen consumption rate (OCR) and extracellular acidification rate (ECAR) were measured using Seahorse XFe96 analyzer (Agilent Technologies, Santa Clara, CA, USA). $7.5x10^3$ cells were plated into 96-well seahorse plates (Agilent, Cat # 103794-100) in a total volume of 100 µl of DMEM LG or HG, supplemented with FBS. On the same day, after cell adherence, the media was replaced by ones without FBS. The next day, cells were treated with palmitate (100 or 200 µmol/L) or vehicle (18.92 or 37.85 µmol/L, respectively) for 24 h. The cartridge hydration was conducted according to manufacturers' instructions. After the treatment, cell culture media was replaced by the XF assay media (Agilent, Cat # 103575-100) supplemented with 10 mmol/L glucose (Agilent, Cat # 103577-100), 2mM L-glutamine (Agilent, Cat # 103579-100) and

1mmol/L pyruvate (Agilent, Cat # 103578-100), sterile filtered and pH adjusted to 7.4. After equipment calibration, the cells underwent to the Mito Stress test kit to measure oxygen consumption and acidification rate (Agilent, Cat # 103015-100). For OCR measurements, first it was measured baseline respiration, and were added, to a final well concentration, 1.5 μmol/L oligomycin (OMY) to determine ATP-linked and proton leak-driven respiration, 0.5 μmol/L Carbonyl cyanide p-(trifluoromethoxy) phenylhydrazone (FCCP), to induce maximal respiratory capacity, and 0.5 μmol/L rotenone/antimycin (ROT/AA) to determine non-mitochondrial respiration (NMR). For ECAR measurements, the baseline was considered as glycolysis rate, since the cells are in the XF assay media supplemented with 10 mmol/L glucose, and after 1.5 μmol/L OMY, it was considered maximum glycolytic capacity (GC). The glycolytic reserve was considered as the difference between GC and glycolysis. 50 mmol/L 2-Deoxy-D-glucose (2-DG) was added at the end of the protocol to assess non-glycolytic acidification (NGA). OCR and ECAR measures were performed within the same plate. In another batch of cells, OCR and ECAR were measured in the same conditions described above, yet, co-treating cells exposed to 200 μmol/L palmitate with 200 μmol/L butyrate for 24h. Protein quantification of the plate was determined by BCA method to normalize the data.

Mitochondrial staining

Primary microglial cells were plated into 96 well plates ($8x10^3$ cells/well). After treatment, cell culture media was replaced by fresh medium containing MitoTracker red at a 1:200 dilution, and incubated for 15 mins. After washing with culture medium, live images were acquired on a Leica Stellaris 5 Confocal microscope. Quantification of total stained MitoTracker area in the cell, reported as percentage, was done on ImageJ software.

Synaptosome uptake and degradation

Primary microglial cells were plated into 2 independent 96 well plates ($8x10^3$ cells/well). After treatment, culture media was replaced by fresh medium containing 6 μg/well of synaptosomes isolated from brains of $CamKII^{cre/+}$; $Rosa26\text{-}TdTomato^{Flox/+}$ mice as previously described (PEDICONE et al., 2022). After 1 hour of synaptosome

exposure, both plates were washed three times with PBS. One plate was fixed with paraformaldehyde 4% (PFA) to determine synaptosome uptake. The other plate returned to the incubator for 6 additional hours before fixing with PFA to determine synaptosome degradation. Cells were imaged on a Leica Stellaris 5 Confocal microscope, and quantification of total TdTomato stained area over total cell area, reported as a percentage, was done on ImageJ software.

Statistical analysis

All data were expressed as mean ± SEM and were analyzed with GraphPad Prism 9.0 (RRID:SCR_002798). ROUT test for identification of extreme values, was applied on the results, and when extreme values were identified, they were removed before analysis. Kolmogorov-Smirnov (KS) normality test was used, and transformation into logarithm function was applied when the data did not reach normality criteria in KS test. Three-way analysis of variance (ANOVA) was used on real time metabolic analysis experiments when butyrate was tested, containing media (low or high), palmitate and butyrate as independent variables, and interaction between the variables were also expressed. One-way ANOVA was used on experiments with primary microglial cells. The other experiments were analyzed with Two-way ANOVA containing media (low or high glucose) and treatment (palmitate) as independent variables, and interaction between both factors were also expressed. Following significant ANOVAs, multiple comparisons were performed using Tukey pos-hoc test. Results were considered statistically significant for $p < 0.05$.

RESULTS

Palmitate promotes cell death and decreases viability in HG-cultured BV2 cells

First, we tested the palmitate toxicity on BV2 cells, evaluating cell death and viability. It was not observed any effect of glucose concentration on cell viability and cell death. Two-way ANOVA revealed significant effects on LDH release in both treatment and media factors (Figure 1A, Treatment Factor: $F_{(2, 40)} = 13.49$, $p < 0.0001$; Media Factor: $F_{(1, 40)} = 18.92$, $p < 0.0001$; Interaction: $F_{(2, 40)} = 7.545$, $p = 0.0017$). *Pos hoc* analysis showed a significant effect of palmitate 200 μmol/L in cells cultured in HG, in

comparison with ones cultured in LG exposed to palmitate 200 µmol/L ($p < 0.0001$), and in HG vehicle and palmitate 100 µmol/L ($p = 0.0002$ and $p < 0.0001$, respectively). On MTT assay, Two-way ANOVA shows a main effect of the palmitate treatment impacting cell viability, with no effect of glucose media concentration (Figure 1B, Treatment Factor: $F_{(2, 36)} = 4.315$, $p = 0.0209$; Media Factor: $F_{(1, 36)} = 0.009$, $p = 0.9219$; Interaction: $F_{(2, 36)} = 1.434$, $p = 0.2517$).

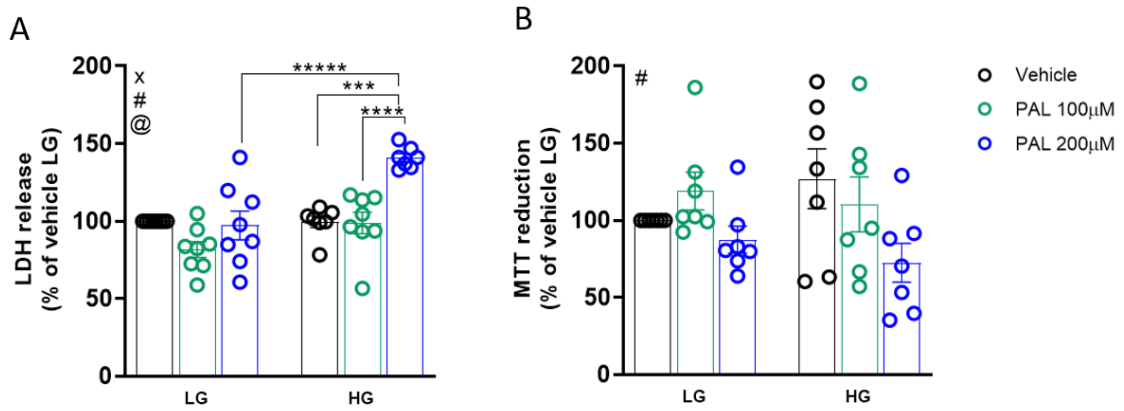

Figure 1. BV2 cells cultured in high glucose medium are more prone to palmitate-induced cell death. (A) LDH release and (B) MTT reduction in BV2 cells treated for 24h with palmitate and cultivated in low glucose (LG, 5.5 mmol/L) or high glucose (HG, 25 mmol/L). Statistical analysis was made by Two-way ANOVA, n = 7/group. ***p<0.001, ****p<0.0001. ANOVA table results: # = Treatment factor, @ = media factor, x = interaction between both factors.

Effect of palmitate on inflammatory and microglial markers in BV2 cells

Next, we evaluated the effect of palmitate on low or high-glucose medium on the expression of genes related to microglial markers and pro-inflammatory cytokines. The cluster of differentiation 68 (CD68) is commonly used as a marker of phagocytic microglia (WALKER; LUE, 2015), and the purinergic receptor P2X7 (P2X7R) has been postulated as a marker of microglial activation and proliferation (MONIF et al., 2009). It was not observed any effect of medium glucose concentration on microglial markers. Two-way ANOVA revealed significant palmitate effect on microglial marker CD68 (Figure 2A, Treatment Factor: $F_{(2, 39)} = 14.44$, $p < 0.0001$; Media Factor: $F_{(1, 39)} = 0.00028$, $p = 0.9867$; Interaction: $F_{(2, 39)} = 1.127$, $p = 0.3345$). *Pos hoc* analysis shows that palmitate increased CD68 expression regardless of medium glucose concentration. This increase was shown on BV2 cells cultured in LG, exposed to 100 µmol/L palmitate, compared to its respective vehicle (Figure 2A, $p = 0.0162$), and in cells cultured in HG in both

palmitate concentrations compared to the respective vehicle (Figure 2A, p = 0.0076 for 100 µmol/L palmitate, and p = 0.005 for 200 µmol/L palmitate). The purinergic receptor P2X7 was not altered by either palmitate or glucose medium conditions (Figure 2B, Treatment Factor: $F_{(2, 39)}$ = 0.5657, p = 0.5726; Media Factor: $F_{(1, 39)}$ = 2.22, p = 0.1443; Interaction: $F_{(2, 39)}$ = 1.24, p = 0.3006).

Inflammatory genes were also evaluated, and we found significant media and palmitate effect on Il-1β expression (Figure 2C, Treatment Factor: $F_{(2, 36)}$ = 6.045, p = 0.0055; Media Factor: $F_{(1, 36)}$ = 7.298, p = 0.0105; Interaction: $F_{(2, 36)}$ =1.711 , p = 0.1951), without changes on IL-6 (Figure 2D, Treatment Factor: $F_{(2, 39)}$ = 2.81, p = 0.0725; Media Factor: $F_{(1, 39)}$ = 1.185, p = 0.2829; Interaction: $F_{(2, 39)}$ = 0.8984, p = 0.4155) and TNF-α expression (Figure 2E, Treatment Factor: $F_{(2, 39)}$ = 1.857, p = 0.1697; Media Factor: $F_{(1, 39)}$ = 0.7797, p = 0.3826; Interaction: $F_{(2, 39)}$ = 0.5362, p = 0.5892). The anti-inflammatory IL-10 gene was also overexpressed due to palmitate treatment (Figure 2F, Treatment Factor: $F_{(2,38)}$ = 15.43, p < 0.0001; Media Factor: $F_{(1, 38)}$ = 0.7563, p = 0.39; Interaction: $F_{(2, 38)}$ = 0.2615, p = 0.7713).

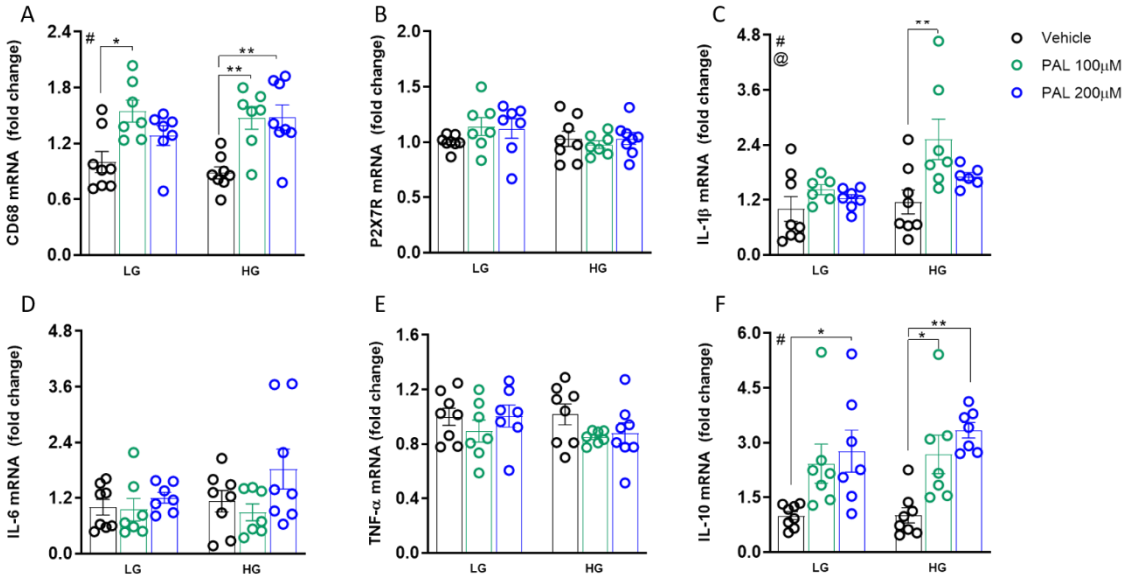

Figure 2. Effect of palmitate on inflammatory and microglial markers in BV2 cells cultured in low or high glucose. mRNA expression of microglial proteins (A) CD68, (B) P2X7R, and the cytokines (C) IL-1β, (D) IL-6, (E) TNF-α and (F) IL-10 in BV2 cells cultured in low (LG, 5.5 mmol/L) or high glucose (HG, 25 mmol/L) medium exposed to palmitate or vehicle. Statistical analysis was made by Two-way ANOVA. n = 7-8 / group. *p< 0.05, **p<0.01. ANOVA table results: # = Treatment factor, @ = media factor.

Palmitate increases lipid metabolism-related genes in BV2 cells

Palmitate exposure increased lipases mRNA expression in BV2 cells. HSL-1 was significantly overexpressed in both palmitate conditions (100 and 200 μmol/L), regardless of glucose media concentration (Figure 3A, Treatment Factor: $F_{(2, 39)} = 37.46$, $p < 0.0001$; Media Factor: $F_{(1, 39)} = 2.58$, $p = 0.1163$; Interaction: $F_{(2, 39)} = 0.6628$, $p = 0.5211$). *Pos hoc* analysis shows that palmitate increased HSL-1 expression, regardless of its concentration and the glucose concentration on cell culture media (Figure 3A, $p < 0.0001$ for palmitate 100 and 200 μmol/L cultured in LG, $p < 0.0001$ for palmitate 100 μmol/L cultured in HG and $p = 0.0008$ for palmitate 200 μmol/L cultured in HG). Palmitate and media effects were also observed on LPL gene expression (Figure 3B, Treatment Factor: $F_{(2, 39)} = 3.239$, $p = 0.05$; Media Factor: $F_{(1, 39)} = 7.784$, $p = 0.0081$; Interaction: $F_{(2, 39)} = 1.055$, $p = 0.3579$). DAGL-β expression was unchanged by either palmitate treatment or differences on medium glucose concentration (Figure 3C, Treatment Factor: $F_{(2, 39)} = 1.788$, $p = 0.1807$; Media Factor: $F_{(1, 39)} = 2.882$, $p = 0.0975$; Interaction: $F_{(2, 39)} = 0.593$, $p = 0.5576$).

Moreover, gene expression of HK-1/2 and Glycogen Synthase, enzymes related to glucose metabolism, were not altered due to glucose medium conditions or palmitate exposure (Figure 3D, Treatment Factor: $F_{(2, 39)} = 0.2268$, $p = 0.7981$; Media Factor: $F_{(1, 39)} = 2.243$, $p = 0.1423$; Interaction: $F_{(2, 39)} = 1.076$, $p = 0.3508$ and Figure 3E, Treatment Factor: $F_{(2, 38)} = 2.833$, $p = 0.0713$; Media Factor: $F_{(1, 38)} = 2.894$, $p = 0.0971$; Interaction: $F_{(2, 38)} = 0.7167$, $p = 0.4984$), respectively.

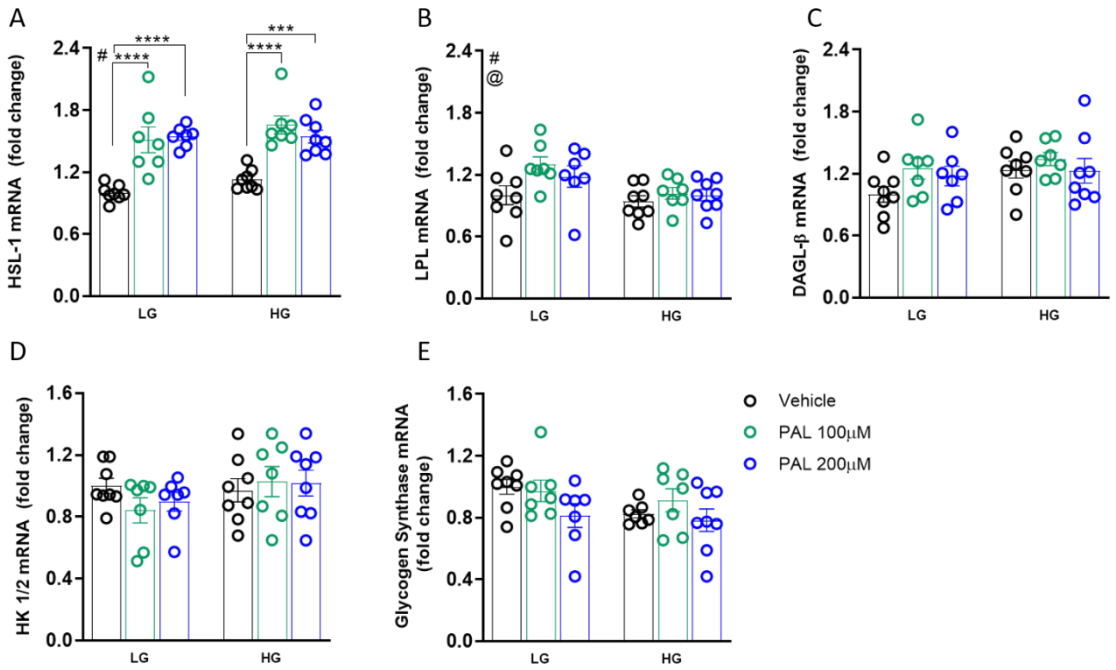

Figure 3. Palmitate increased lipase gene expression. mRNA expression of lipases (A) HSL, (B) LPL and (C) DAGL-β and glucose metabolism-related enzymes (D) Hexokinase 1/2 and (E) Glycogen Synthase in BV2 cells cultured in low (LG, 5.5 mmol/L) or high glucose (HG, 25 mmol/L) medium exposed to palmitate or vehicle. Statistical analysis was made by Two-way ANOVA. n = 7-8 / group. ***p<0.001, ****p<0.0001. ANOVA table results: # = Treatment factor, @ = media factor.

Palmitate impacts microglial oxidative phosphorylation

The availability of glucose in the medium and the palmitate exposure significantly affected the cellular metabolism of BV2 cells. Figure 4A presents a representative trace obtained by measuring real-time oxygen consumption using Seahorse XFe96. Baseline respiration of the cells was higher when BV2 cells were cultured in high glucose media, while palmitate, regardless of its concentration, downregulated the OCR in both low or high glucose conditions (Figure 4B, Treatment Factor: $F_{(3, 39)} = 4.049$, $p = 0.0134$; Media Factor: $F_{(1, 39)} = 5.254$, $p = 0.0274$; Interaction: $F_{(3, 39)} = 0.292$, $p = 0.8303$). Proton leak driven OCR was also decreased with palmitate exposure (Figure 4C, Treatment Factor: $F_{(3, 39)} = 4.535$, $p = 0.008$; Media Factor: $F_{(1, 39)} = 3.254$, $p = 0.079$; Interaction: $F_{(3, 39)} = 0.57$, $p = 0.6375$). Two-way ANOVA showed the effect of glucose medium condition and palmitate on ATP-linked respiration. The data indicated that the effect of high glucose condition increased ATP-linked OCR, while both palmitate concentrations decreased ATP-linked respiration, regardless of glucose medium condition (Figure 4D, Treatment Factor: $F_{(3, 39)} = 3.481$, $p = 0.0248$; Media Factor: $F_{(1, 39)} = 5.448$, $p = 0.0248$; Interaction:

$F_{(3\ ,39)}$ = 0.207, p = 0.8912). Maximum respiration was affected only by palmitate, showing decreased raw rates of oxygen consumption (Figure 4E, Treatment Factor: $F_{(3, 39)}$ = 3.166, p = 0.035; Media Factor: $F_{(1, 39)}$ = 1.054, p = 0.3109; Interaction: $F_{(3, 39)}$ = 0.2621, p = 0.8523). The respiratory reserve capacity was unaffected by either glucose in the media or palmitate exposure (Figure 4F, Treatment Factor: $F_{(3, 39)}$ = 2.222, p = 0.1008; Media Factor: $F_{(1, 39)}$ = 0.113, p = 0.7386; Interaction: $F_{(3, 39)}$ = 0.4077, p = 0.7483).

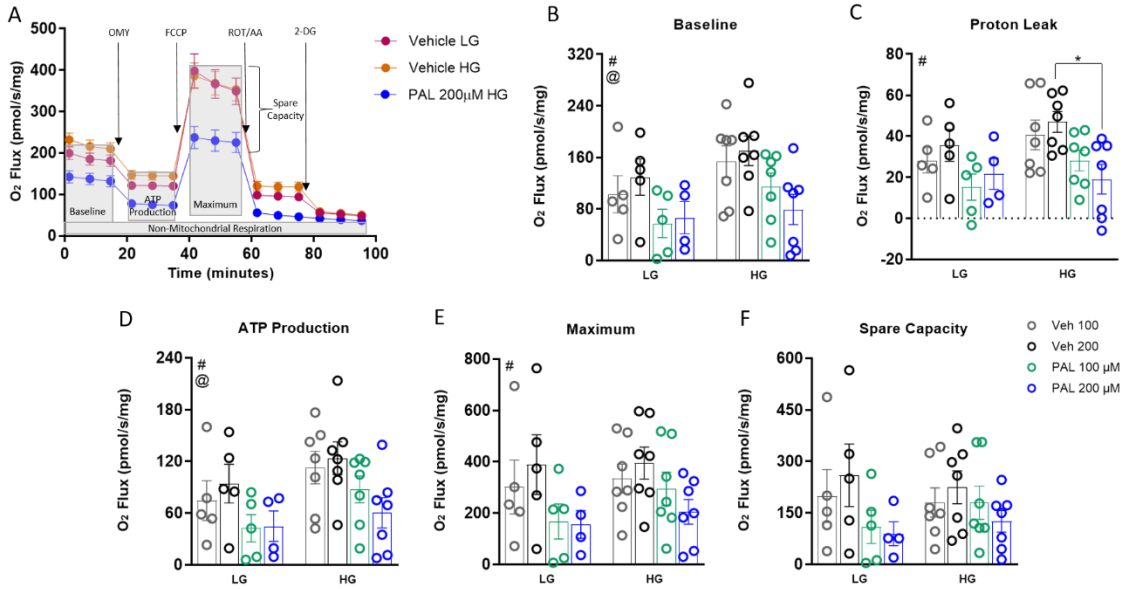

Figure 4. Palmitate exposure decreased oxidative phosphorylation in BV2 cells. (A) Real-time OCR was recorded after 24 h incubation of BV2 in low (LG, 5.5 mmol/L) or high glucose (HG, 25 mmol/L) medium exposed to palmitate (PAL) or vehicle (Veh). Mitochondrial respiratory states calculated as: (B) Baseline respiration (Baseline - NMR), (C) Proton leak (OMY - NMR), (D) ATP-linked respiration (Baseline - proton leak), (E) Maximum respiration (FCCP – NMR), and (F) Spare capacity (Maximum – Baseline). Statistical analysis was made by Two-way ANOVA. n = 5-7 / group. OMY: oligomycin; FCCP: carbonyl cyanide-p-trifluoromethoxy-phenylhydrazone; Rot: rotenone; AA: antimycin A; 2-DG: 2-Deoxy-D-glucose; OCR: oxygen consumption rate. *p<0.05. ANOVA table results: # = Treatment factor, @ = media factor.

Palmitate impacts microglial glycolytic flux

To assess adaptations in glycolytic flow, we measured ECAR in the same conditions that underwent OCR measurements, using MitoStress kit. Two-way ANOVA revealed the effect of HG medium condition in increasing baseline extracellular acidification, while palmitate, regardless of concentration, decreased ECAR in both LG and HG medium conditions (Figure 5B, Treatment Factor: $F_{(3, 39)}$ = 6.639, p = 0.001; Media Factor: $F_{(1, 39)}$ = 5.071, p = 0.003; Interaction: $F_{(3, 39)}$ = 0.5677, p = 0.6396). The

maximum glycolytic capacity, measured after ATP-synthase blockage by oligomycin, was decreased by palmitate exposure, regardless of medium conditions (Figure 5C, Treatment Factor: $F_{(3, 39)} = 9.621$, $p < 0.0001$; Media Factor: $F_{(1, 39)} = 3.147$, $p = 0.0839$; Interaction: $F_{(3, 39)} = 0.3779$, $p = 0.7694$). Glycolytic reserve also was diminished by palmitate exposure in BV2 cells (Figure 5D, Treatment Factor: $F_{(3, 39)} = 5.658$, $p = 0.0026$; Media Factor: $F_{(1, 39)} = 0.2216$, $p = 0.6404$; Interaction: $F_{(3, 39)} = 0.075$, $p = 0.9731$).

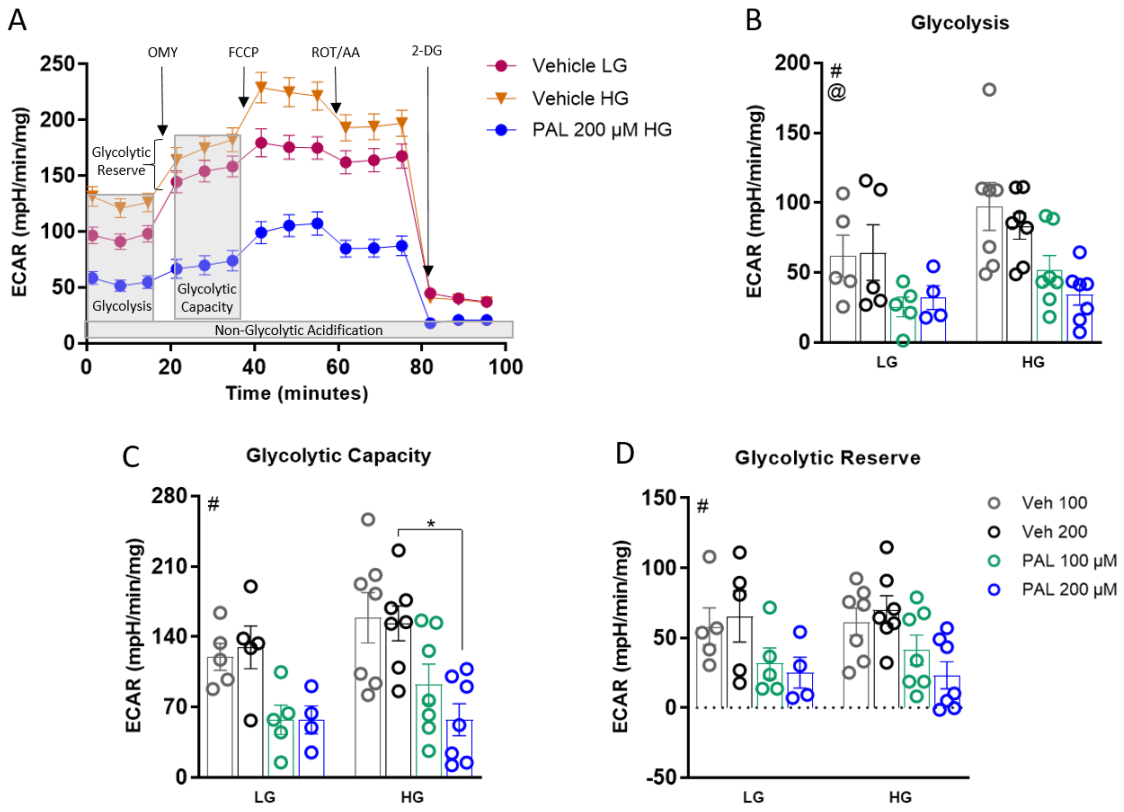

Figure 5. Palmitate exposure decreased extracellular acidification rate in BV2 cells. (A) Real time ECAR recorded after 24 h incubation of BV2 cells in low (LG, 5.5 mmol/L) or high glucose (HG, 25 mmol/L) medium exposed to palmitate (PAL) or vehicle (Veh). Metabolic states calculated as: (B) Glycolysis (Baseline extracellular acidification rate - NGA), (C) Glycolytic Capacity (OMY - NGA), and (D) Glycolytic Reserve (Glycolytic Capacity - Glycolysis). Statistical analysis was made by Two-way ANOVA. n = 5-7 / group. OMY: oligomycin; FCCP: carbonyl cyanide-p-trifluoromethoxy-phenylhydrazone; Rot: rotenone; AA: antimycin A; 2-DG: 2-Deoxy-D-glucose; ECAR: extracellular acidification rate; NGA: non-glycolytic acidification. ANOVA table results: # = Treatment factor, @ = media factor.

Butyrate did not prevent palmitate-induced changes in microglial cellular metabolism

As the SCFA butyrate has been shown to impact positively mitochondrial function in neuronal cells (CHO et al., 2024; XU et al., 2021), we evaluated its effect in mitigating the changes induced by palmitate in BV2 cellular metabolism. We observed that the HG medium increased oxygen consumption in BV2 cells in a similar pattern as observed before. Importantly, we replicated the effect of palmitate (200 µmol/L) in reducing all respiratory states. While butyrate itself did not disturb cellular metabolism, it was not effective in preserving the changes in OCR caused by palmitate exposure at baseline (Figure 6A, Palmitate Effect: $F_{(1, 24)} = 12.99$, $p = 0.0014$; Media Effect: $F_{(1, 24)} = 0.57$, $p = 0.4573$; Butyrate Effect: $F_{(1, 24)} = 3.551$, $p = 0.0717$; Media x Palmitate Interaction: $F_{(1, 24)} = 8.691$, $p = 0.007$), ATP-linked respiration (Figure 6C, Palmitate Effect: $F_{(1, 24)} = 12.94$, $p = 0.0014$; Media Effect: $F_{(1, 24)} = 0.8$, $p = 0.3788$; Butyrate Effect: $F_{(1, 24)} = 3.094$, $p = 0.0913$; Media x Palmitate Interaction: $F_{(1, 24)} = 9.343$, $p = 0.0054$), maximum respiration (Figure 6D, Palmitate Effect: $F_{(1, 24)} = 19.54$, $p = 0.0002$; Media Effect: $F_{(1, 24)} = 0.1998$, $p = 0.6589$; Butyrate Effect: $F_{(1, 24)} = 2.412$, $p = 0.1335$; Media x Palmitate Interaction: $F_{(1, 24)} = 7.199$, $p = 0.0130$) and spare capacity (Figure 6E, Palmitate Effect: $F_{(1, 24)} = 20.96$, $p = 0.0001$; Media Effect: $F_{(1, 24)} = 0.01$, $p = 0.9217$; Butyrate Effect: $F_{(1, 24)} = 1.069$, $p = 0.3115$; Media x Palmitate Interaction $F_{(1, 24)} = 4.294$, $p = 0.0492$). Palmitate and Butyrate themselves impacted proton leak-driven respiration (Figure 6B, Palmitate Effect: $F_{(1, 24)} = 12.22$, $p = 0.0019$; Media Effect: $F_{(1, 24)} = 0.098$, $p = 0.7574$; Butyrate Effect: $F_{(1, 24)} = 4.783$, $p = 0.0387$; Media x Palmitate Interaction: $F_{(1, 24)} = 6.362$, $p = 0.0187$).

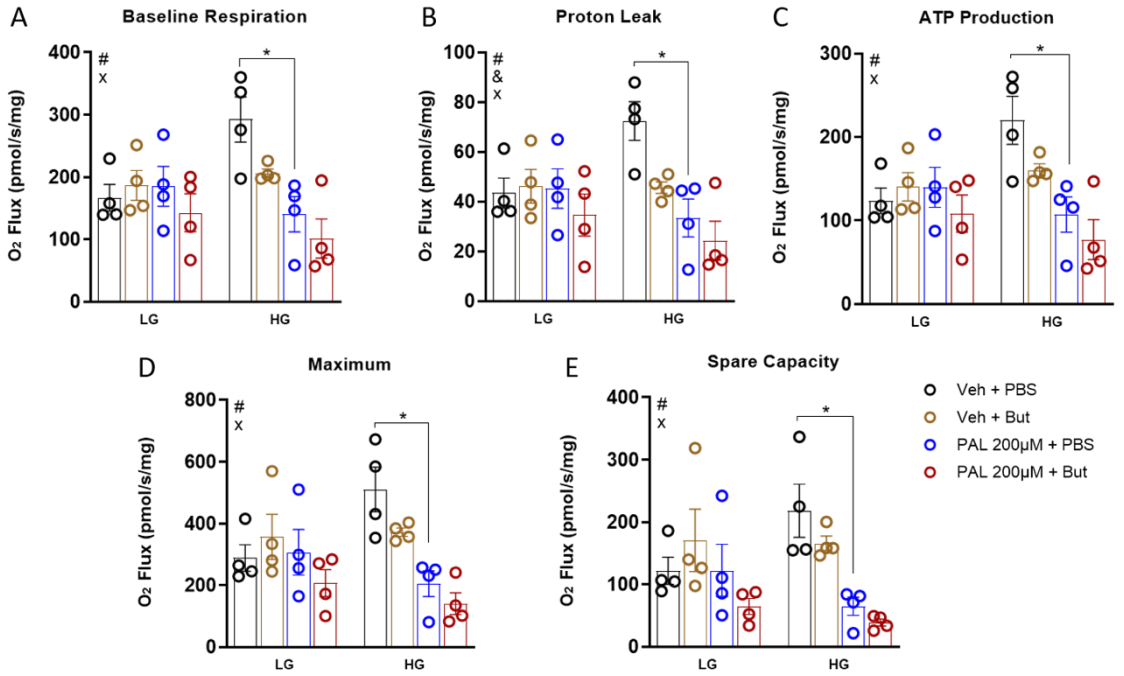

Figure 6. Butyrate did not prevent palmitate-induced mitochondrial dysfunction in BV2 cells. Real-time OCR was recorded after 24 h incubation of BV2 in low (LG, 5.5 mmol/L) or high glucose (HG, 25 mmol/L) medium exposed to palmitate (PAL), Butyrate (But) or vehicle (Veh). Mitochondrial respiratory states calculated as: (A) Baseline respiration (Baseline - NMR), (B) Proton leak (OMY - NMR), (C) ATP-linked respiration (Baseline - proton leak), (D) Maximum respiration (FCCP – NMR), and (E) Spare capacity (Maximum – Baseline). Statistical analysis was made by Three-way ANOVA, n = 4 / group. *p<0.05. ANOVA table results: # = palmitate effect, & = butyrate effect, x = interaction between palmitate and media factors.

The effect of butyrate on ECAR in BV2 cells was also addressed. The effect of HG medium and palmitate on ECAR were here reproduced. Butyrate itself had an impact on baseline acidification rate (Figure 7A, Palmitate Effect: $F_{(1, 24)}$ = 30.14, p < 0.0001; Media Effect: $F_{(1, 24)}$ = 1.017, p = 0.3232; Butyrate Effect: $F_{(1, 24)}$ = 10.23, p = 0.0039; Media x Palmitate Interaction: $F_{(1, 24)}$ = 6.992, p = 0.0142), with no impact on glycolytic capacity (Figure 7B, Palmitate Effect: $F_{(1, 24)}$ = 73.92, p <0.0001; Media Effect: $F_{(1, 24)}$ = 0.2724, p = 0.6065; Butyrate Effect: $F_{(1, 24)}$ = 3.023, p = 0.0949; Media x Palmitate Interaction: $F_{(1, 24)}$ = 7.658, p = 0.0107) and it had an interacting with palmitate on glycolytic reserve (Figure 7C, Palmitate Effect: $F_{(1, 24)}$ = 106.2, p <0.0001; Media Effect: $F_{(1, 24)}$ = 0.02, p = 0.877; Butyrate Effect: $F_{(1, 24)}$ = 0.111, p = 0.7419; Media x Palmitate Interaction: $F_{(1, 24)}$ = 5.297, p = 0.0303; Palmitate x Butyrate Interaction $F_{(1, 24)}$ = 5.19, p = 0.0319.

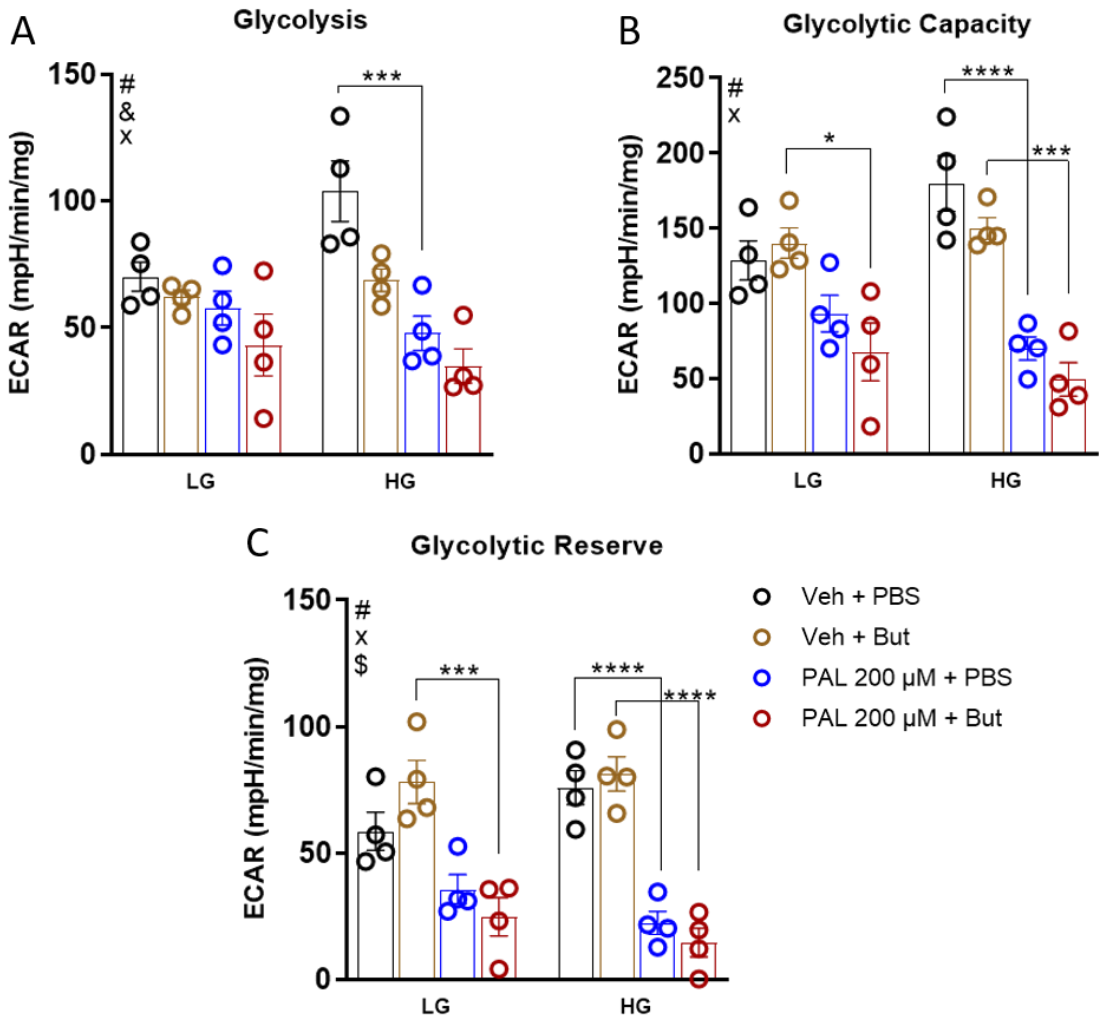

Figure 7. Butyrate did not prevent palmitate-induced changes in extracellular acidification rate of BV2 cells. Extracellular acidification rate (ECAR) of BV2 cells cultured for 24 h in low (LG, 5.5 mmol/L) or high glucose (HG, 25 mmol/L) medium exposed to palmitate (PAL), butyrate (But) or vehicles (Veh) in different metabolic states: (A) Glycolysis (Baseline acidification rate - NGA), (B) Glycolytic Capacity (OMY - NGA), and (C) Glycolytic Reserve (Glycolytic Capacity - Glycolysis). Statistical analysis was made by Three-way ANOVA. n = 4 / group. *p<0.05, ***p<0.001, ****p<0.0001. ANOVA table results: # = palmitate effect, & = butyrate effect, x = interaction between palmitate and media factors, $ = interaction between palmitate and butyrate factors.

Palmitate exposure did not alter mitochondrial area in primary microglia

Further, we investigated if palmitate would affect mitochondrial area in primary microglia cells cultured in HG. For that, we used MitoTracker probe, and no changes in cell area, and mitochondrial area were observed with 24h exposition of both 100 or 200 µmol/L palmitate (Figure 8A and B, $F_{(3, 12)} = 0.6011$, $p = 0.6265$ and Figure 8A and C, $F_{(3, 12)} = 0.126$, $p = 0.9429$, respectively).

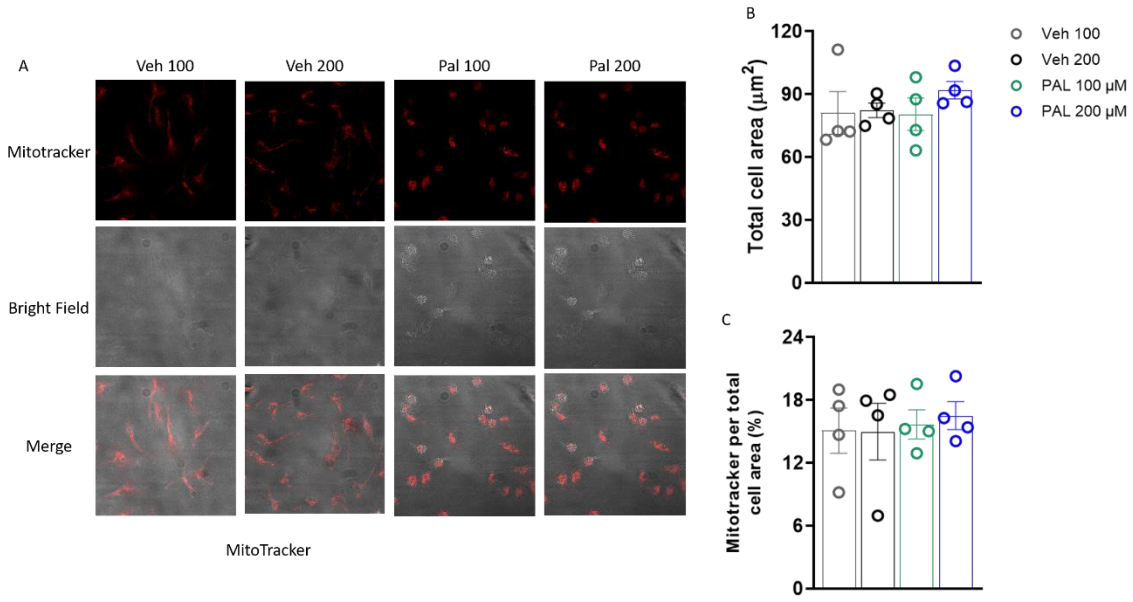

Figure 8. Palmitate did not induce changes in mitochondrial area in primary microglia. (A, C) MitoTracker total stained area per cell of primary microglial cells treated with palmitate (100 or 200 µmol/L) or vehicle (18.92 or 37.85 µmol/L BSA) for 24h. (B) Total cell area in μm^2. Statistical analysis was made by one-way ANOVA. n = 3-4/ group.

Palmitate exposure did not disturb external cargo metabolism by primary microglia

We also performed a functional phagocytic assay in primary microglia cells cultured in HG. The cells were exposed to a Td-Tomato-labeled synaptossomal cargo and the amount of cargo uptaken and degraded were evaluated. The vehicle cells were able to uptake the cargo proportionally to about 5% of total cell area, and degraded half of it in a period of 6 hours after synaptossomal removal. Both concentrations of palmitate did not induce any change in cargo uptake (Figure 9A and 9C, $F_{(3, 11)} = 0.1445$, $p = 0.9311$) or degradation (Figure 9B and 9C, $F_{(3, 8)} = 0.289$, $p = 0.8321$).

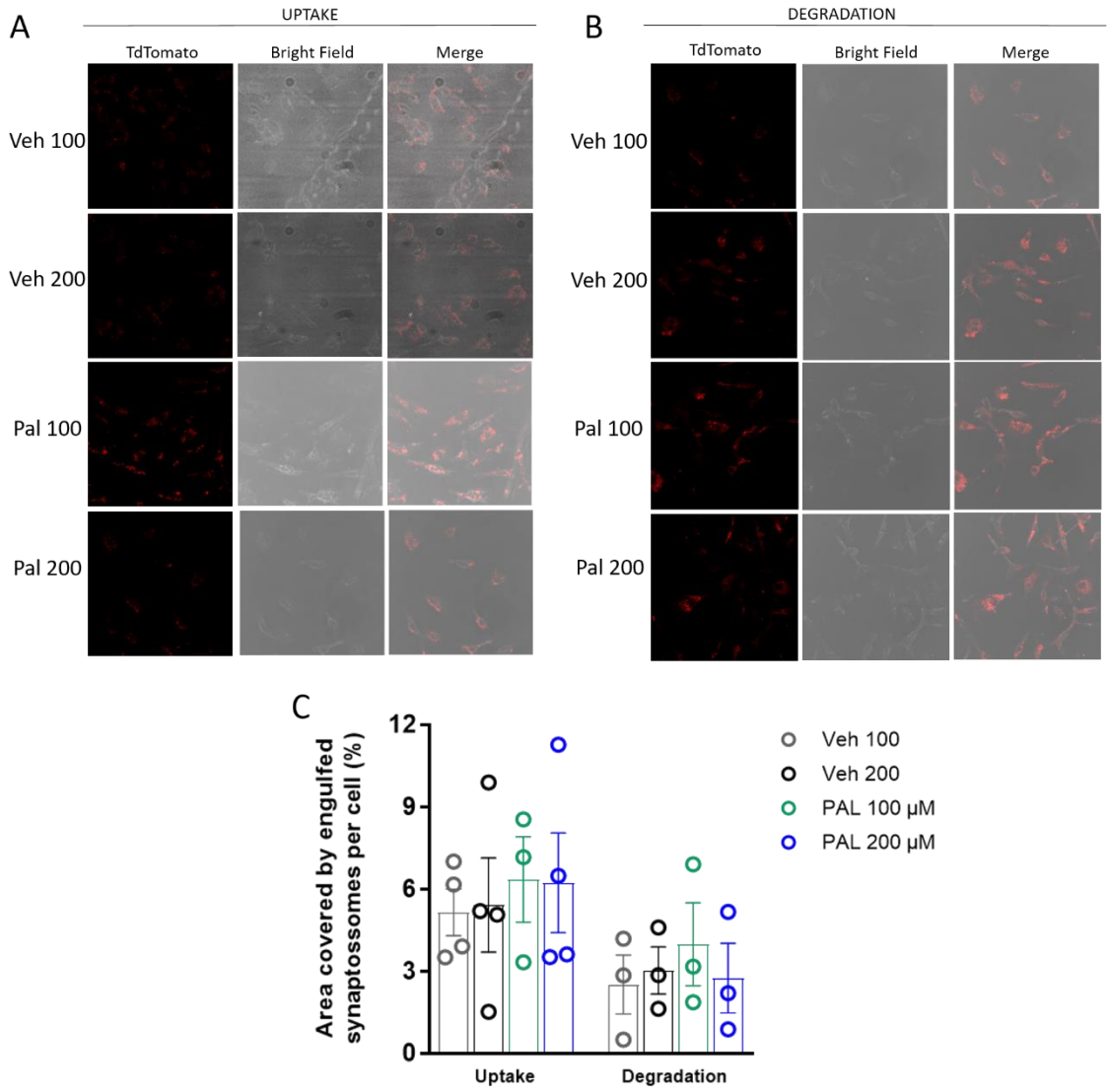

Figure 9. Palmitate did not induce changes in cargo uptake and degradation in primary microglia. (A) TdTomato signal after 1h synaptosome exposure and wash out, and (B) Td-Tomato signal 6 hours after the wash out. TdTomato-labeled synaptosomes expressed as total stained area per cell of primary microglial cells treated with palmitate (100 or 200 µmol/L) or vehicle (18.92 or 37.85 µmol/L BSA) for 24h. Statistical analysis was made by one-way ANOVA. n = 3-4/ group.

DISCUSSION

Cell culture conditions, especially the glucose concentration, may vary substantially according to cell type (primary vs lineage), and between different primary cells and lineages themselves. In this study we evaluated the metabolic and inflammatory status of BV2 microglial cells, by modifying glucose concentrations on cell culture media, combined with a palmitate-induced lipotoxicity model. Culturing BV2 cells in 25 mmol/L

glucose, although not impacting their inflammatory status, increased their metabolic activity and made them more susceptible to palmitate-induced lipotoxicity. Palmitate itself increased inflammatory markers and lipid-metabolism-related genes, and downregulated both oxidative and glycolytic metabolism. The SCFA butyrate did not mitigate palmitate-induced changes in cellular metabolism. Additionally, palmitate did not alter mitochondrial area and cargo metabolism in primary microglial cells.

HG media has been reported to impact BV2 cells by increasing cell proliferation, oxidative stress and inflammatory status compared to LG media. HG media also sensitized the cells to a greater inflammatory response to LPS compared to those cultured in LG (HSIEH et al., 2019). Our findings align with this, as we observed that palmitate increased LDH release only in HG condition. This suggests that HG predispose BV2 cells to heightened sensitivity to TLR4 ligands. Supporting studies have demonstrated that the same concentration of palmitate used here (100 μmol/L) decreased cell viability and increased the release of proinflammatory cytokines (TNF-α, IL-1β and Il-6) in BV2 cells cultured in high glucose media (WANG et al., 2012; YANG, Y. et al., 2023). Furthermore, the conditioned medium from BV2 cells exposed to 100 μmol/L palmitate was sufficient to induce apoptosis in primary neurons, indicating that microglial priming by fatty acids, or more specifically, the secreted products from these microglia, plays a role in neuronal health. This inflammatory effect is reported to be mediated trough NF-κB and TLR4 signaling, which triggers an inflammatory response in BV2 microglia (WANG et al., 2012).

In HepG2 cells, it has been reported that changes in glucose concentration in the media impact cells' susceptibility to palmitate-induced toxicity and oxidative stress. Interestingly, HG itself promoted a higher rate of apoptosis and decreased mitochondrial complex IV activity and ATP levels compared to LG (ALNAHDI et al., 2019). Although we did not investigate the specific type of cell death in our protocol, previous studies have shown that palmitate induces cell death in BV2 via apoptosis and pyroptosis (YU et al., 2024).

Our data demonstrated that palmitate modulates the gene expression of proteins related to microglial polarization and inflammation. Regardless of the glucose concentration in the media, palmitate impacted the expression of CD68 and IL-1β in BV2 cells. A similar pattern of cytokine upregulation was observed in experimental models of traumatic brain injuries, suggesting that microglial are recruited to repair damaged areas

(TURTZO et al., 2014). Moreover, CD68 expression is increased on a mice model related to amyloidosis and behavioral phenotypes related to Alzheimer's Disease. As CD68 is a robust marker of phagocytosis, it has relevant implications for synaptic degeneration, since excessive synaptic pruning is believed to contribute to synaptic degeneration in neurodegenerative disorders (EVANS et al., 2020).

IL-1β is considered one of the key contributors to microglial-driven inflammation and is prominently present in polarized microglia localized in amyloid plaques (SHENG; MRAK; GRIFFIN, 1995). The increase in IL-1β release may be related to enhanced inflammasome formation, which has been shown to be induced by palmitate in hepatic cells (DONG et al., 2020) and also in microglia (YU et al., 2024). However, conflicting our findings, Chausse et al., showed no palmitate-induced increase on TNF-α and IL-1β mRNA expression in BV2 cells cultured in HG (CHAUSSE et al., 2019). Consistent with our findings, cell viability in primary rat microglia cultured in glucose concentrations ranging from 25 to 50 mmol/L was not affected. However, when these cells were stimulated with LPS, the magnitude of TNF-α and IL-6 release was directly proportional to the glucose concentrations in the media. This data reinforces that glucose levels in culture media can modulate the intensity of microglia response to stimuli (ZHANG et al., 2015).

Vuong and colleagues (2017) found that palmitate increased the expression of inflammatory genes in primary microglia cultured in LG. Surprisingly, when these cells are cultured in 3x more glucose, the palmitate -induced increase in inflammatory markers IL-3 and interferon-γ was abolished. This changes are correlated with an amoeboid shape in cells cultured in HG, and palmitate markedly enhanced this amoeboid phenotype. Their findings suggest that palmitate plays a more substantial role in shifting microglia towards a non- homeostatic state than elevated glucose concentrations alone (VUONG et al., 2017).

HFD induce features of type 2 diabetes mellitus, such as hyperinsulinemia and elevated blood glucose levels (YANG, X. et al., 2022). The high glucose condition we exposed BV2 in our study may be comparable with glucose overload seen in T2DM patients and experimental models. In a model of hyperinsulinemia *in vitro,* increased inflammatory cytokines and mitochondrial dysfunction were observed and accompanied by decreased GLUT4 expression in both BV2 and primary microglia (YANG, X. et al., 2022). It would be important not only to define the concentration of glucose given to the

cell, but to estimate how much of this available amount is actually used, and the impacts for the cell of the amount not uptaken.

In our study, palmitate upregulated HSL and LPL, enzymes related to lipid metabolism, without affecting Hexokinase 1/2 and Glycogen Synthase, which are key enzymes in glucose metabolism. Microglial lipid metabolism plays a critical role in regulating microglial responsiveness and effector functions, including migration, phagocytosis and inflammatory signaling (CHAUSSE; KAKIMOTO; KANN, 2021). Along with other markers, the upregulation of LPL in microglia from AD-transgenic mice was associated with a microglia phenotype linked to neurodegenerative disease (KEREN-SHAUL et al., 2017). Gao and colleagues reported that just three days of an energy-dense diet were sufficient to increase LPL gene expression in mouse microglia. Moreover, mice lacking LPL in microglia exhibited exaggerated metabolic disorders and microglia mitochondria dysmorphologies under the same diet conditions, which accompains reduced microglial immune reactivity (GAO et al., 2017). These findings suggest that LPL homeostasis may be crucial for proper microglial function. HSL has not been previously explored in microglia, and its specific role in microglial health and disease warrants further investigation.

As previous studies have shown a shift from OXPHOS to glycolysis in microglia following LPS exposure (VOLOBOUEVA et al., 2013), we evaluated the effect of palmitate, another TLR4 ligand, on mitochondrial function under both low and high glucose conditions. The high glucose condition itself had a significant impact, increasing basal respiration and ATP production as measured by OCR, as well the glycolysis rate indicated by ECAR. Switching the culture media from LG to HG in mixed glial cultures also affected mitochondria function, leading to a decrease in mitochondria membrane potential and ATP levels (HUANG et al., 2022). Interestingly, we evidenced that palmitate caused downregulation of all parameters measured by both OCR and ECAR in BV2 cells. The literature reports varying effects of palmitate on BV2 metabolism, including an increase in glycolytic flux without affecting OCR (CHAUSSE et al., 2019), and an overall decrease in OCR, particularly in BV2 cultured in HG (BUTLER et al., 2023). Butler and colleagues also emphasized a more pronounced downregulation of basal respiration in BV2, compared to HippoE-14 neurons, suggesting that microglia may be more vulnerable to palmitate-induced injury than neurons (BUTLER et al., 2023). In a recent study from our group, palmitate shifted the metabolism from OXPHOS to

glycolysis in BV2 cells cultured in LG (DE PAULA et al., 2024). These findings underscore the importance of the glucose concentration on cell culture media, as it may determine the nature and intensity of the metabolic response to palmitate.

The body of evidence suggest that the Warburg effect, which is implied in microglia under inflammatory stress, is stimulus-dependent. LPS, for instance, consistently induces a shift from OXPHOS to glycolysis (CHAUSSE et al., 2019; DE PAULA et al., 2024; NAIR et al., 2019; VOLOBOUEVA et al., 2013). However, studies on palmitate yield highly controversial results: some report no effect on this metabolic shift (CHAUSSE et al., 2019), while another demonstrated a shift towards glycolysis (DE PAULA et al., 2024), and we observed decrease in both OCR and ECAR. Our data indicate that palmitate toxicity disrupts the entire cellular machinery, impairing both aerobic and anaerobic energy production, which ultimately leads to prolonged microglial dysfunction.

This downregulation in both OCR and ECAR may be related to oxidative stress, as already been reported in increased ROS production in BV2 cells exposed to palmitate (WANG et al., 2012). This excessive ROS may damage mitochondrial complexes, being the cause of a direct impact on decreased mitochondrial OCR (GUO et al., 2013). Another possible mechanism may be altered mitochondrial dynamics, which is indispensable for proper mitochondrial function. Supporting this, LPS-treated microglia presented increased mitochondrial fragmentation and shifted the metabolism to glycolytic, features that were substantially restored after blocking mitochondrial fission (NAIR et al., 2019).

Interestingly, *in vitro* microglial glycolysis blockage with 2-DG rapidly depletes ATP microglial content, which consistently culminates in cell death. This blockage didn't induce cell death in neurons or astrocytes (VILALTA; BROWN, 2014). This data shows the importance of glycolysis in microglia fitness, evidencing that only OXPHOS is not enough to keep microglia healthy in challenging conditions, highlighting the key role of metabolic flexibility as well. This data agrees with our evidence that palmitate induces microglia bioenergetics crisis, which makes microglia prone to dysfunction and death.

We evaluated the potential effects of the SCFA butyrate in mitigating palmitate-induced metabolic outcomes. In our protocol butyrate itself did not have an impact in either cellular metabolism or in preventing palmitate-induced stress. Butyrate has been

postulated to keep energy balance in favor of obesity control and metabolic diseases. In the brain, butyrate protects neurons from ischemia damage, improves memory and attenuates neurodegeneration (STILLING et al., 2016). High doses of sodium butyrate *in vivo* (2.5g/kg) induce hypothalamic mitochondrial swelling and upregulation of glycolytic and OXPHOS metabolites, and a mixed effect on citric acid cycle enzymes. Moreover, 10 or 20 mM sodium butyrate in Neuro-2a cells increased overall OXPHOS compared to control cells (XU et al., 2021). It is worth to highlight that the dose we used in BV2 was 200 µM butyrate, which may have not been enough to produce significant effects in baseline and palmitate-induced changes in metabolism. Moreover, sodium butyrate ameliorated HG-induced neuronal mitochondrial dysfunction by recovering mitophagy *in vitro*, and hippocampal mitophagy in a streptozotocin-induced diabetes mouse model (CHO et al., 2024). In microglia, sodium butyrate regulates LPS response *in vitro* (LI, H. et al., 2021), however, there are still few studies on butyrate impacting microglial mitochondrial function.

Phagocytic capacity is critical to maintaining optimal synaptic transmission and plasticity, and in conditions of neuroinflammation, microglia have been shown to over-prune synapses, resulting in aberrant neuronal plasticity (BUTLER et al., 2023). Our results show no impact of palmitate in microglial mitochondrial total area and their ability to uptake and degrade cargo. In our previous study, we found no impact of palmitate on total Mitoracker area in BV2 cells (DE PAULA et al., 2024). A previous study has shown no impact of palmitate alone on primary microglial phagocytosis, but a significant decrease when cells were co-exposed to palmitate and interferon-γ. These findings were explained as palmitate being able to decrease microglial ability to migrate under inflammatory conditions (YANGUAS-CASAS et al., 2018). Butler and colleagues added more evidence that BV2 cells exposed to palmitate did not have an impairment in engulfing synapses from aged HFD-fed mice (BUTLER et al., 2023). Our findings are in accordance with these, reinforcing that palmitate alone is not sufficient to impair microglial phagocytic capacity, but it potentiates microglial impairment when another stressful stimulus is present.

In conclusion, our study demonstrates that high glucose concentration on cell culture media enhances BV2 susceptibility to lipid-induced toxicity and increases mitochondrial oxidative and glycolytic activity. We add more evidence that palmitate induces overexpression of inflammatory and lipid metabolism-related genes, and

downregulates mitochondrial metabolism in BV2 microglia, with no impact on mitochondrial mass and phagocytic functions in primary microglia. Moreover, we suggest the authors who work with cell culture to fully describe the media composition used in their study, to make them reproducible, and to avoid undesired priming or preconditioning of the cells.

REFERENCES

ALNAHDI, A.; JOHN, A.; RAZA, H. Augmentation of Glucotoxicity, Oxidative Stress, Apoptosis and Mitochondrial Dysfunction in HepG2 Cells by Palmitic Acid. **Nutrients,** v. 11, n. 9, Aug 22 2019.

BERNIER, L. P.; YORK, E. M.; MACVICAR, B. A. Immunometabolism in the Brain: How Metabolism Shapes Microglial Function. **Trends Neurosci,** v. 43, n. 11, p. 854-869, Nov 2020.

BUTLER, M. J. et al. Fatty food, fatty acids, and microglial priming in the adult and aged hippocampus and amygdala. **Brain Behav Immun,** v. 89, p. 145-158, Oct 2020.

BUTLER, M. J. et al. Dietary fatty acids differentially impact phagocytosis, inflammatory gene expression, and mitochondrial respiration in microglial and neuronal cell models. **Front Cell Neurosci,** v. 17, p. 1227241, 2023.

CAETANO-SILVA, M. E. et al. Inhibition of inflammatory microglia by dietary fiber and short-chain fatty acids. **Sci Rep,** v. 13, n. 1, p. 2819, Feb 16 2023.

CHAUSSE, B. et al. Distinct metabolic patterns during microglial remodeling by oleate and palmitate. **Biosci Rep,** v. 39, n. 4, Apr 30 2019.

CHAUSSE, B.; KAKIMOTO, P. A.; KANN, O. Microglia and lipids: how metabolism controls brain innate immunity. **Semin Cell Dev Biol,** v. 112, p. 137-144, Apr 2021.

CHO, J. H. et al. Sodium butyrate ameliorates high glucose-suppressed neuronal mitophagy by restoring PRKN expression via inhibiting the RELA-HDAC8 complex. **Autophagy,** v. 20, n. 7, p. 1505-1522, Jul 2024.

CHUNCHAI, T. et al. Decreased microglial activation through gut-brain axis by prebiotics, probiotics, or synbiotics effectively restored cognitive function in obese-insulin resistant rats. **J Neuroinflammation,** v. 15, n. 1, p. 11, Jan 9 2018.

COPE, E. C. et al. Microglia Play an Active Role in Obesity-Associated Cognitive Decline. **J Neurosci,** v. 38, n. 41, p. 8889-8904, Oct 10 2018.

DAI, X. J. et al. Activation of BV2 microglia by lipopolysaccharide triggers an inflammatory reaction in PC12 cell apoptosis through a toll-like receptor 4-dependent pathway. **Cell Stress Chaperones,** v. 20, n. 2, p. 321-31, Mar 2015.

DE PAULA, G. C. et al. Extracellular vesicles released from microglia after palmitate exposure impact brain function. **J Neuroinflammation,** v. 21, n. 1, p. 173, Jul 16 2024.

DONG, Z. et al. Palmitic acid stimulates NLRP3 inflammasome activation through TLR4-NF-kappaB signal pathway in hepatic stellate cells. **Ann Transl Med,** v. 8, n. 5, p. 168, Mar 2020.

EVANS, A. K. et al. Beta-adrenergic receptor antagonism is proinflammatory and exacerbates neuroinflammation in a mouse model of Alzheimer's Disease. **Neurobiol Dis,** v. 146, p. 105089, Dec 2020.

GAO, Y. et al. Lipoprotein Lipase Maintains Microglial Innate Immunity in Obesity. **Cell Rep,** v. 20, n. 13, p. 3034-3042, Sep 26 2017.

GUO, C. et al. Oxidative stress, mitochondrial damage and neurodegenerative diseases. **Neural Regen Res,** v. 8, n. 21, p. 2003-14, Jul 25 2013.

HICKMAN, S. et al. Microglia in neurodegeneration. **Nat Neurosci,** v. 21, n. 10, p. 1359-1369, Oct 2018.

HSIEH, C. F. et al. Acute glucose fluctuation impacts microglial activity, leading to inflammatory activation or self-degradation. **Sci Rep,** v. 9, n. 1, p. 840, Jan 29 2019.

HUANG, Y. C. et al. Reduced mitochondria membrane potential and lysosomal acidification are associated with decreased oligomeric Abeta degradation induced by hyperglycemia: A study of mixed glia cultures. **PLoS One,** v. 17, n. 1, p. e0260966, 2022.

KEREN-SHAUL, H. et al. A Unique Microglia Type Associated with Restricting Development of Alzheimer's Disease. **Cell,** v. 169, n. 7, p. 1276-1290 e17, Jun 15 2017.

KOH, A. et al. From Dietary Fiber to Host Physiology: Short-Chain Fatty Acids as Key Bacterial Metabolites. **Cell,** v. 165, n. 6, p. 1332-1345, Jun 2 2016.

LI, H. et al. Rifaximin-mediated gut microbiota regulation modulates the function of microglia and protects against CUMS-induced depression-like behaviors in adolescent rat. **J Neuroinflammation,** v. 18, n. 1, p. 254, Nov 4 2021.

LI, Y. et al. Mitochondrial dysfunction in microglia: a novel perspective for pathogenesis of Alzheimer's disease. **J Neuroinflammation,** v. 19, n. 1, p. 248, Oct 6 2022.

MICHELL-ROBINSON, M. A. et al. Roles of microglia in brain development, tissue maintenance and repair. **Brain,** v. 138, n. Pt 5, p. 1138-59, May 2015.

MISHRA, S. P. et al. Free Fatty Acid Receptors 2 and 3 as Microbial Metabolite Sensors to Shape Host Health: Pharmacophysiological View. **Biomedicines,** v. 8, n. 6, Jun 8 2020.

MONIF, M. et al. The P2X7 receptor drives microglial activation and proliferation: a trophic role for P2X7R pore. **J Neurosci,** v. 29, n. 12, p. 3781-91, Mar 25 2009.

MONSORNO, K. et al. Loss of microglial MCT4 leads to defective synaptic pruning and anxiety-like behavior in mice. **Nat Commun,** v. 14, n. 1, p. 5749, Sep 16 2023.

NAIR, S. et al. Lipopolysaccharide-induced alteration of mitochondrial morphology induces a metabolic shift in microglia modulating the inflammatory response in vitro and in vivo. **Glia,** v. 67, n. 6, p. 1047-1061, Jun 2019.

NAKAJIMA, S. et al. Central activation of the fatty acid sensor GPR120 suppresses microglia reactivity and alleviates sickness- and anxiety-like behaviors. **J Neuroinflammation,** v. 20, n. 1, p. 302, Dec 19 2023.

PAOLICELLI, R. C.; ANGIARI, S. Microglia immunometabolism: From metabolic disorders to single cell metabolism. **Semin Cell Dev Biol,** v. 94, p. 129-137, Oct 2019.

PAOLICELLI, R. C. et al. Synaptic pruning by microglia is necessary for normal brain development. **Science,** v. 333, n. 6048, p. 1456-8, Sep 9 2011.

PAOLICELLI, R. C. et al. Microglia states and nomenclature: A field at its crossroads. **Neuron,** v. 110, n. 21, p. 3458-3483, Nov 2 2022.

PEDICONE, C. et al. Discovery of a novel SHIP1 agonist that promotes degradation of lipid-laden phagocytic cargo by microglia. **iScience,** v. 25, n. 4, p. 104170, Apr 15 2022.

QIU, T. et al. Obesity-induced elevated palmitic acid promotes inflammation and glucose metabolism disorders through GPRs/NF-kappaB/KLF7 pathway. **Nutr Diabetes,** v. 12, n. 1, p. 23, Apr 20 2022.

SHENG, J. G.; MRAK, R. E.; GRIFFIN, W. S. Microglial interleukin-1 alpha expression in brain regions in Alzheimer's disease: correlation with neuritic plaque distribution. **Neuropathol Appl Neurobiol,** v. 21, n. 4, p. 290-301, Aug 1995.

SQUARZONI, P.; THION, M. S.; GAREL, S. Neuronal and microglial regulators of cortical wiring: usual and novel guideposts. **Front Neurosci,** v. 9, p. 248, 2015.

STILLING, R. M. et al. The neuropharmacology of butyrate: The bread and butter of the microbiota-gut-brain axis? **Neurochem Int,** v. 99, p. 110-132, Oct 2016.

THALER, J. P. et al. Obesity is associated with hypothalamic injury in rodents and humans. **J Clin Invest,** v. 122, n. 1, p. 153-62, Jan 2012.

TURTZO, L. C. et al. Macrophagic and microglial responses after focal traumatic brain injury in the female rat. **J Neuroinflammation,** v. 11, p. 82, Apr 24 2014.

VALDEARCOS, M. et al. Microglial Inflammatory Signaling Orchestrates the Hypothalamic Immune Response to Dietary Excess and Mediates Obesity Susceptibility. **Cell Metab,** v. 26, n. 1, p. 185-197 e3, Jul 5 2017.

VILALTA, A.; BROWN, G. C. Deoxyglucose prevents neurodegeneration in culture by eliminating microglia. **J Neuroinflammation,** v. 11, p. 58, Mar 26 2014.

VOLOBOUEVA, L. A. et al. Inflammatory response of microglial BV-2 cells includes a glycolytic shift and is modulated by mitochondrial glucose-regulated protein 75/mortalin. **FEBS Lett,** v. 587, n. 6, p. 756-62, Mar 18 2013.

VUONG, B. et al. Exposure to gestational diabetes mellitus induces neuroinflammation, derangement of hippocampal neurons, and cognitive changes in rat offspring. **J Neuroinflammation,** v. 14, n. 1, p. 80, Apr 7 2017.

WALKER, D. G.; LUE, L. F. Immune phenotypes of microglia in human neurodegenerative disease: challenges to detecting microglial polarization in human brains. **Alzheimers Res Ther,** v. 7, n. 1, p. 56, Aug 19 2015.

WANG, Z. et al. Saturated fatty acids activate microglia via Toll-like receptor 4/NF-kappaB signalling. **Br J Nutr,** v. 107, n. 2, p. 229-41, Jan 2012.

XU, Y. et al. High doses of butyrate induce a reversible body temperature drop through transient proton leak in mitochondria of brain neurons. **Life Sci,** v. 278, p. 119614, Aug 1 2021.

YANG, X. et al. Hyperinsulinemia-induced microglial mitochondrial dynamic and metabolic alterations lead to neuroinflammation in vivo and in vitro. **Front Neurosci,** v. 16, p. 1036872, 2022.

YANG, Y. et al. Palmitate lipotoxicity is closely associated with the fatty acid-albumin complexes in BV-2 microglia. **PLoS One,** v. 18, n. 4, p. e0281189, 2023.

YANGUAS-CASAS, N. et al. Sex differences in the phagocytic and migratory activity of microglia and their impairment by palmitic acid. **Glia,** v. 66, n. 3, p. 522-537, Mar 2018.

YU, Q. et al. Palmitoleic acid protects microglia from palmitate-induced neurotoxicity in vitro. **PLoS One,** v. 19, n. 1, p. e0297031, 2024.

ZHANG, X. et al. Enhancement of LPS-induced microglial inflammation response via TLR4 under high glucose conditions. **Cell Physiol Biochem,** v. 35, n. 4, p. 1571-81, 2015.

ZHOU, Y. et al. Dietary Fiber and Microbiota Metabolite Receptors Enhance Cognition and Alleviate Disease in the 5xFAD Mouse Model of Alzheimer's Disease. **J Neurosci,** v. 43, n. 37, p. 6460-6475, Sep 13 2023.

Parte III

6. CONCLUSÕES E PERSPECTIVAS FUTURAS

O consumo de dietas ricas em gordura saturada, carboidratos refinados e pobre em fibras, além de induzir alterações metabólicas periféricas, impacta direta e severamente o SNC (ROCHA et al., 2017; ZHANG, R. et al., 2024). Especialmente no hipocampo, o consumo desse padrão alimentar desequilibrado é fortemente associado com alterações morfológicas e bioquímicas, como neuroinflamação, disfunção mitocondrial e estresse oxidativo, e redução do volume hipocampal e da massa cinzenta cerebral (DE BEM et al., 2020; DE PAULA et al., 2021; ZHANG, R. et al., 2024). A microglia desempenha papel essencial na manutenção da homeostase das funções cerebrais como um todo, sendo afetada funcional e morfologicamente pelo consumo de dietas hiperlipídicas e obesidade (COPE et al., 2018; THALER et al., 2012). O nosso grupo de pesquisa vem contribuindo para o entendimento de como o SNC reage e é afetado pela sobrecarga de gorduras saturadas oriundas da dieta. Em nossos estudos recentes reportamos que as alterações cognitivas induzidas pela dieta hiperlipídica está associada a alterações mitocondriais das células hipocampais (VILELA, W. R. et al., 2023). Desta forma, esta tese de doutorado investigou os efeitos da sobrecarga de lipídeos saturados *in vivo*, no metabolismo periférico e na função cognitiva e mitocondrial cerebral, e *in vitro*, em células de microglia.

No Capítulo I, estabelecemos um modelo de disfunção metabólica induzida por DH + L-NAME em ratos Wistar. O modelo foi capaz de induzir obesidade, elevação da pressão arterial e aumento nos níveis séricos colesterol total. Associado às alterações metabólicas verificamos que os ratos submetidos a DH + L-NAME apresentaram prejuízo de aprendizagem em tarefas de memória espacial, altamente dependente de funções hipocampais, e que exige uma alta taxa metabólica das células neurais. Observamos também um prejuízo bioenergético das células hipocampais e alteração na expressão da proteína de dinâmica mitocondrial OPA-1, sem alterações funcionais das mitocôndrias neocorticais.

No capítulo II, transpomos esse modelo de sobrecarga lipídica, juntamente com uma sobrecarga de glicose, para a cultura celular de microglia. A sobrecarga lipídica foi feita pela exposição de células BV2 ao palmitato, e a sobrecarga glicídica foi realizada aumentando as concentrações de glicose diluídas no meio de cultivo celular. A sobrecarga de glicose propiciou às células a sofrerem em maior extensão os efeitos do palmitato na

viabilidade celular, e induziu aumento dos fluxos oxidativo e glicolítico. A sobrecarga lipídica polarizou a célula para um perfil mais inflamatório, comprometendo a viabilidade celular e aumentando marcadores de metabolismo lipídico, e com evidente impacto no metabolismo mitocondrial, reduzindo parâmetros bioenergéticos oxidativos e glicolíticos. O palmitato não modulou a dinâmica de fagocitose de sinaptossomas pela microglia. Ademais, a modulação terapêutica com o butirato não foi capaz de prevenir as alterações bioenergéticas causadas pelo palmitato.

Por fim, estabelecemos um modelo de disfunção metabólica *in vivo* e *in vitro* pela sobrecarga de ácidos graxos saturados. Em ambos os modelos, obtivemos disfunção mitocondrial, especialmente bioenergética, decorrente do estresse metabólico aplicado. Esses dados colocam a fisiologia mitocondrial em evidência nas alterações fenotípicas e funcionais neurais, sendo a neuroenergética particularmente sensível aos efeitos de estressores metabólicos.

Futuros trabalhos em nosso laboratório pretendem explorar o papel da microbiota intestinal e seus metabólitos na disfunção cerebral induzida por modelos de sobrecarga lipídica *in vitro* e *in vivo*. Além disso, pretendemos caracterizar morfologicamente a mitocôndria nesses modelos, bem como realizar ensaios bioenergéticos na microglia oriunda de animais expostos à DH, para avaliar isoladamente a contribuição da disfunção bioenergética microglial, nas alterações fenotípicas observadas.

7. REFERÊNCIAS BIBLIOGRÁFICAS

ALAMNIA, T. T.; SARGENT, G. M.; KELLY, M. Dietary patterns and associations with metabolic risk factors for non-communicable disease. **Sci Rep,** v. 13, n. 1, p. 21028, Nov 29 2023.

ALAVI, M. V.; FUHRMANN, N. Dominant optic atrophy, OPA1, and mitochondrial quality control: understanding mitochondrial network dynamics. **Mol Neurodegener,** v. 8, p. 32, Sep 25 2013.

ALLEN, N. J.; BARRES, B. A. Neuroscience: Glia - more than just brain glue. **Nature,** v. 457, n. 7230, p. 675-7, Feb 5 2009.

ALNAHDI, A.; JOHN, A.; RAZA, H. Augmentation of Glucotoxicity, Oxidative Stress, Apoptosis and Mitochondrial Dysfunction in HepG2 Cells by Palmitic Acid. **Nutrients,** v. 11, n. 9, Aug 22 2019.

ATTWELL, D.; LAUGHLIN, S. B. An energy budget for signaling in the grey matter of the brain. **J Cereb Blood Flow Metab,** v. 21, n. 10, p. 1133-45, Oct 2001.

BAKER, N.; PATEL, J.; KHACHO, M. Linking mitochondrial dynamics, cristae remodeling and supercomplex formation: How mitochondrial structure can regulate bioenergetics. **Mitochondrion,** v. 49, p. 259-268, Nov 2019.

BERNIER, L. P.; YORK, E. M.; MACVICAR, B. A. Immunometabolism in the Brain: How Metabolism Shapes Microglial Function. **Trends Neurosci,** v. 43, n. 11, p. 854-869, Nov 2020.

BUTLER, M. J. et al. Fatty food, fatty acids, and microglial priming in the adult and aged hippocampus and amygdala. **Brain Behav Immun,** v. 89, p. 145-158, Oct 2020.

BUTLER, M. J. et al. Dietary fatty acids differentially impact phagocytosis, inflammatory gene expression, and mitochondrial respiration in microglial and neuronal cell models. **Front Cell Neurosci,** v. 17, p. 1227241, 2023.

CAETANO-SILVA, M. E. et al. Inhibition of inflammatory microglia by dietary fiber and short-chain fatty acids. **Sci Rep,** v. 13, n. 1, p. 2819, Feb 16 2023.

CAVALIERE, G. et al. Butyrate Improves Neuroinflammation and Mitochondrial Impairment in Cerebral Cortex and Synaptic Fraction in an Animal Model of Diet-Induced Obesity. **Antioxidants (Basel),** v. 12, n. 1, Dec 20 2022.

CHAUSSE, B. et al. Distinct metabolic patterns during microglial remodeling by oleate and palmitate. **Biosci Rep,** v. 39, n. 4, Apr 30 2019.

CHEN, W.; ZHAO, H.; LI, Y. Mitochondrial dynamics in health and disease: mechanisms and potential targets. **Signal Transduct Target Ther,** v. 8, n. 1, p. 333, Sep 6 2023.

CHO, J. H. et al. Sodium butyrate ameliorates high glucose-suppressed neuronal mitophagy by restoring PRKN expression via inhibiting the RELA-HDAC8 complex. **Autophagy,** v. 20, n. 7, p. 1505-1522, Jul 2024.

CHUNCHAI, T. et al. Decreased microglial activation through gut-brain axis by prebiotics, probiotics, or synbiotics effectively restored cognitive function in obese-insulin resistant rats. **J Neuroinflammation,** v. 15, n. 1, p. 11, Jan 9 2018.

COLE, M. A. et al. A high fat diet increases mitochondrial fatty acid oxidation and uncoupling to decrease efficiency in rat heart. **Basic Res Cardiol,** v. 106, n. 3, p. 447-57, May 2011.

COLONNA, M.; BUTOVSKY, O. Microglia Function in the Central Nervous System During Health and Neurodegeneration. **Annu Rev Immunol,** v. 35, p. 441-468, Apr 26 2017.

COPE, E. C. et al. Microglia Play an Active Role in Obesity-Associated Cognitive Decline. **J Neurosci,** v. 38, n. 41, p. 8889-8904, Oct 10 2018.

CORDERO-HERRERA, I. et al. Head-to-head comparison of inorganic nitrate and metformin in a mouse model of cardiometabolic disease. **Nitric Oxide,** v. 97, p. 48-56, Apr 1 2020.

DAI, X. J. et al. Activation of BV2 microglia by lipopolysaccharide triggers an inflammatory reaction in PC12 cell apoptosis through a toll-like receptor 4-dependent pathway. **Cell Stress Chaperones,** v. 20, n. 2, p. 321-31, Mar 2015.

DE BEM, A. F. et al. Animal Models of Metabolic Disorders in the Study of Neurodegenerative Diseases: An Overview. **Front Neurosci,** v. 14, p. 604150, 2020.

DE PAULA, G. C. et al. Extracellular vesicles released from microglia after palmitate exposure impact brain function. **J Neuroinflammation,** v. 21, n. 1, p. 173, Jul 16 2024.

DE PAULA, G. C. et al. Hippocampal Function Is Impaired by a Short-Term High-Fat Diet in Mice: Increased Blood-Brain Barrier Permeability and Neuroinflammation as Triggering Events. **Front Neurosci,** v. 15, p. 734158, 2021.

DIAZ, A. et al. Metforminium Decavanadate (MetfDeca) Treatment Ameliorates Hippocampal Neurodegeneration and Recognition Memory in a Metabolic Syndrome Model. **Neurochem Res,** v. 46, n. 5, p. 1151-1165, May 2021.

DUTHEIL, S. et al. High-Fat Diet Induced Anxiety and Anhedonia: Impact on Brain Homeostasis and Inflammation. **Neuropsychopharmacology,** v. 41, n. 7, p. 1874-87, Jun 2016.

EVANS, A. K. et al. Beta-adrenergic receptor antagonism is proinflammatory and exacerbates neuroinflammation in a mouse model of Alzheimer's Disease. **Neurobiol Dis,** v. 146, p. 105089, Dec 2020.

FOLICK, A.; KOLIWAD, S. K.; VALDEARCOS, M. Microglial Lipid Biology in the Hypothalamic Regulation of Metabolic Homeostasis. **Front Endocrinol (Lausanne),** v. 12, p. 668396, 2021.

FRIEDMAN, J. R.; NUNNARI, J. Mitochondrial form and function. **Nature,** v. 505, n. 7483, p. 335-43, Jan 16 2014.

FUSCO, W. et al. Short-Chain Fatty-Acid-Producing Bacteria: Key Components of the Human Gut Microbiota. **Nutrients,** v. 15, n. 9, May 6 2023.

GAO, M.; MA, Y.; LIU, D. High-fat diet-induced adiposity, adipose inflammation, hepatic steatosis and hyperinsulinemia in outbred CD-1 mice. **PLoS One,** v. 10, n. 3, p. e0119784, 2015.

GAO, Z. et al. Butyrate improves insulin sensitivity and increases energy expenditure in mice. **Diabetes,** v. 58, n. 7, p. 1509-17, Jul 2009.

GOMES GONCALVES, N. et al. Association Between Consumption of Ultraprocessed Foods and Cognitive Decline. **JAMA Neurol,** v. 80, n. 2, p. 142-150, Feb 1 2023.

GOYAL, M. S. et al. Aerobic glycolysis in the human brain is associated with development and neotenous gene expression. **Cell Metab,** v. 19, n. 1, p. 49-57, Jan 7 2014.

GRASSO, D. et al. Mitochondria in cancer. **Cell Stress,** v. 4, n. 6, p. 114-146, May 11 2020.

GUILLAMON-VIVANCOS, T.; GOMEZ-PINEDO, U.; MATIAS-GUIU, J. Astrocytes in neurodegenerative diseases (I): function and molecular description. **Neurologia,** v. 30, n. 2, p. 119-29, Mar 2015.

HAKALA, J. O. et al. Cardiovascular Risk Factor Trajectories Since Childhood and Cognitive Performance in Midlife: The Cardiovascular Risk in Young Finns Study. **Circulation,** v. 143, n. 20, p. 1949-1961, May 18 2021.

HAO, S. et al. Dietary obesity reversibly induces synaptic stripping by microglia and impairs hippocampal plasticity. **Brain Behav Immun,** v. 51, p. 230-239, Jan 2016.

HENAGAN, T. M. et al. Sodium butyrate epigenetically modulates high-fat diet-induced skeletal muscle mitochondrial adaptation, obesity and insulin resistance through nucleosome positioning. **Br J Pharmacol,** v. 172, n. 11, p. 2782-98, Jun 2015.

HICKMAN, S. et al. Microglia in neurodegeneration. **Nat Neurosci,** v. 21, n. 10, p. 1359-1369, Oct 2018.

HSIEH, C. F. et al. Acute glucose fluctuation impacts microglial activity, leading to inflammatory activation or self-degradation. **Sci Rep,** v. 9, n. 1, p. 840, Jan 29 2019.

ISHIMOTO, T. et al. High-fat and high-sucrose (western) diet induces steatohepatitis that is dependent on fructokinase. **Hepatology,** v. 58, n. 5, p. 1632-43, Nov 2013.

JEON, B. T. et al. Resveratrol attenuates obesity-associated peripheral and central inflammation and improves memory deficit in mice fed a high-fat diet. **Diabetes,** v. 61, n. 6, p. 1444-54, Jun 2012.

JOKINEN, E. Obesity and cardiovascular disease. **Minerva Pediatr,** v. 67, n. 1, p. 25-32, Feb 2015.

KAPOGIANNIS, D.; AVGERINOS, K. I. Brain glucose and ketone utilization in brain aging and neurodegenerative diseases. **Int Rev Neurobiol,** v. 154, p. 79-110, 2020.

KATOH, M. et al. Polymorphic regulation of mitochondrial fission and fusion modifies phenotypes of microglia in neuroinflammation. **Sci Rep,** v. 7, n. 1, p. 4942, Jul 10 2017.

KHEIRANDISH, M. et al. The association between dietary patterns and metabolic syndrome among Iranian adults, a cross-sectional population-based study (findings from Bandare-Kong non-communicable disease cohort study). **BMC Endocr Disord,** v. 24, n. 1, p. 57, Apr 30 2024.

KNIGHT, E. M. et al. High-fat diet-induced memory impairment in triple-transgenic Alzheimer's disease (3xTgAD) mice is independent of changes in amyloid and tau pathology. **Neurobiol Aging,** v. 35, n. 8, p. 1821-32, Aug 2014.

KOH, A. et al. From Dietary Fiber to Host Physiology: Short-Chain Fatty Acids as Key Bacterial Metabolites. **Cell,** v. 165, n. 6, p. 1332-1345, Jun 2 2016.

LEE, Y. A. et al. Associations between Dietary Patterns and Metabolic Syndrome: Findings of the Korean National Health and Nutrition Examination Survey. **Nutrients,** v. 15, n. 12, Jun 8 2023.

LIU, H. et al. Butyrate: A Double-Edged Sword for Health? **Adv Nutr,** v. 9, n. 1, p. 21-29, Jan 1 2018.

LOUZADA, M. et al. Consumption of ultra-processed foods in Brazil: distribution and temporal evolution 2008-2018. **Rev Saude Publica,** v. 57, p. 12, 2023.

LUQUE-CONTRERAS, D. et al. Oxidative stress and metabolic syndrome: cause or consequence of Alzheimer's disease? **Oxid Med Cell Longev,** v. 2014, p. 497802, 2014.

MANDWIE, M. et al. Metformin Treatment Attenuates Brain Inflammation and Rescues PACAP/VIP Neuropeptide Alterations in Mice Fed a High-Fat Diet. **Int J Mol Sci,** v. 22, n. 24, Dec 20 2021.

MARKOWIAK-KOPEC, P.; SLIZEWSKA, K. The Effect of Probiotics on the Production of Short-Chain Fatty Acids by Human Intestinal Microbiome. **Nutrients,** v. 12, n. 4, Apr 16 2020.

MCDONALD, A. J.; MOTT, D. D. Functional neuroanatomy of amygdalohippocampal interconnections and their role in learning and memory. **J Neurosci Res,** v. 95, n. 3, p. 797-820, Mar 2017.

MELO, H. M. et al. Palmitate Is Increased in the Cerebrospinal Fluid of Humans with Obesity and Induces Memory Impairment in Mice via Pro-inflammatory TNF-alpha. **Cell Rep,** v. 30, n. 7, p. 2180-2194 e8, Feb 18 2020.

MICHELL-ROBINSON, M. A. et al. Roles of microglia in brain development, tissue maintenance and repair. **Brain,** v. 138, n. Pt 5, p. 1138-59, May 2015.

MISHRA, P.; CHAN, D. C. Metabolic regulation of mitochondrial dynamics. **J Cell Biol,** v. 212, n. 4, p. 379-87, Feb 15 2016.

MISHRA, S. P. et al. Free Fatty Acid Receptors 2 and 3 as Microbial Metabolite Sensors to Shape Host Health: Pharmacophysiological View. **Biomedicines,** v. 8, n. 6, Jun 8 2020.

NAIR, S. et al. Lipopolysaccharide-induced alteration of mitochondrial morphology induces a metabolic shift in microglia modulating the inflammatory response in vitro and in vivo. **Glia,** v. 67, n. 6, p. 1047-1061, Jun 2019.

NUNNARI, J.; SUOMALAINEN, A. Mitochondria: in sickness and in health. **Cell,** v. 148, n. 6, p. 1145-59, Mar 16 2012.

OSELLAME, L. D.; BLACKER, T. S.; DUCHEN, M. R. Cellular and molecular mechanisms of mitochondrial function. **Best Pract Res Clin Endocrinol Metab,** v. 26, n. 6, p. 711-23, Dec 2012.

PAOLICELLI, R. C. et al. Synaptic pruning by microglia is necessary for normal brain development. **Science,** v. 333, n. 6048, p. 1456-8, Sep 9 2011.

PARK, H. S.; CHO, H. S.; KIM, T. W. Physical exercise promotes memory capability by enhancing hippocampal mitochondrial functions and inhibiting apoptosis in obesity-induced insulin resistance by high fat diet. **Metab Brain Dis,** v. 33, n. 1, p. 283-292, Feb 2018.

PATCHING, S. G. Glucose Transporters at the Blood-Brain Barrier: Function, Regulation and Gateways for Drug Delivery. **Mol Neurobiol,** v. 54, n. 2, p. 1046-1077, Mar 2017.

REMPEL-CLOWER, N. L. et al. Three cases of enduring memory impairment after bilateral damage limited to the hippocampal formation. **J Neurosci,** v. 16, n. 16, p. 5233-55, Aug 15 1996.

ROCHA, N. P. et al. Association between dietary pattern and cardiometabolic risk in children and adolescents: a systematic review. **J Pediatr (Rio J),** v. 93, n. 3, p. 214-222, May-Jun 2017.

RUEGSEGGER, G. N. et al. Exercise and metformin counteract altered mitochondrial function in the insulin-resistant brain. **JCI Insight,** v. 4, n. 18, Sep 19 2019.

SCHIATTARELLA, G. G. et al. Nitrosative stress drives heart failure with preserved ejection fraction. **Nature,** v. 568, n. 7752, p. 351-356, Apr 2019.

SQUARZONI, P.; THION, M. S.; GAREL, S. Neuronal and microglial regulators of cortical wiring: usual and novel guideposts. **Front Neurosci,** v. 9, p. 248, 2015.

STILLING, R. M. et al. The neuropharmacology of butyrate: The bread and butter of the microbiota-gut-brain axis? **Neurochem Int,** v. 99, p. 110-132, Oct 2016.

SUN, Q. et al. Mitochondrial fatty acid oxidation is the major source of cardiac adenosine triphosphate production in heart failure with preserved ejection fraction. **Cardiovasc Res,** v. 120, n. 4, p. 360-371, Mar 30 2024.

TAN, J. et al. The role of short-chain fatty acids in health and disease. **Adv Immunol,** v. 121, p. 91-119, 2014.

THALER, J. P. et al. Obesity is associated with hypothalamic injury in rodents and humans. **J Clin Invest,** v. 122, n. 1, p. 153-62, Jan 2012.

TREVINO, S. et al. A high calorie diet causes memory loss, metabolic syndrome and oxidative stress into hippocampus and temporal cortex of rats. **Synapse,** v. 69, n. 9, p. 421-33, Sep 2015.

TREVINO, S. et al. Metabolic syndrome causes recognition impairments and reduced hippocampal neuronal plasticity in rats. **J Chem Neuroanat,** v. 82, p. 65-75, Jul 2017.

TUTUNCHI, H. et al. Association between Dietary Patterns and Non-alcoholic Fatty Liver Disease: Results from a Case-Control Study. **Arch Iran Med,** v. 24, n. 1, p. 35-42, Jan 1 2021.

VALDEARCOS, M. et al. Microglial Inflammatory Signaling Orchestrates the Hypothalamic Immune Response to Dietary Excess and Mediates Obesity Susceptibility. **Cell Metab,** v. 26, n. 1, p. 185-197 e3, Jul 5 2017.

VEZZANI, A.; VIVIANI, B. Neuromodulatory properties of inflammatory cytokines and their impact on neuronal excitability. **Neuropharmacology,** v. 96, n. Pt A, p. 70-82, Sep 2015.

VILAS-BOAS, E. A. et al. Goldilocks calcium concentrations and the regulation of oxidative phosphorylation: Too much, too little, or just right. **J Biol Chem,** v. 299, n. 3, p. 102904, Mar 2023.

VILELA, W. R. et al. Early-life metabolic dysfunction impairs cognition and mitochondrial function in mice. **J Nutr Biochem,** v. 117, p. 109352, Jul 2023.

VILELA, W. R. et al. Metabolic dysfunction induced by HFD + L-NAME preferentially affects hippocampal mitochondria, impacting spatial memory in rats. **Journal of Bioenergetics and Biomembranes**, 2024/02/20 2024.

VUONG, B. et al. Exposure to gestational diabetes mellitus induces neuroinflammation, derangement of hippocampal neurons, and cognitive changes in rat offspring. **J Neuroinflammation,** v. 14, n. 1, p. 80, Apr 7 2017.

WANG, Z. et al. Saturated fatty acids activate microglia via Toll-like receptor 4/NF-kappaB signalling. **Br J Nutr,** v. 107, n. 2, p. 229-41, Jan 2012.

WHO. Obesity and Overweight. World Health Organization. 2020.

WU, Z. et al. Publisher Correction: Inhibition of eNOS by L-NAME resulting in rat hind limb developmental defects through PFKFB3 mediated angiogenetic pathway. **Sci Rep,** v. 11, n. 1, p. 4298, Feb 16 2021.

XIAO, S. et al. Analysis of the association between dietary patterns and nonalcoholic fatty liver disease in a county in Guangxi. **BMC Gastroenterol,** v. 23, n. 1, p. 309, Sep 13 2023.

XU, Y. et al. High doses of butyrate induce a reversible body temperature drop through transient proton leak in mitochondria of brain neurons. **Life Sci,** v. 278, p. 119614, Aug 1 2021.

YANG, C. et al. Exogenous IGF-1 alleviates depression-like behavior and hippocampal mitochondrial dysfunction in high-fat diet mice. **Physiol Behav,** v. 229, p. 113236, Feb 1 2021.

YASSINE, H. N. et al. Nutritional metabolism and cerebral bioenergetics in Alzheimer's disease and related dementias. **Alzheimers Dement,** v. 19, n. 3, p. 1041-1066, Mar 2023.

ZHANG, R. et al. Associations of dietary patterns with brain health from behavioral, neuroimaging, biochemical and genetic analyses. **Nature Mental Health,** v. 2, n. 5, p. 535-552, 2024.

ZHANG, X. et al. Enhancement of LPS-induced microglial inflammation response via TLR4 under high glucose conditions. **Cell Physiol Biochem,** v. 35, n. 4, p. 1571-81, 2015.

ZHUANG, H. et al. Long-term high-fat diet consumption by mice throughout adulthood induces neurobehavioral alterations and hippocampal neuronal remodeling accompanied by augmented microglial lipid accumulation. **Brain Behav Immun,** v. 100, p. 155-171, Feb 2022.

ZOLA-MORGAN, S.; SQUIRE, L. R.; AMARAL, D. G. Human amnesia and the medial temporal region: enduring memory impairment following a bilateral lesion limited to field CA1 of the hippocampus. **J Neurosci,** v. 6, n. 10, p. 2950-67, Oct 1986.

8. ANEXOS

Aprovação do projeto pela Comissão de Ética no Uso de Animais da Universidade de São Paulo

Instituto de Ciências Biomédicas
ICB USP Excelência em Ensino e Pesquisa

Universidade de São Paulo
Comissão de Ética no Uso de Animais

São Paulo, 10 de junho de 2021
CEUA N 9236210120

Ilmo(a). Sr(a).
Responsável: Julio Cesar Batista Ferreira
Área: Anatomia

Título da proposta: "SAMbA: UMA NOVA ESTRATÉGIA TERAPÊUTICA PARA INSUFICIÊNCIA CARDÍACA COM FRAÇÃO DE EJEÇÃO PRESERVADA".

Parecer Consubstanciado da Comissão de Ética no Uso de Animais ICB (ID 001557)

A Comissão de Ética no Uso de Animais da Instituto de Ciências Biomédicas (Universidade de São Paulo), no cumprimento das suas atribuições, analisou e **APROVOU** a Emenda (versão de 04/junho/2021) da proposta acima referenciada.

Resumo apresentado pelo pesquisador: "Inclusão de membro da equipe.".

Comentário da CEUA: "O Colegiado da CEUA autoriza a inclusão de Wembley Rodrigues Vilela ao protocolo aprovado. ".

Profa. Dra. Luciane Valéria Sita
Coordenadora da Comissão de Ética no Uso de Animais
Instituto de Ciências Biomédicas (Universidade de São Paulo)

Dr. Alexandre Ceroni
Vice-Coordenador da Comissão de Ética no Uso de Animais
Instituto de Ciências Biomédicas (Universidade de São Paulo)